

AD-A102 262

MASSACHUSETTS UNIV AMHERST ASTRONOMY RESEARCH FACILITY

F/G 7/4

SCRIBE I DATA ANALYSIS (U)

APR 81 M SAKAI

F19628-79-C-0062

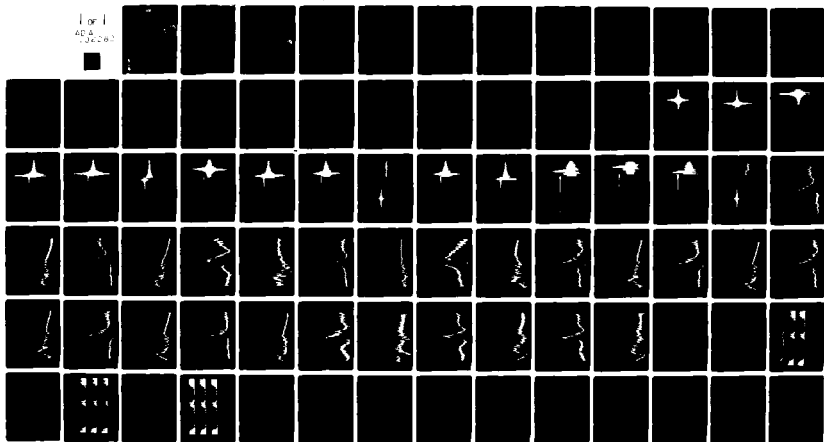
UNCLASSIFIED

UMASS-ARF-81-315

AFGL-TR-81-0129

NL

1 of 1  
484  
100000



END  
DATE  
FILMED  
9-81  
DTIC

**LEVEL II**

12 72

AD A102262

AFGL-TR-81-0129

SCRIBE I DATA ANALYSIS

Hajime Sakai

Astronomy Research Facility  
University of Massachusetts  
Amherst MA 01003

**DTIC  
ELECTED  
JUL 31 1981**  
C

Approved for public release; distribution unlimited.

April 1981

Scientific Report No. 1

AIR FORCE GEOPHYSICS LABORATORY  
AIR FORCE SYSTEMS COMMAND  
UNITED STATES AIR FORCE  
HANSCOM AFB, MASSACHUSETTS 01731

81 7 31 108

FILE COPY  
96

**Qualified requestors may obtain additional copies from the Defense Technical Information Center. All others should apply to the National Technical Information Service.**

UNCLASSIFIED

SECURITY CLASSIFICATION OF THIS PAGE (When Data Entered)

REPORT DOCUMENTATION PAGE		READ INSTRUCTIONS BEFORE COMPLETING FORM
1. REPORT NUMBER AFGL-TR-81-0129 ✓	2. GOVT ACCESSION NO. AD-A102262	3. RECIPIENT'S CATALOG NUMBER
4. TITLE (and Subtitle) SCRIBE I DATA ANALYSIS	5. TYPE OF REPORT & PERIOD COVERED Scientific Report No. 1	
7. AUTHOR(s) Hajime/Sakai	6. PERFORMING ORG. REPORT NUMBER UMASS-ARF-81-315	SCIENTIFIC
9. PERFORMING ORGANIZATION NAME AND ADDRESS Astronomy Research Facility University of Massachusetts Amherst MA 01003	8. CONTRACT OR GRANT NUMBER(s) F19628-79-C-0062	10. PROGRAM ELEMENT, PROJECT, TASK AREA & WORK UNIT NUMBERS 61102F 2310GLAL
11. CONTROLLING OFFICE NAME AND ADDRESS Air Force Geophysics Laboratory Hanscom AFB, Massachusetts 01731 Monitor/George Vanasse/OPI	12. REPORT DATE April 1981	13. NUMBER OF PAGES 81
14. MONITORING AGENCY NAME & ADDRESS (if different from Controlling Office)	15. SECURITY CLASS. (of this report) Unclassified	
16. DISTRIBUTION STATEMENT (of this Report)  Approved for public release; distribution unlimited.		
17. DISTRIBUTION STATEMENT (of the abstract entered in Block 20, if different from Report)		
18. SUPPLEMENTARY NOTES		
19. KEY WORDS (Continue on reverse side if necessary and identify by block number) Atmospheric emission      H <sub>2</sub> O Cryogenic interferometer      CO <sub>2</sub> Fourier spectroscopy      O <sub>3</sub>		
20. ABSTRACT (Continue on reverse side if necessary and identify by block number)  The data collected by the SCRIBE October 1980 flight were analyzed. The obtained results are reported in this report, together with the hardware and the software developed.		

DTIC  
 SELECTED  
 JUL 31 1981  
 C

480 989

## SCRIBE\* I Data Analysis

### Introduction

A LiN<sub>2</sub> cooled cat's eye interferometer was flown on October 8, 1980, at Holloman AFB under the SCRIBE program. We at the University of Massachusetts took a responsibility for the post-flight data analysis which can be divided into three major functions: (1) extraction of the interferogram data from the PCM telemetry record; (2) recovery of the spectral data from the extracted interferograms; and (3) analysis of the spectral data in terms of the atmospheric molecular parameters. The experiment was successful only during the first 20 minutes of flight. The balloon-borne instrument failed to produce the interferogram data after the balloon reached an altitude of 6 km.

Our major effort up to the present can be summarized in the following four major categories: (1) to assemble the electronics interface to receive the output data of the PCM decommutator and to modify them in a proper format for the PDP11/20 computer; (2) to implement a scheme for recording the interferogram data extracted from the PCM record onto a digital magnetic recording tape; (3) to develop a scheme for processing the produced interferogram data recorded on a magnetic tape; and (4) to improve the analysis scheme on the recovered spectral data. Our efforts in all of these activities were successful in that we were able to obtain the atmospheric emission spectra from the telemetry record. Unfortunately, the flight data did not provide

---

\* Stratospheric Cryogenic Interferometer Balloon Experiment. The technical detail of the program and of the October 8, 1980, flight is given in G. Vanasse, AFGL Report (1981).

a full test of our developed scheme. The quality of the flight data did not reach the expected level due to the interferometer scanning problem. In addition, mere 16 interferogram data extracted from the telemetry record were not sufficient to provide a solid basis for studying the infrared atmospheric emission as a function of the altitude.

The present scientific report summarizes our effort which was carried out for processing of the October 1980 data. Included in the report are a description of the interferogram electronics hardware constructed for our decommutation scheme, the PDP11 software employed in conjunction with our decommutation scheme, and the CDC software written for the spectral recovery from the interferogram data recorded on a PDP11/RT11 format magnetic tape.

Accession For	<input checked="" type="checkbox"/>	<input type="checkbox"/>
NTIS GRA&I	<input type="checkbox"/>	<input type="checkbox"/>
DTIC TAB		
Unannounced		
Justification		
By		
Distribution/		
Availability Codes		
Avail and/or		
Special		
Dist		
A		

### Decommutation of the Telemetry Data

The data obtained during the flight were sent to the ground station through a telemetry radio link. The scheme used for the telemetry is shown in a block diagram of Fig. 1. The digitized interferogram data together with other signals were fed into the PCM encoder, which produced the PCM telemetry signal as a proper bit sequence. The telemetry signal transmitter in the balloon-borne package and the receiver in the ground station formed a radio link between the data obtained by the balloon-borne instruments and the ground station recording device. The SABRE IV magnetic tape recorder was used to record the telemetry signal on a 1/2" analog tape in a direct recording mode. The recording was done at 800 K BPS at 60 IPS.

The telemetry signal was formatted in a 72 bit per frame, which consisted of a 20-bit synchronization word, a 4-bit frame-identification word, a 16-bit interferogram data word, and four 8-bit words for other data. The synchronization-word bit pattern is given in Table I. The interferogram data were made of a 12-bit word representing the A/D converter output and a 4-bit control status word, as shown in Table I. The interferometer was scanned at an approximate rate of .3 cm OPD/sec. The interferogram data were sampled at twice the HeNe laser line wavelength of 6329 Å (in vacuum). The telemetry rate of 11, 1 K frame-per-second was considerably higher than the interferogram data sampling rate which was less than 2 K word-per-second. This scheme was designed to accommodate fluctuating interferogram sampling intervals by making the telemetry signal transmission deliberately faster than the interferogram sampling rate. It was devised in such a way that the data transmission was never caught up by the data sampling. Within the interferometer scanning

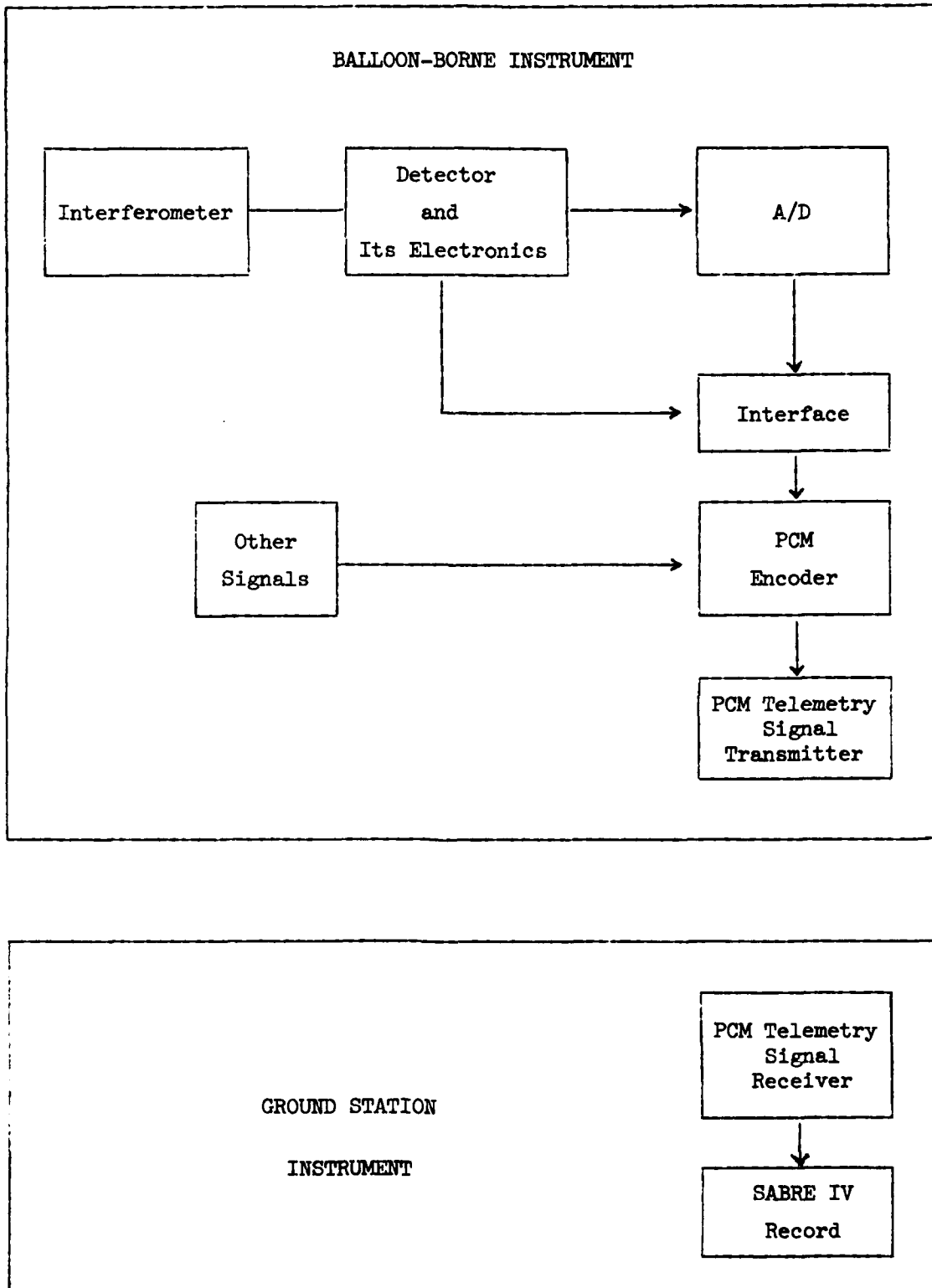
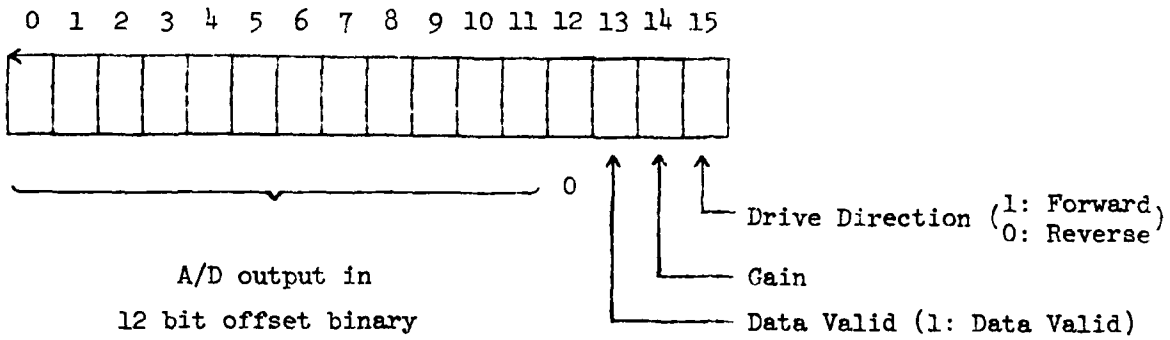


Figure 1

Table I  
Interferogram Data Bit Format



A/D output in  
12 bit offset binary

-10V 000 000 000 000  
0V 100 000 000 000  
10V 111 111 111 111

Synchronization Word (20-bit)  
111 010 111 001 000 000 00

tolerance, no interferogram data should be lost in the transmission. The on-board electronics produced a sequence of zero-word data after the sampled interferogram signal was transmitted until the next sampled interferogram signal became ready for the transmission. The data status was coded in a 4-bit word shown in Table I.

Fig. 2 shows an overall scheme for our data extraction electronics. The PCM decommutator manufactured originally by the Monitor System provides two functions: it finds a clock-rate of the telemetry signal which is play-backed by SABRE IV, and it generates a clock-pulse stream synchronized with the telemetry signal. The unit was modified by us to accept a bit rate of 800 K BPS. The produced output was a serial 72-bit string together with the synchronization clock pulse, if the unit succeeds to detect a bit pattern of the synchronization word. When a detection failure occurs, the clock pulse stops and the error flag is raised. The error status continues until the reset switch is manually intervened.

The interface electronics provides two major functions: (1) an extraction of a proper 16-bit word from a serial 72-bit string of the telemetry; and (2) a parallel 16-bit output to DR11B parallel I/O interface of PDP11/20. The unit accepts three signals provided by the PCM decommutator: (1) PCMIN signal of a serial 72-bit data word; (2) a clock signal synchronized with PCMIN, and (3) FTO signal indicating a completion of each PCMIN signal transmission. The logic used in our scheme is shown in a block diagram of Fig. 3. The WORD SELECT logic accepts either a command from a manual switch on the front panel, or an external control signal provided by the PDP11. The HAND SHAKE circuit provides an ordinary flag logic for indicating that the data are ready for transfer to the CPU. Figs. 4 through 8 show the component circuits

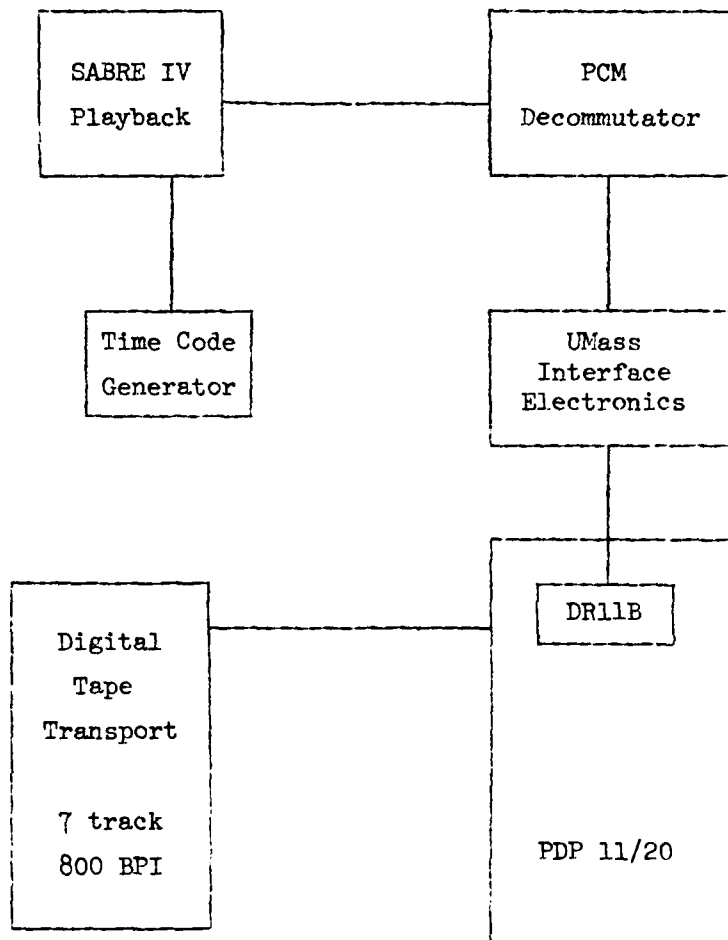


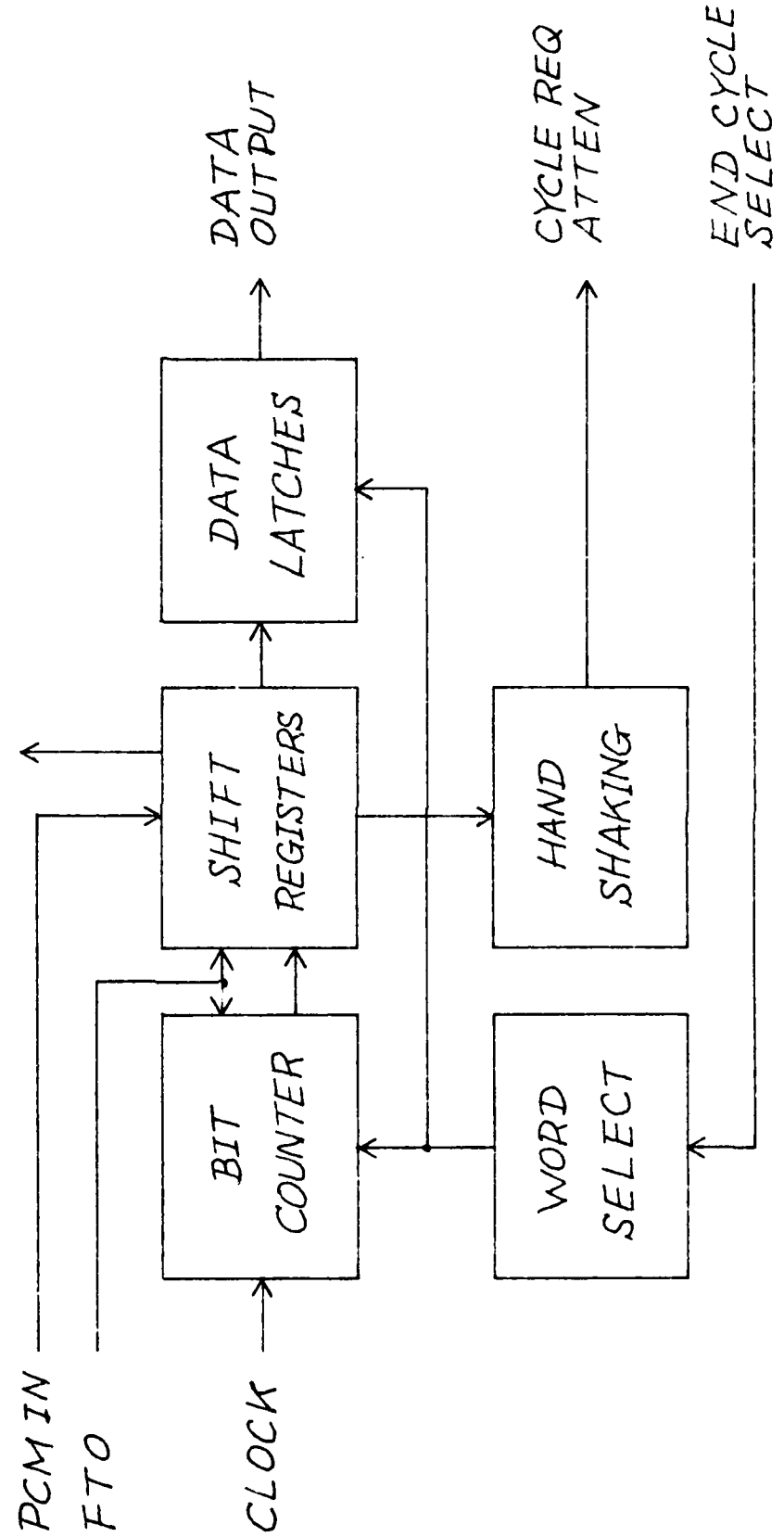
Figure 2

in detail.

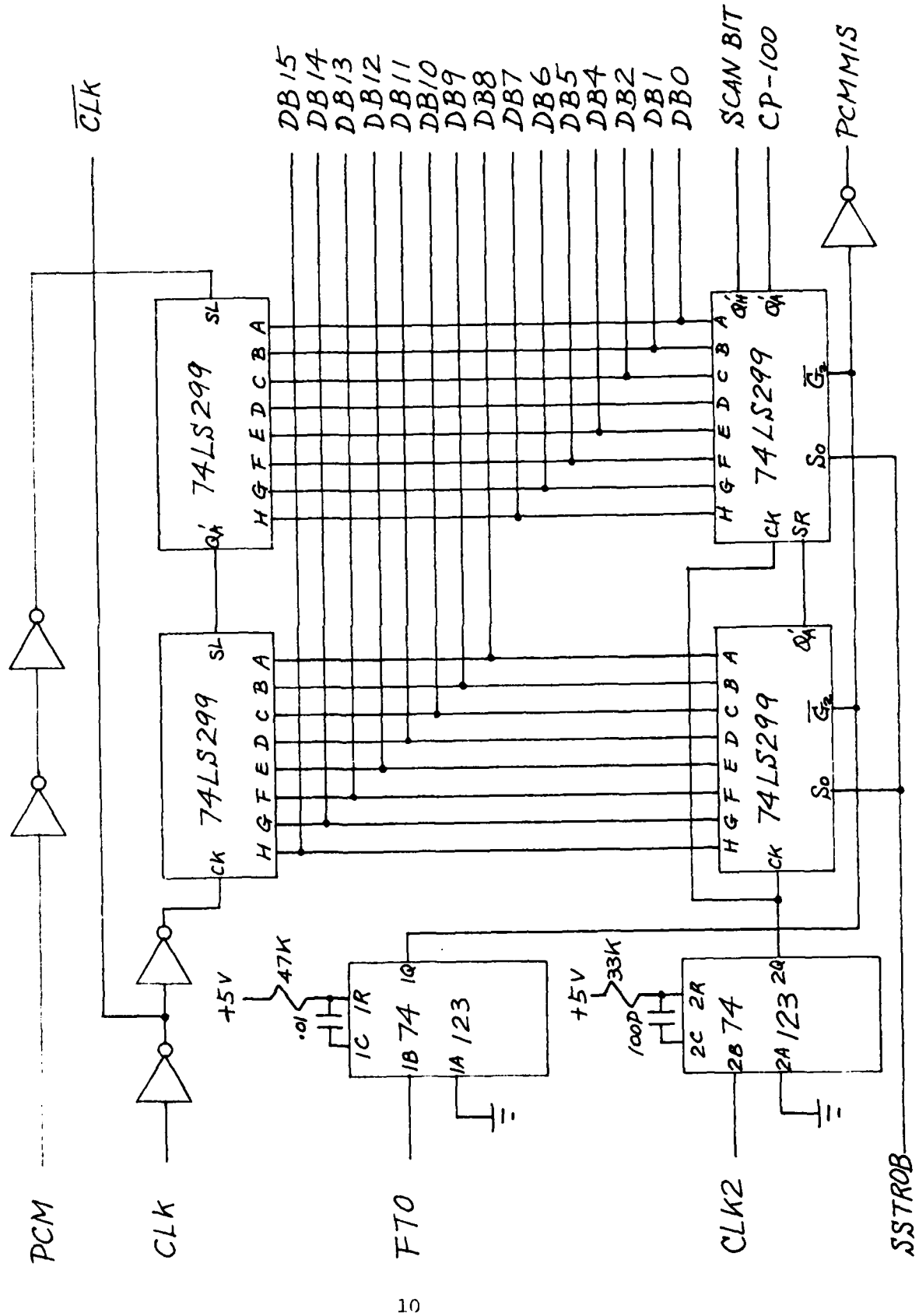
The PDP11/20 mainframe accepts the parallel 16-bit data via DR11B parallel I/O interface. The first program disregards the bit pattern of the control status word, and transfers the entire 16-bit word to RKL disk memory without discriminating the zero words interspersed in the interferogram signal. The second program examines the data stored on RKL for their validation. Only the proper data are selected to transfer to DTO. The generated data files on DTO are recorded with the standard RT11 format. The data transfer from DTO to MT is done using the standard RT11 peripheral interchange software PIP. The final data recorded on MT are formatted on 800 BPI, 7 track, odd parity magnetic tape blocked by 256 16-bit words, which are composed by 4 6-bit bytes with a parity bit accompanying to each byte. The software programs loaded on PDP11/20 for these operations are listed in APPENDIX.

# DATA ACQUISITION INTERFACE

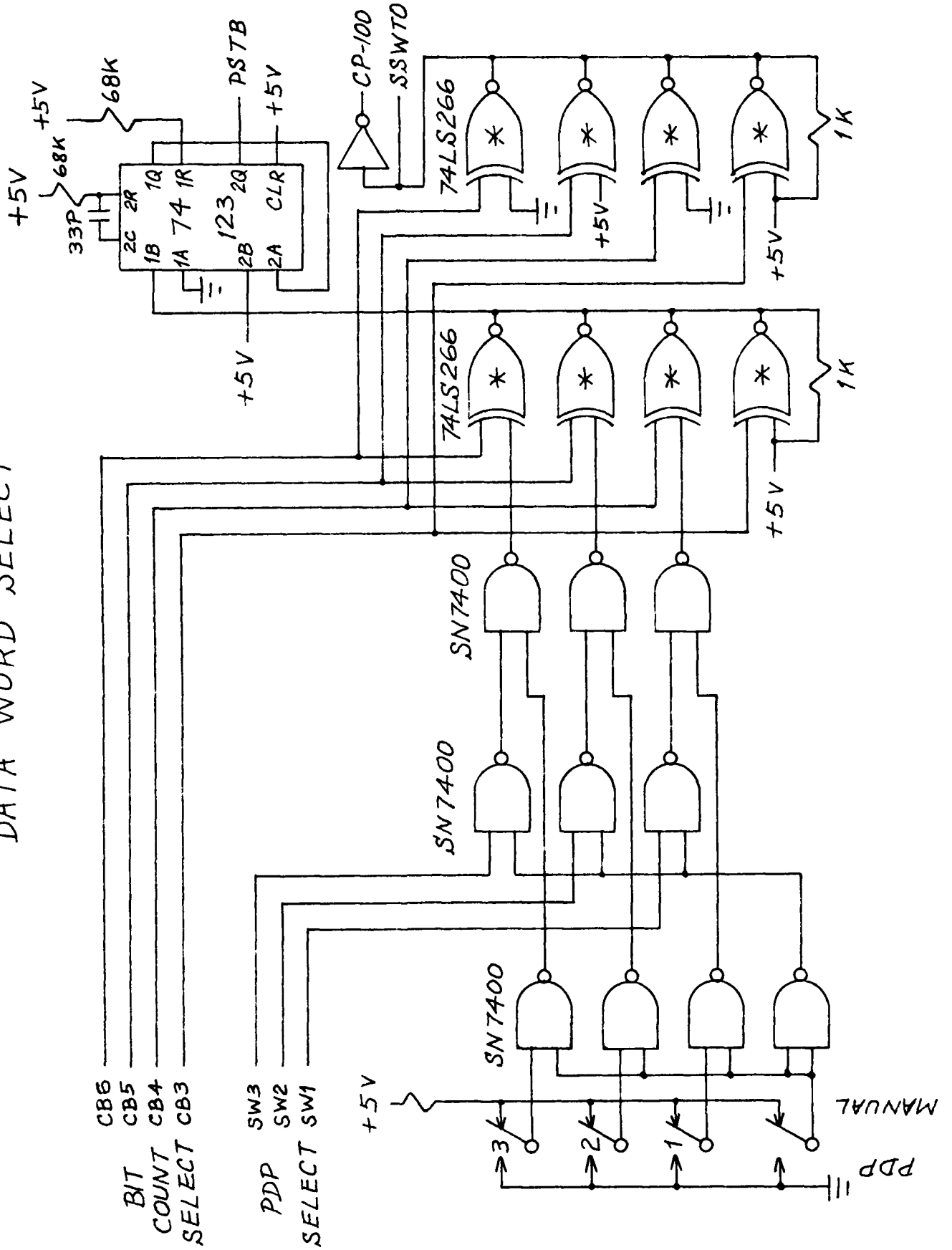
FROM PCM DECOMMUTATOR TO PDP 11



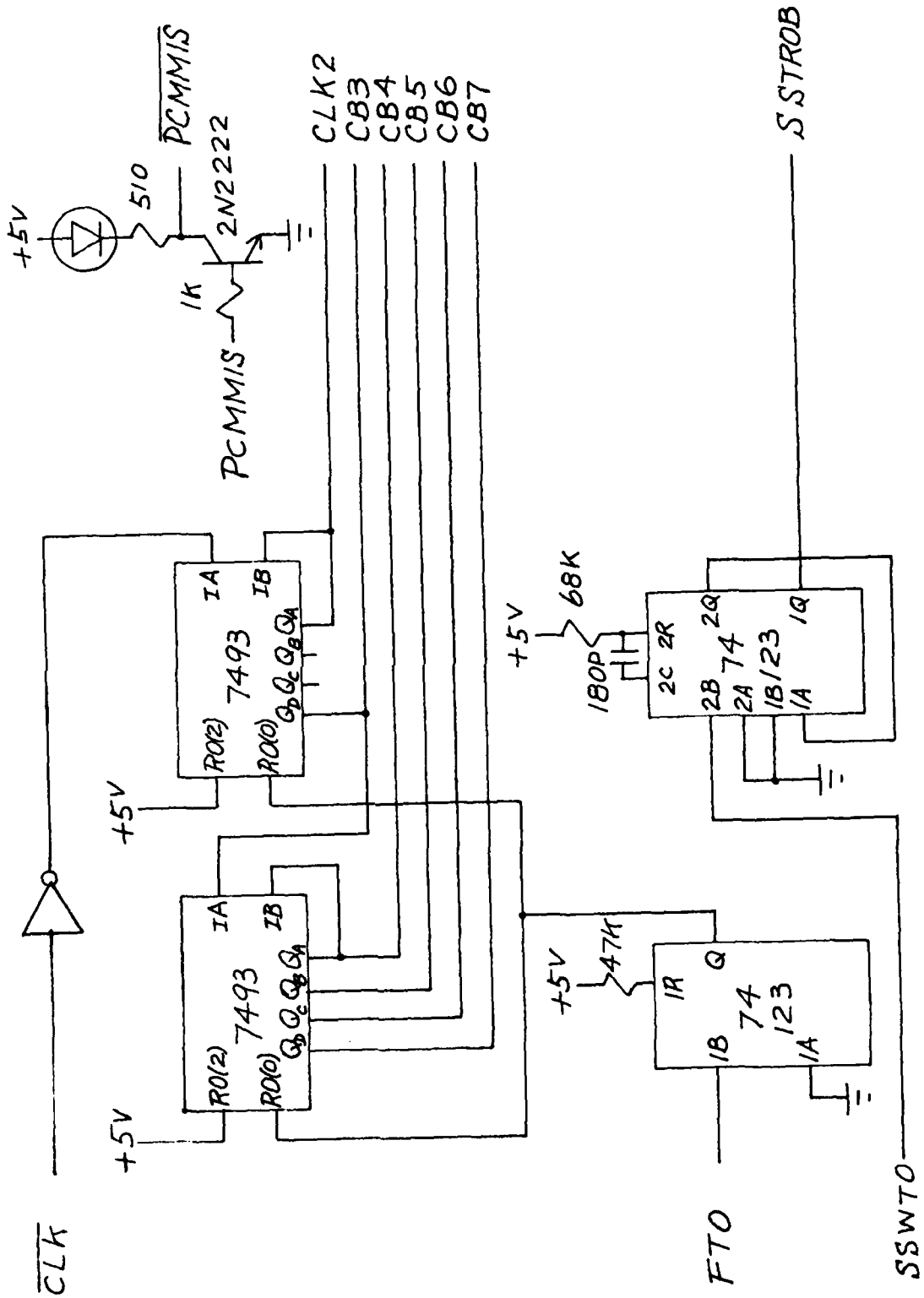
# SHIFT/STORAGE REGISTERS



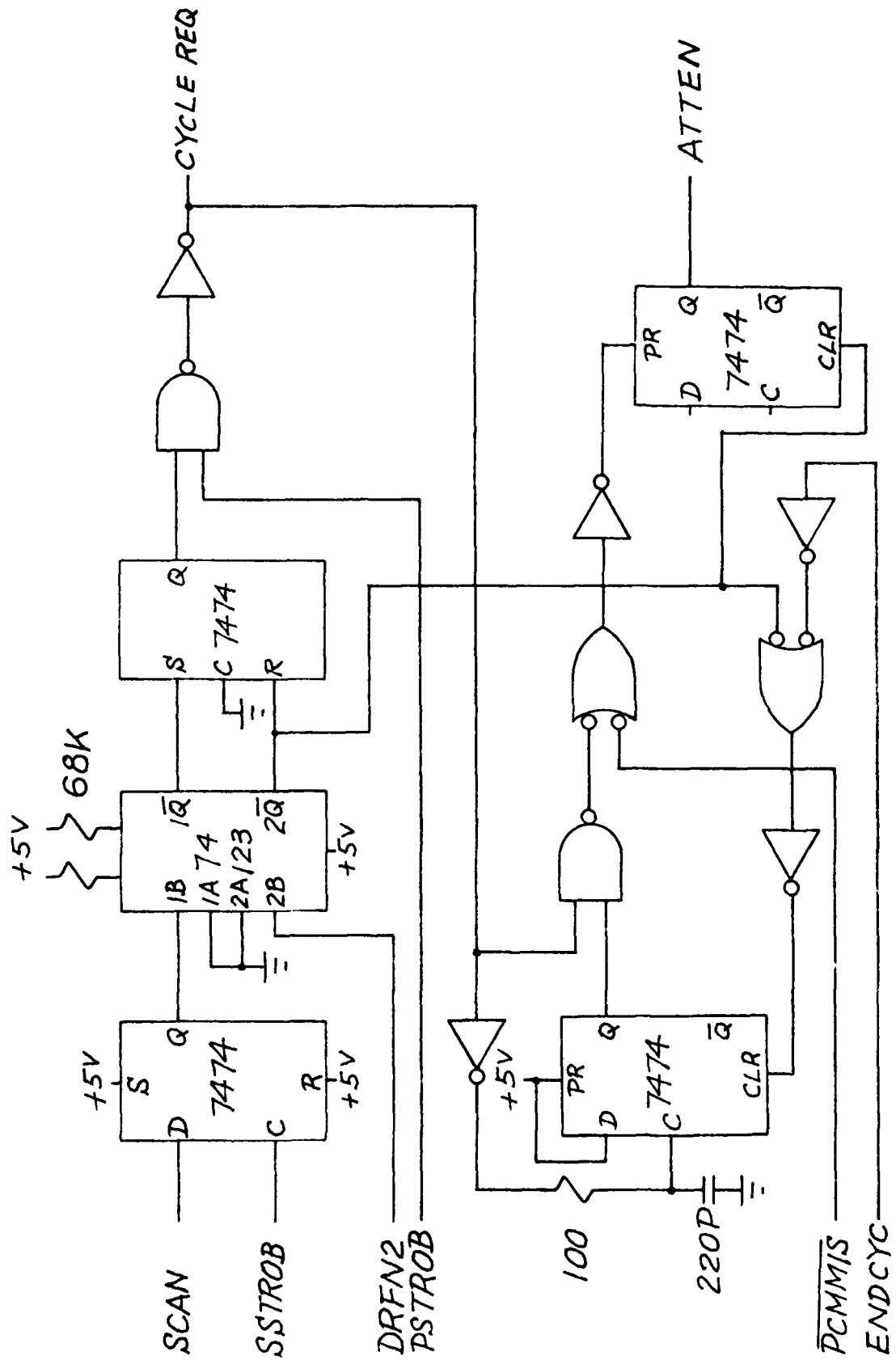
# DATA WORD SELECT



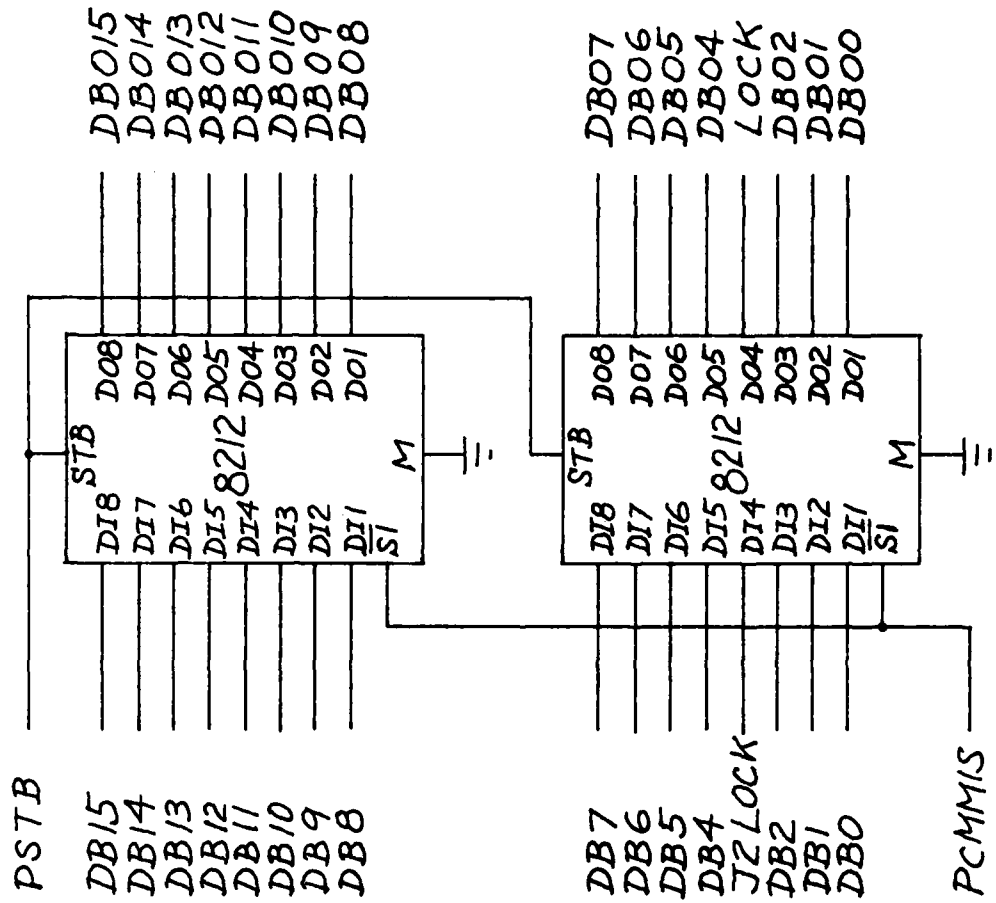
# BIT COUNTERS



# DRIIB HAND SHAKING



# BUFFERED DATA LATCHES



### Spectral Recovery Process on CDC Cyber

The interferogram data on a 7-track, 800 BPI magnetic tape are recorded under control of the PDP/RT11 operating system. The general scheme for spectral recovery shown in a block diagram of Fig. 9 has consequently an extra step required for a conversion of the RT11 format word to the CDC internal format. The CDC's COPYBF command under the NOS operating system provides a satisfactory data transfer to the CDC disk memory for our data generated by the PDP/RT11 system. The conversion of the data to the CDC Cyber format is carried out by SXREAD listed in APPENDIX. The gain change in the interferogram data is adjusted by SKXREAD, also listed in APPENDIX. These two programs were developed by us for this operation. The rest of the numerical computation process is our standard routine used for general purpose spectral recovery in our Fourier spectroscopy effort. The Appendices provide a listing of the entire software package. The final outputs are generally produced with (16I5) format with the highest peak value of the recovered spectrum normalized to 1000.

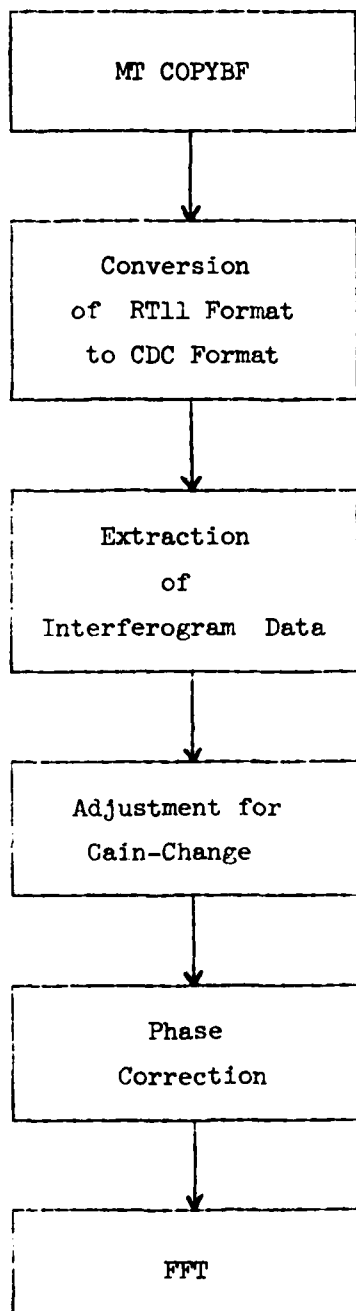


Figure 9

### Interferogram Data

The interferogram data extracted from the telemetry record are summarized in Table II. The time-code generator failed to function at the time of our data extraction effort. The extracted interferogram data were identified by reading the SABRE IV footage counter. Included in the Table are the approximate balloon altitudes. We found two major trouble spots in the telemetry record, where the PCM decommutator failed to establish a lock-in, (1) between 1600 ft. and 2300 ft., and (2) between 4150 ft. and 4340 ft. The telemetry record beyond 4340 ft. produced the interferogram data not extending to the full optical path difference. The PCM decommutator was able to lock-in to the synchronization word for those data.

We observed that the interferogram data starting position varied considerably among these sixteen extracted from the telemetry record. The gain-change scheme was implemented under the basic design assumption that the interferometer would commence to take data without a narrow proximity centered at a pre-fixed position. The first several hundred data points would be measured with a low gain setting, since they would fall in a region of the central modulation. After these data points, the detector amplifier would be set at a high gain (a factor of 5.6 times the gain in the first region). The interferometer did not scan in accordance with this design during the flight. The gain-change scheme lost its function and a majority of the interferogram data were recorded with a single gain. In addition to the gain-switching scheme, the detector amplifier was designed to accommodate a gain-adjustment in accordance with the preceding interferogram modulation in the ZPD region. Because the gain-switching position did not provide a required

Table II

<u>Designation</u>	<u>SABRE IV Footage Reading</u>	<u>Balloon Altitude</u>
A	1100	2700 m
B	1200	2800
C	1340	2900
D	1480	3050
E	2300	3800
F	2400	3950
G	2560	4100
H	2700	4200
K	2840	4350
L	2980	4500
M	3110	4600
N	3400	4900
P	3510	5000
Q	3650	5150
R	3790	5250
S	3930	5400
T*	4340	5800
U*	4470	5900
V*	4600	6050
X*	4745	6150

\*The PCM decommutator was able to lock-in, but the interferogram data were fragmentary.

synchronization with the interferogram ZPD position due to the trouble described above, a considerable gain fluctuation was resulted among the data. The central modulation of some data was found to be saturated.

A critical inspection of the data quality became necessary in our effort because of the difficulties in the interferometer scanning. We devised to observe the phase curve of the ZPD region for all the interferogram data extracted, and found it varying from one interferogram data to another in a substantial degree.

The S/N in the recovered spectra was found far below the figure expected. The interferogram data were not measured with a dynamic range originally planned because of the interferometer scanning problem. We believe that a correction of the interferogram scanning difficulty is essential for achieving overall improvement of the spectrometry.

The data were sampled at an interval of twice the HeNe laser line wavelength. We do not believe that the sampling scheme used for the October 1980 flight would add any advantages to the scheme which we planned originally. The resulted disadvantage was far greater than otherwise. We strongly recommend to adopt the originally planned sampling interval.

We found that the 4-bit status word for the interferogram data produced no consistency to what the data indicated. The gain-bit registered in the status word did not conform with the actual gain-setting of the detector amplifier. We judged the amplifier gain by inspecting the off-set bias voltage in the data, the scheme implemented by the University of Denver. A problem faced us with the U. Denver scheme was that we found it rather difficult to write a fail-safe software for accommodating the gain-adjustment. The software listed in APPENDIX

provided a service for a majority of the cases. We did not bother to re-write it for broadening its coverage of the cases which fall outside of its applicability. We knew that its applicability was limited and that several cases could not be processed by using the scheme. The gain adjustment for those cases was implemented manually by inspecting the raw data. The procedure that we adopted for the present case cannot produce a sufficient efficiency for the case where the processing involves several hundred of the interferogram data. For future flights, we hope that the status word would furnish a true reflection of the interferogram data.

Figures 10 through 25 show the raw interferogram data extracted from the telemetry record. Figures 26 through 38 show the spectra recovered with a resolution of  $.5 \text{ cm}^{-1}$ . The data F, L and S had its central modulation recorded in the low gain setting. A dynamic range of their recording was extremely small, resulting in the recovered spectra of an exceptionally low S/N. They are not shown because of excessive noise content. The phase curves shown in Figure 39 are obtained with a spectral resolution of approximately  $125 \text{ cm}^{-1}$ . They are not stable principally because of the dynamic range saturation in the CM region. It was found that among these interferograms processed, the data N was free from these problems.

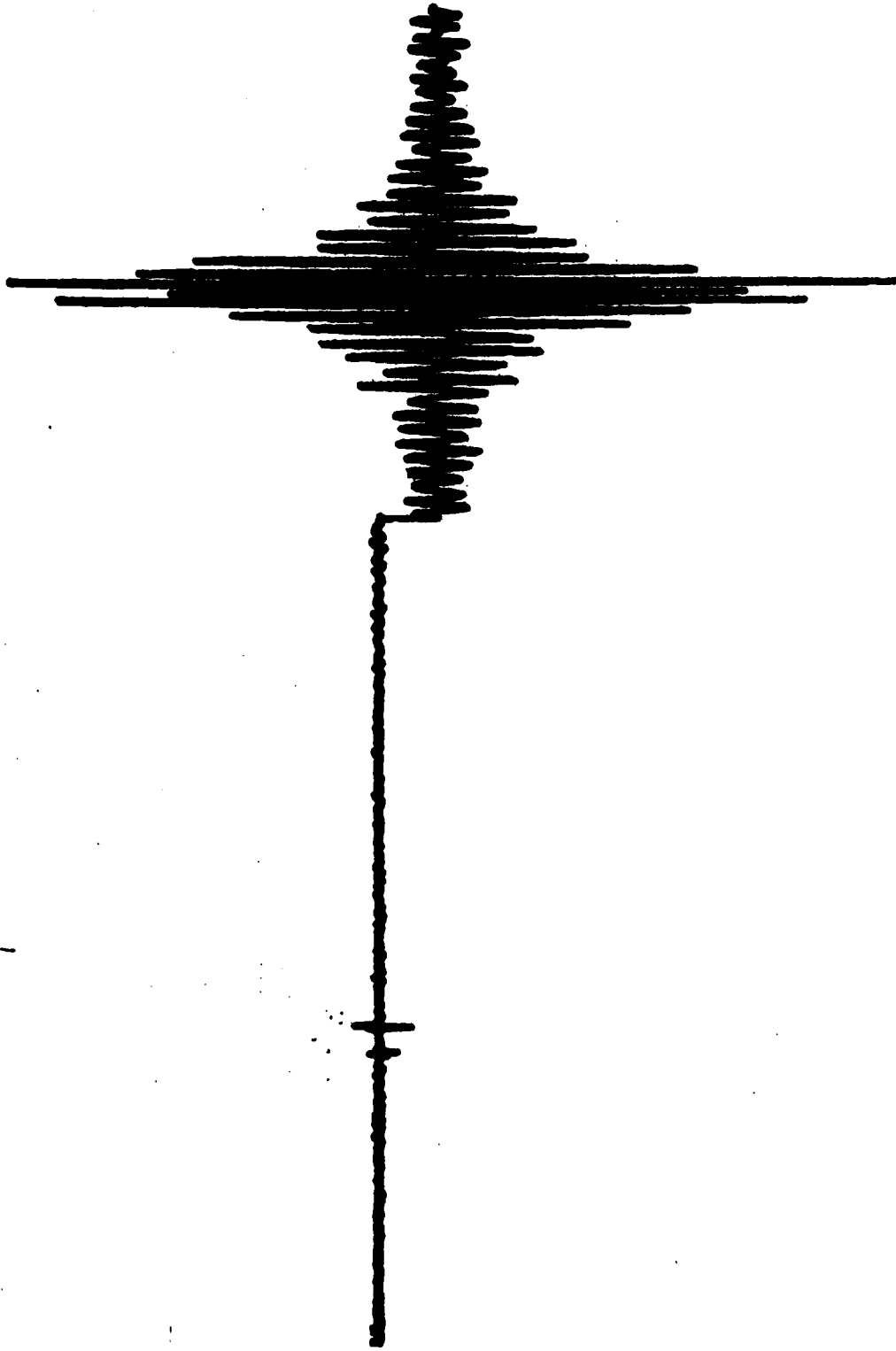


Fig. 10 Interferogram A

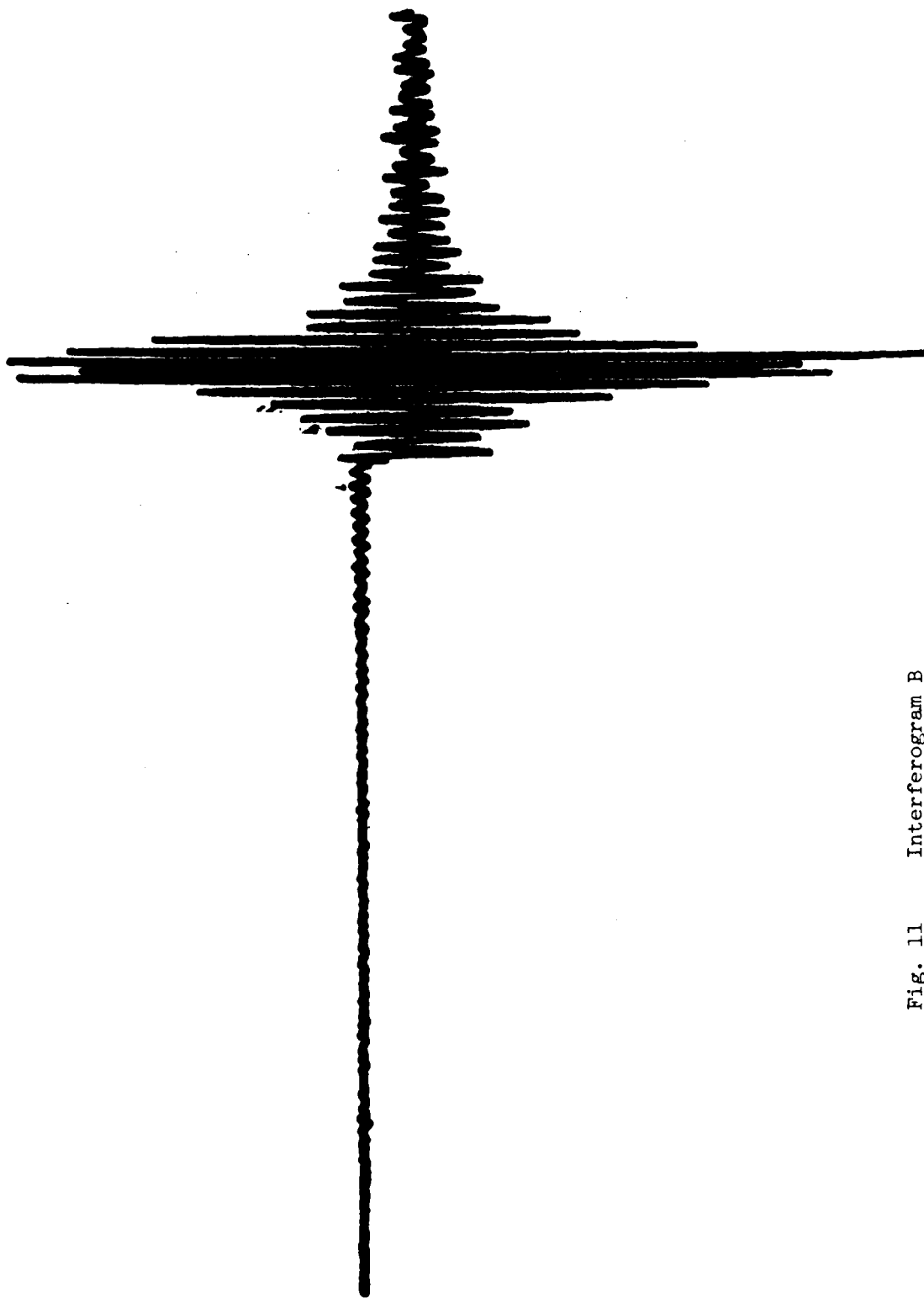


Fig. 11 Interferogram B

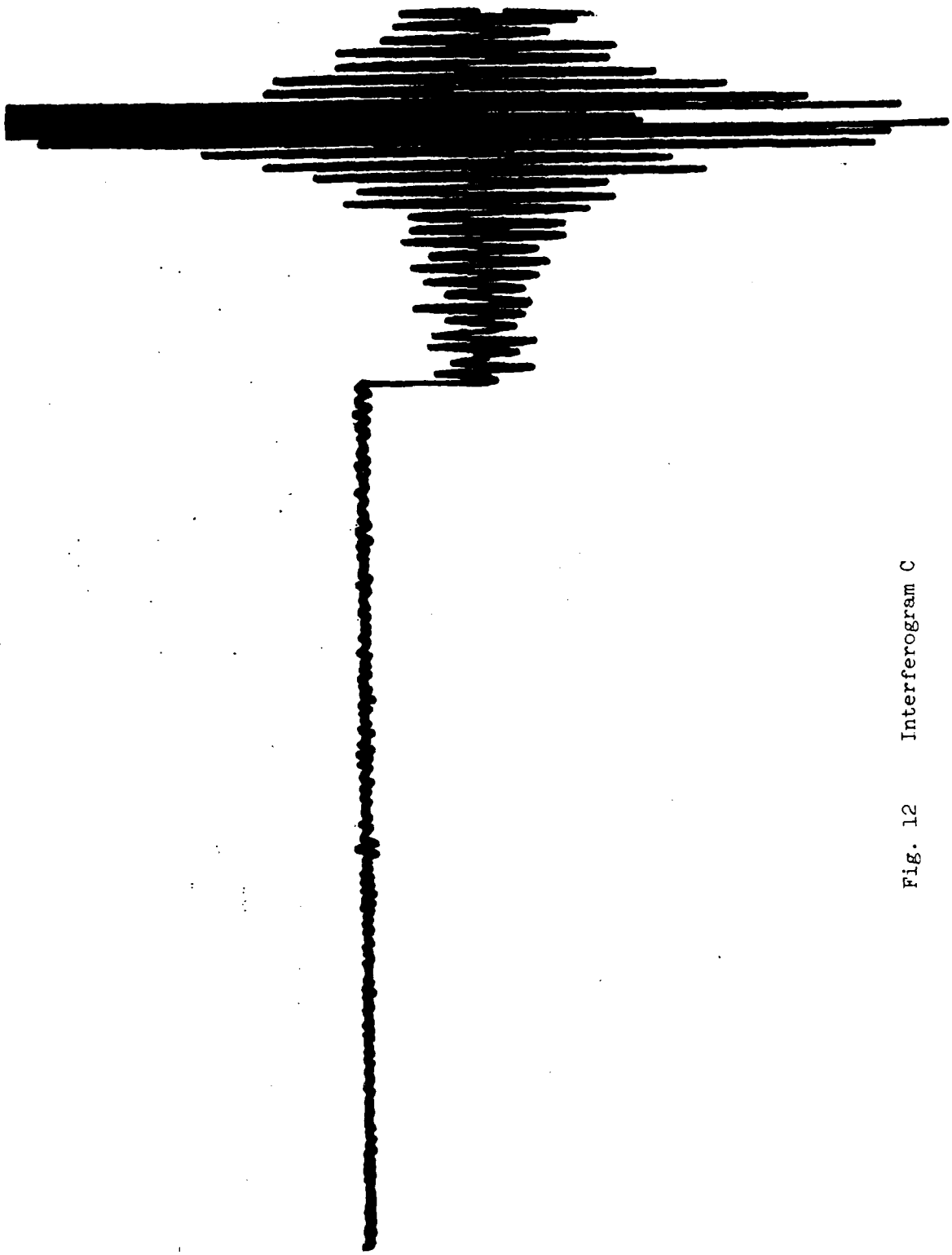


Fig. 12 Interferogram C

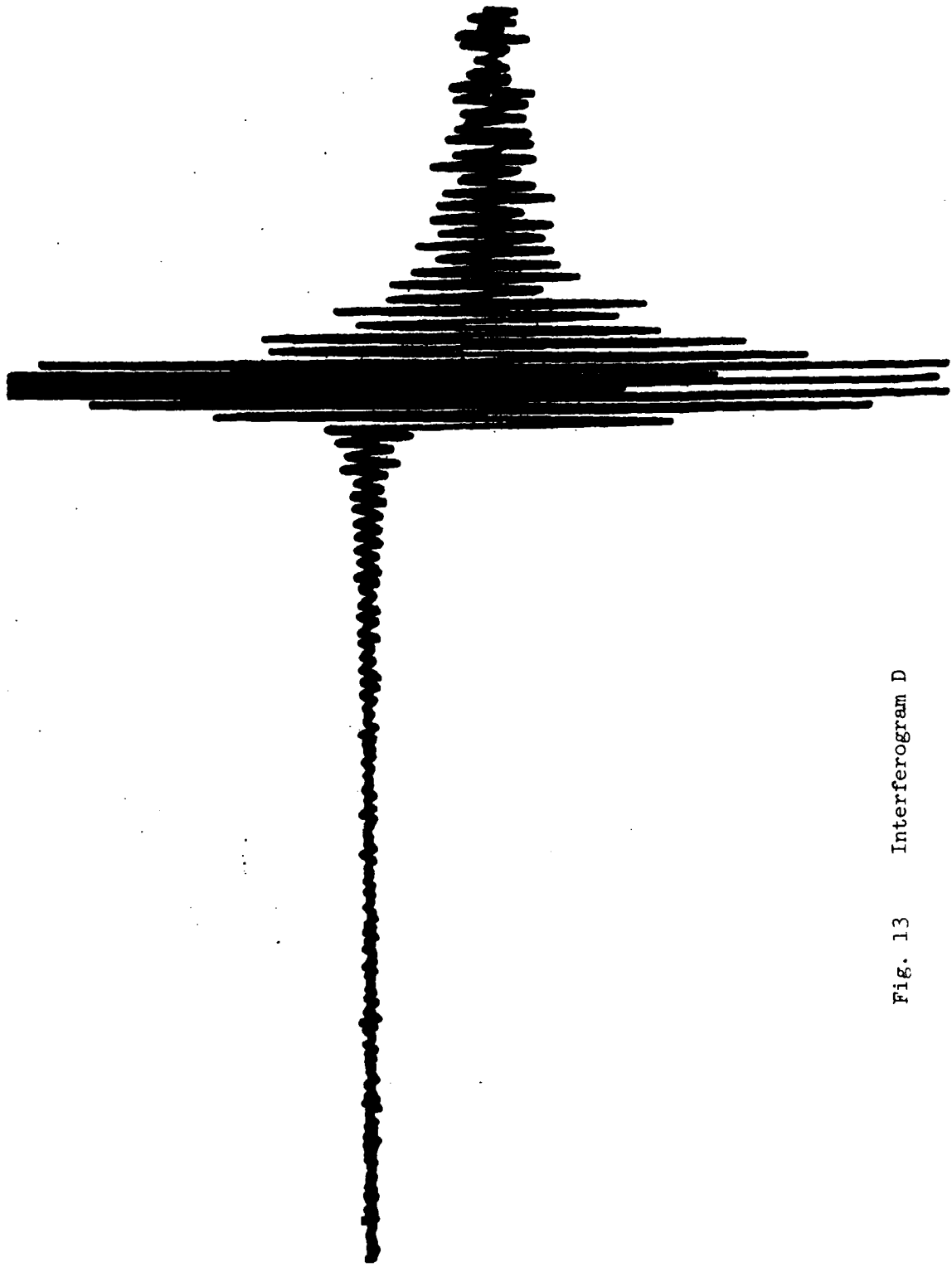


Fig. 13 Interferogram D

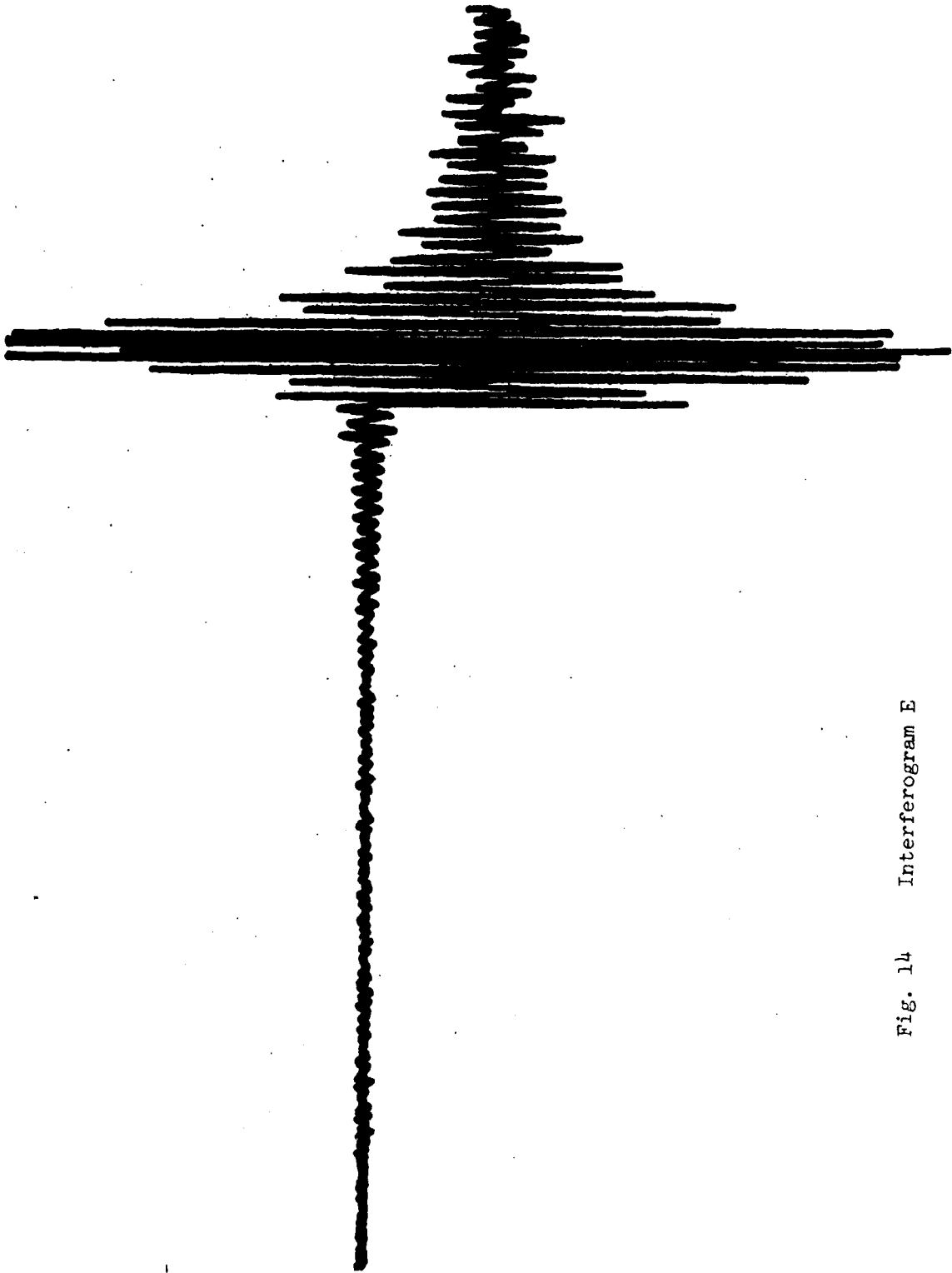


Fig. 14 Interferogram E

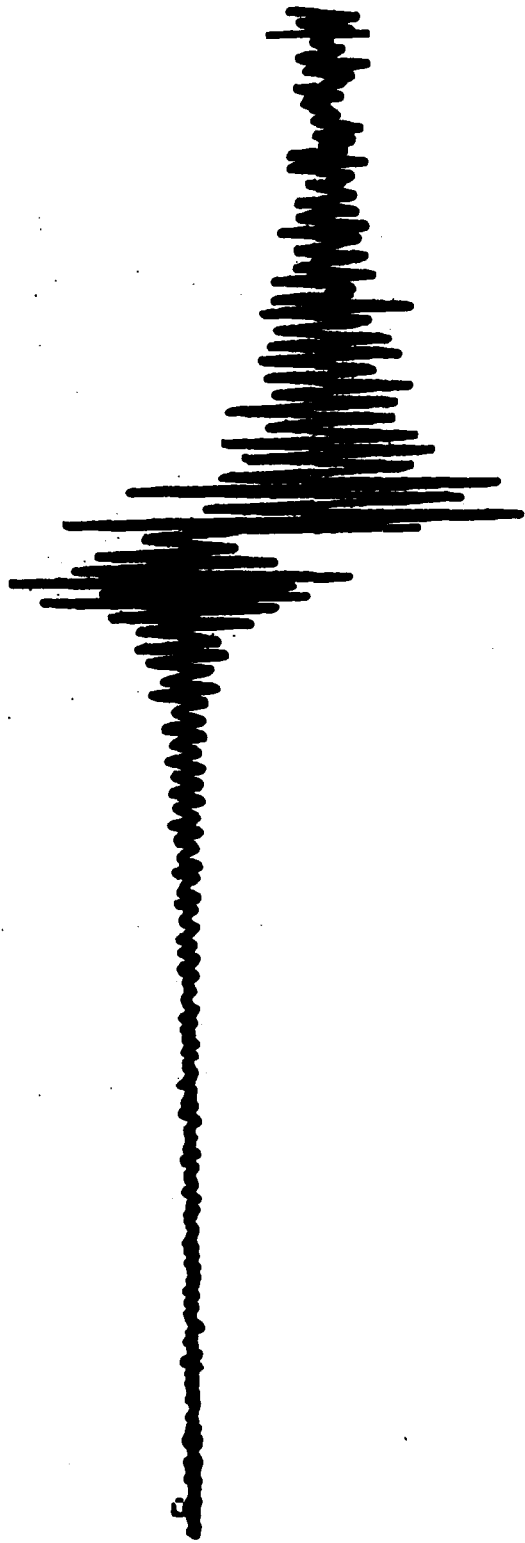


Fig. 15 Interferogram F

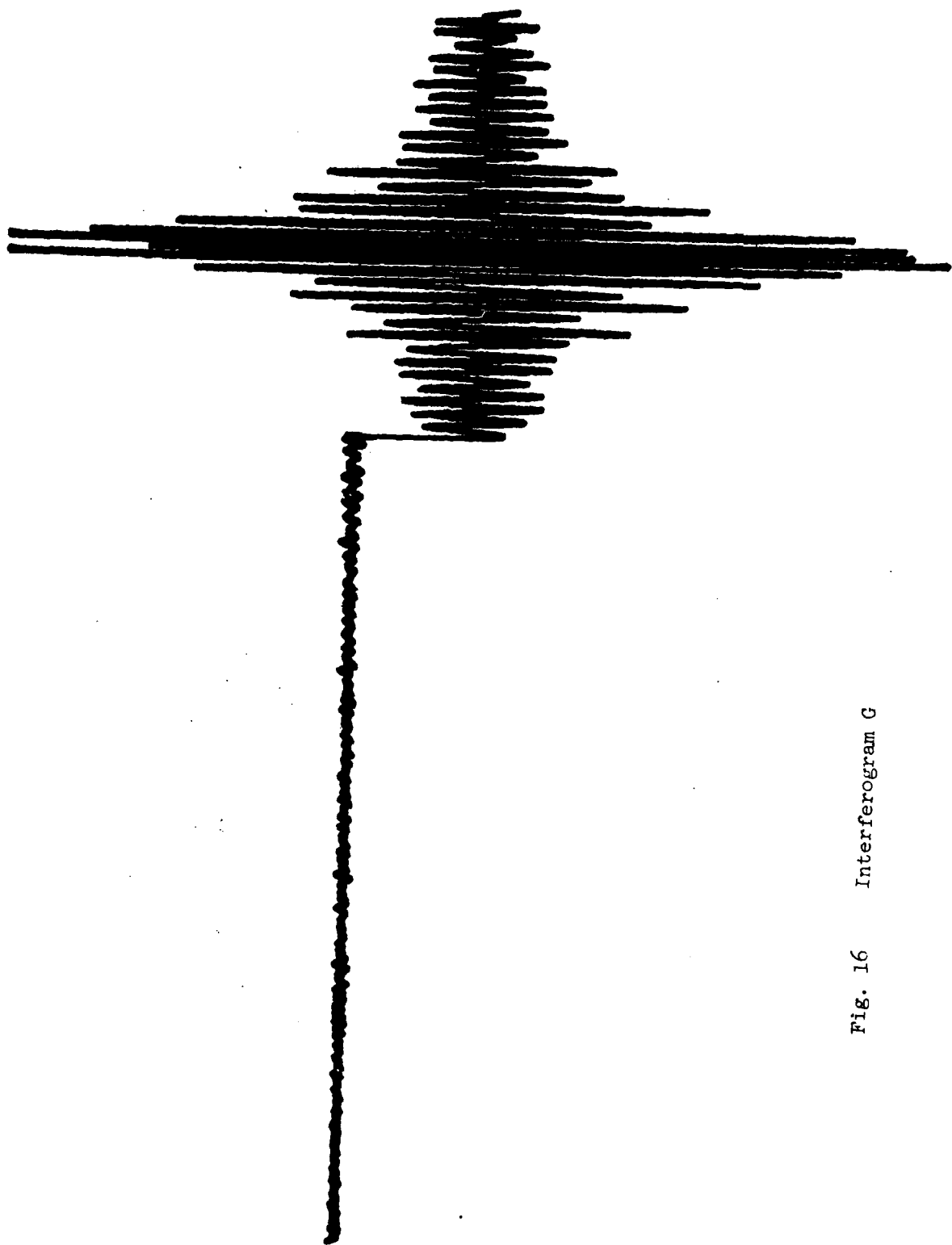


Fig. 16 Interferogram G

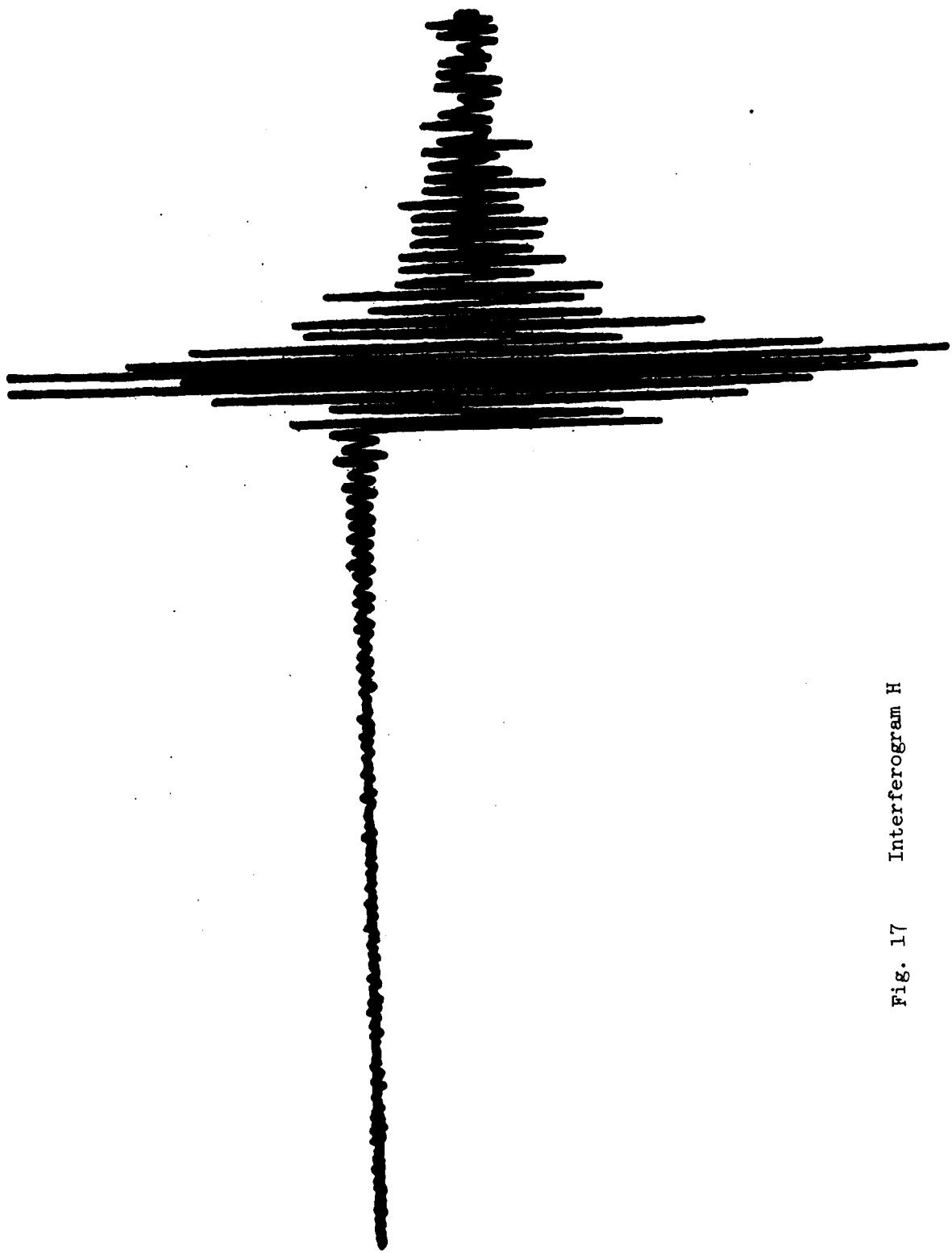


Fig. 17 Interferogram H

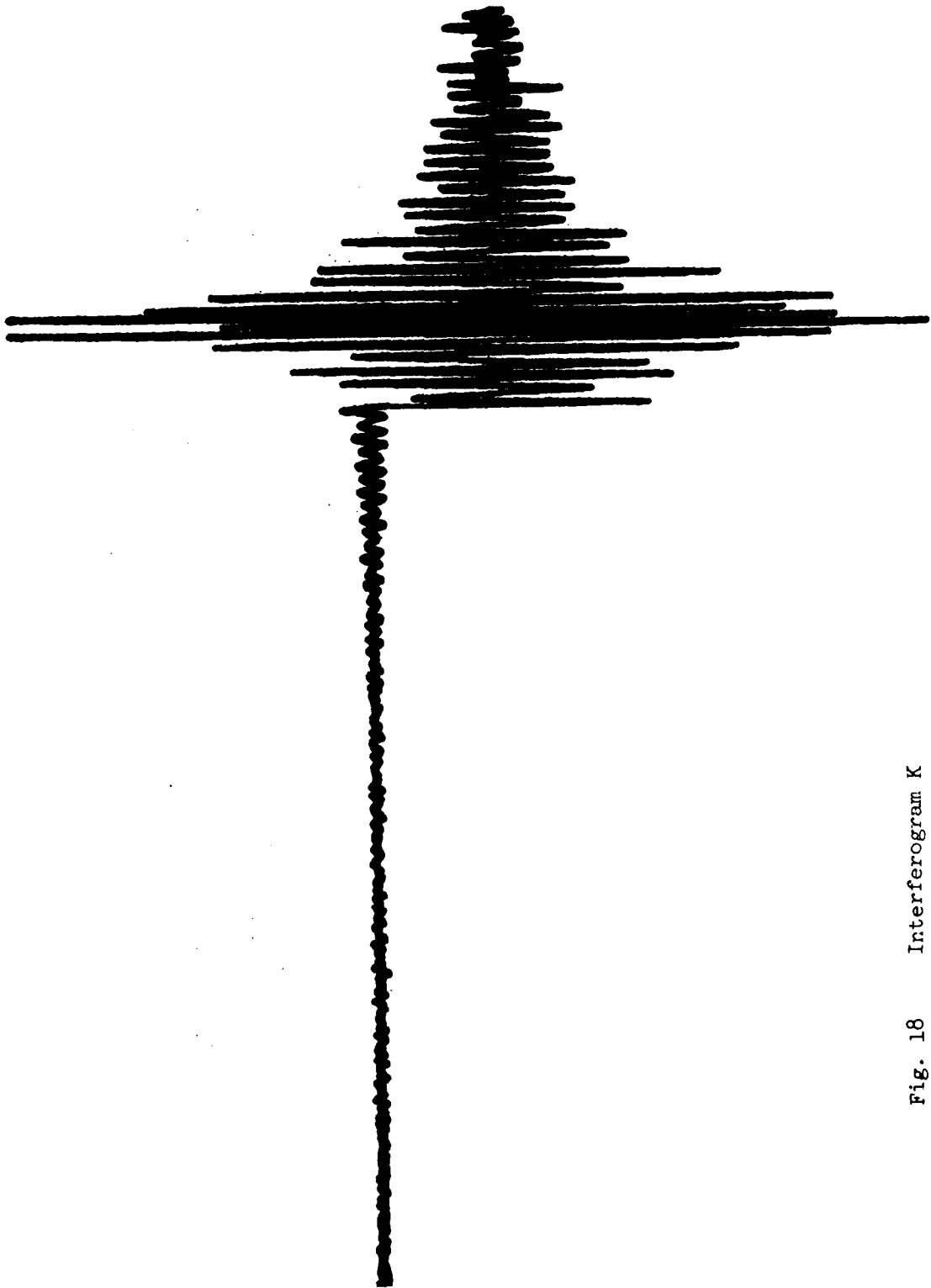


Fig. 18 Interferogram K

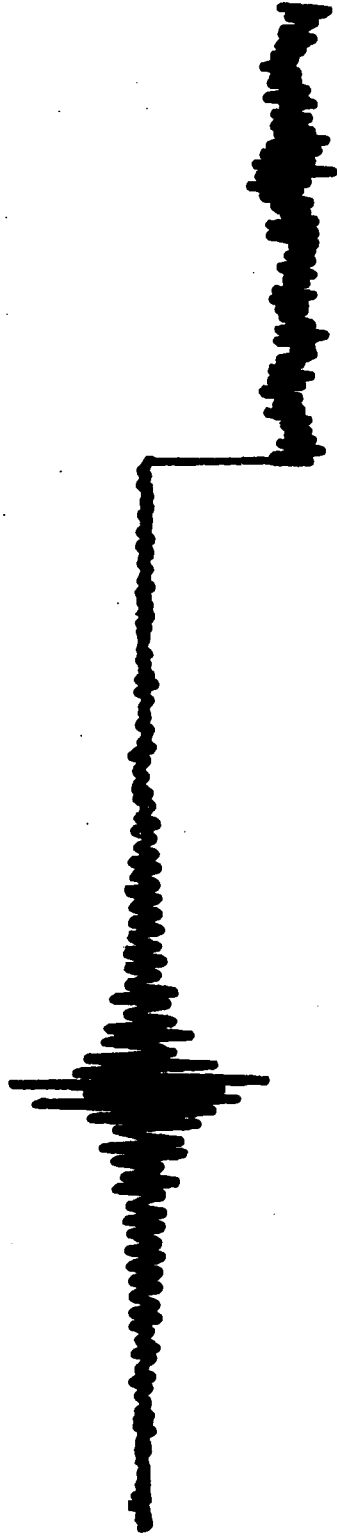


Fig. 19 Interferogram L

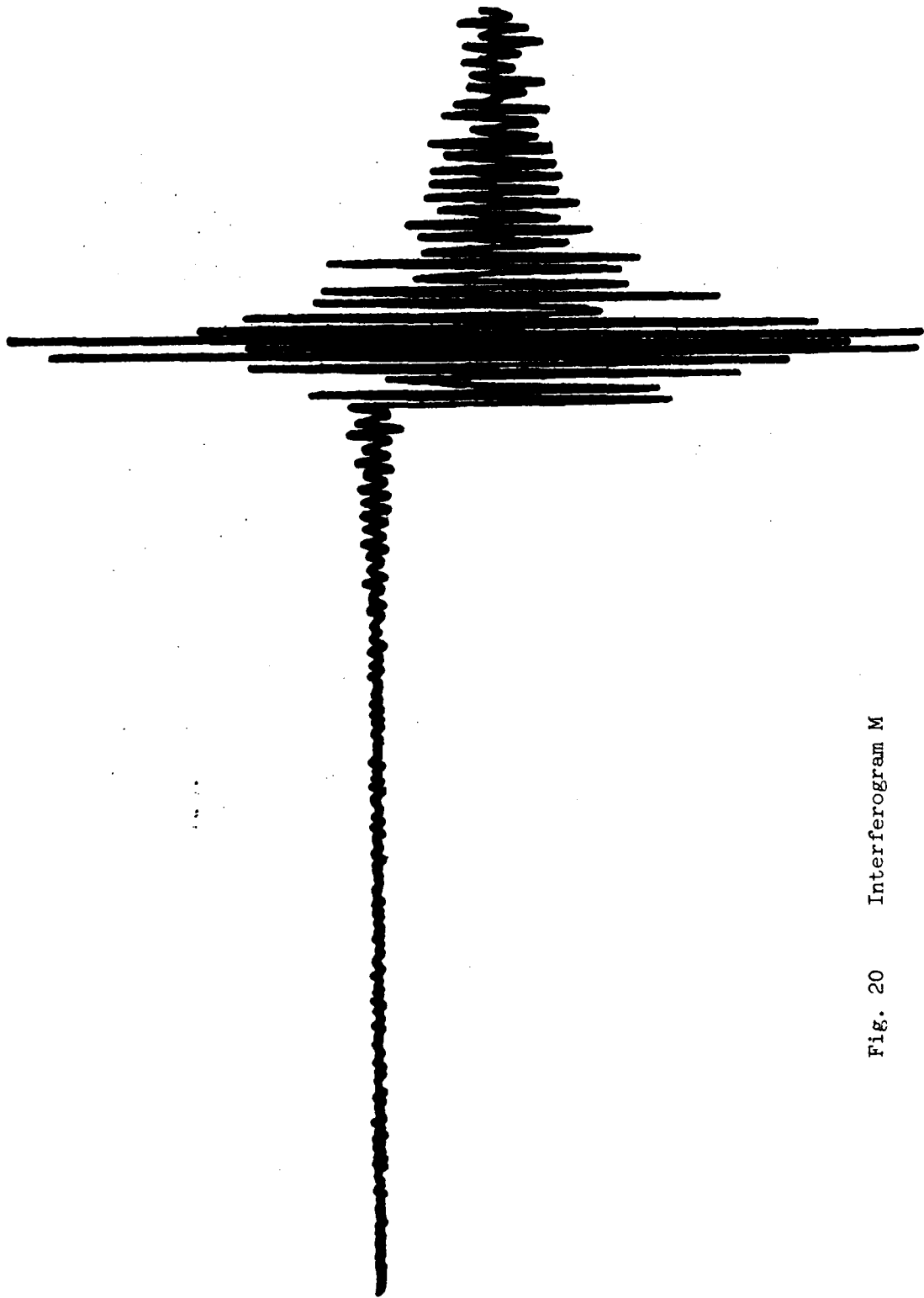


Fig. 20 Interferogram M

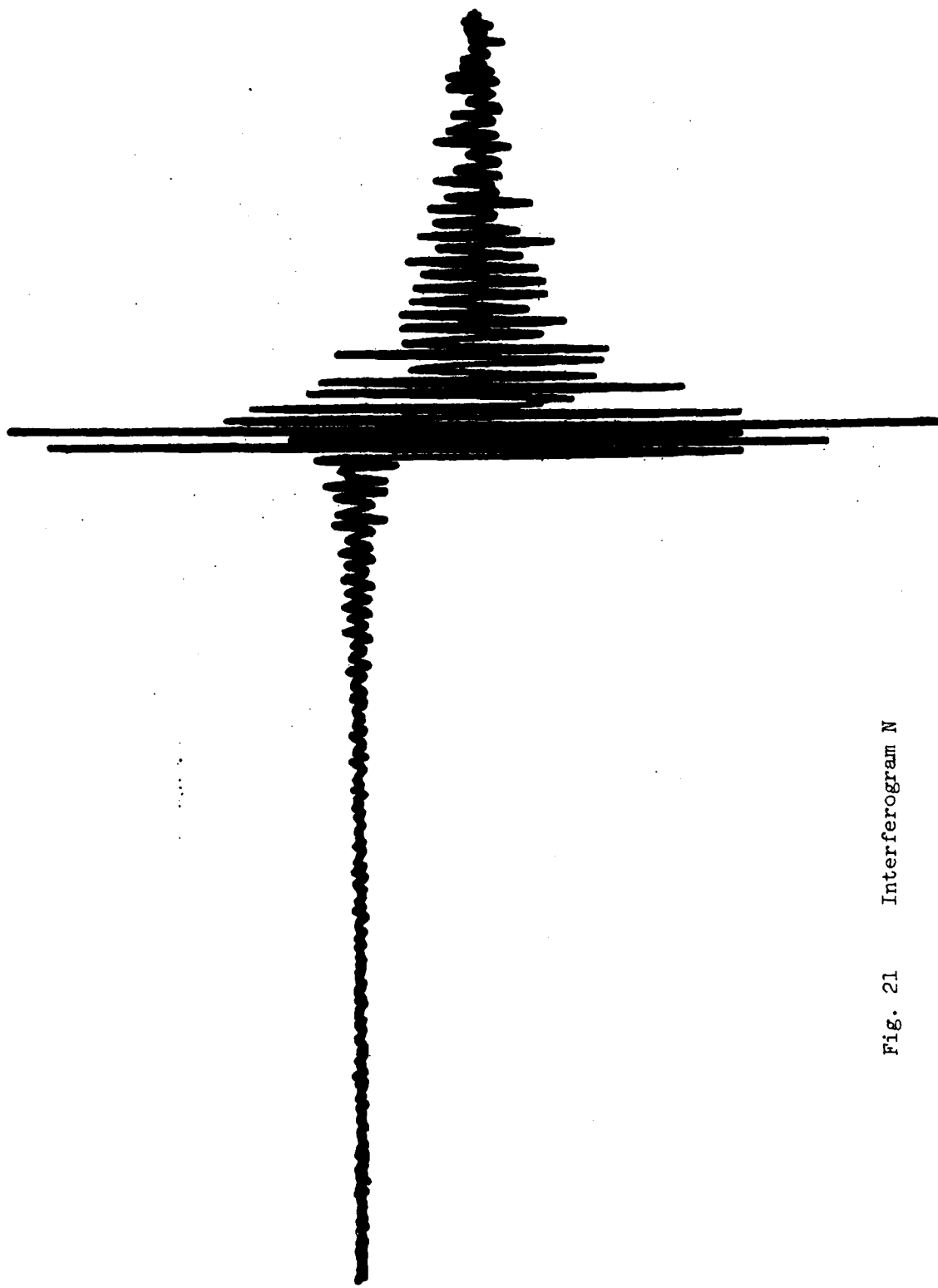


Fig. 21 Interferogram N

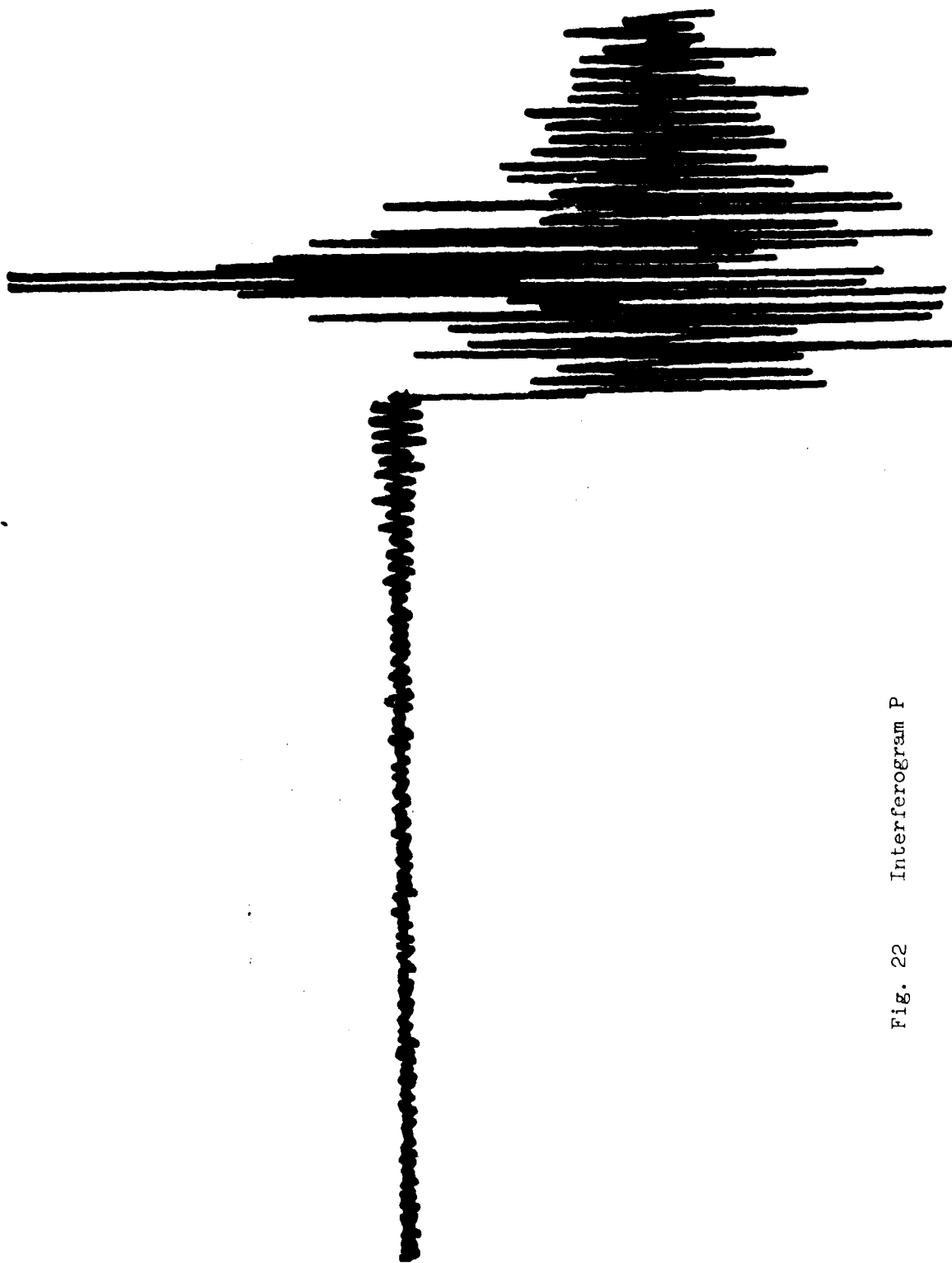


Fig. 22 Interferogram P

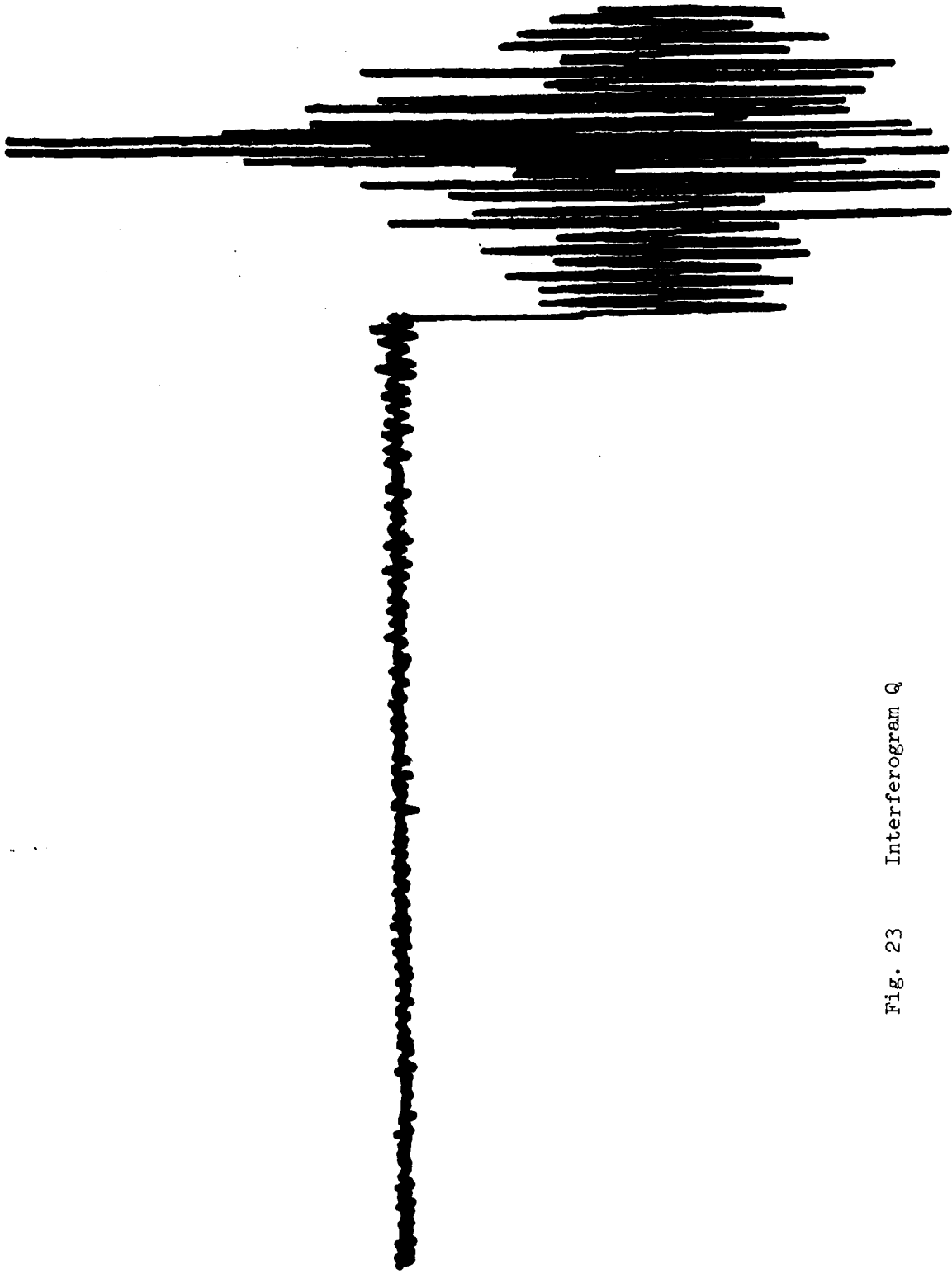


Fig. 23 Interferogram Q

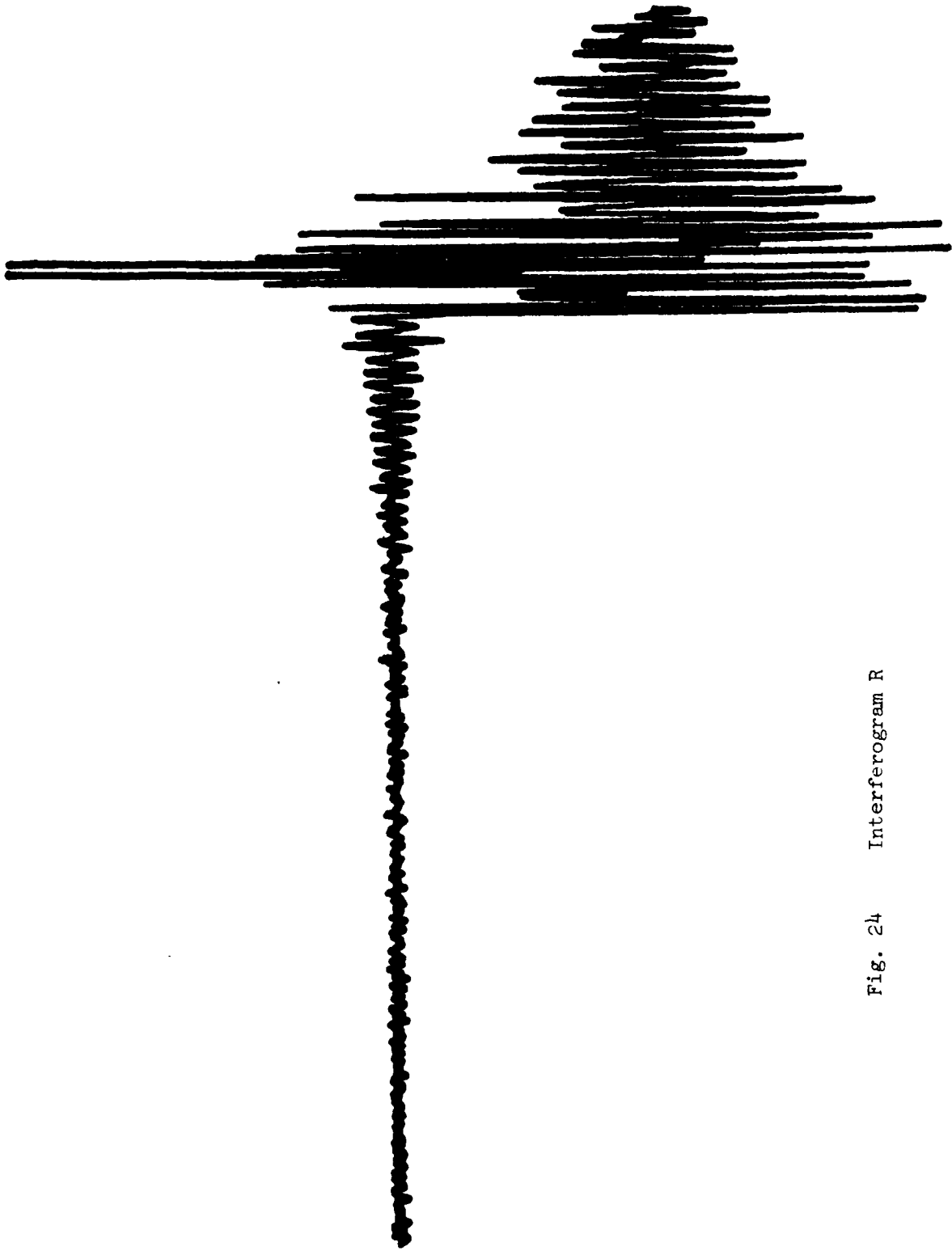


Fig. 24 Interferogram R

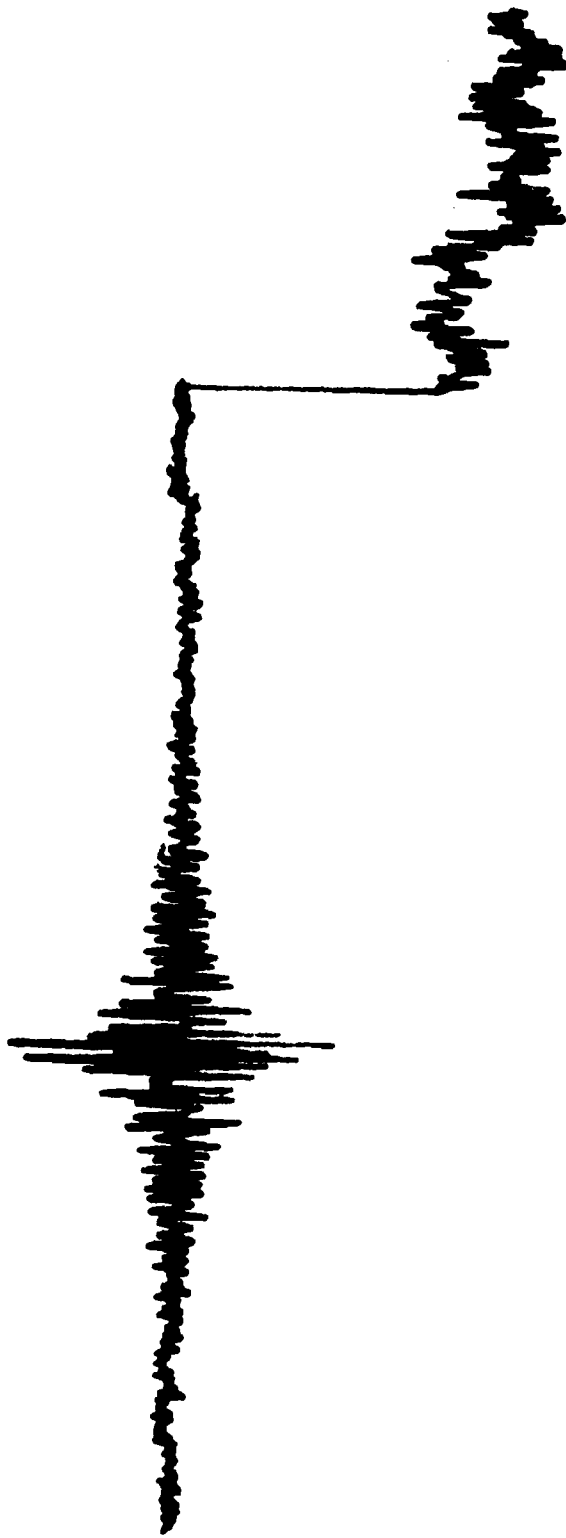


Fig. 25 Interferogram S

Fig. 26 (a) Spectrum A  $500 \text{ cm}^{-1} \sim 1000 \text{ cm}^{-1}$

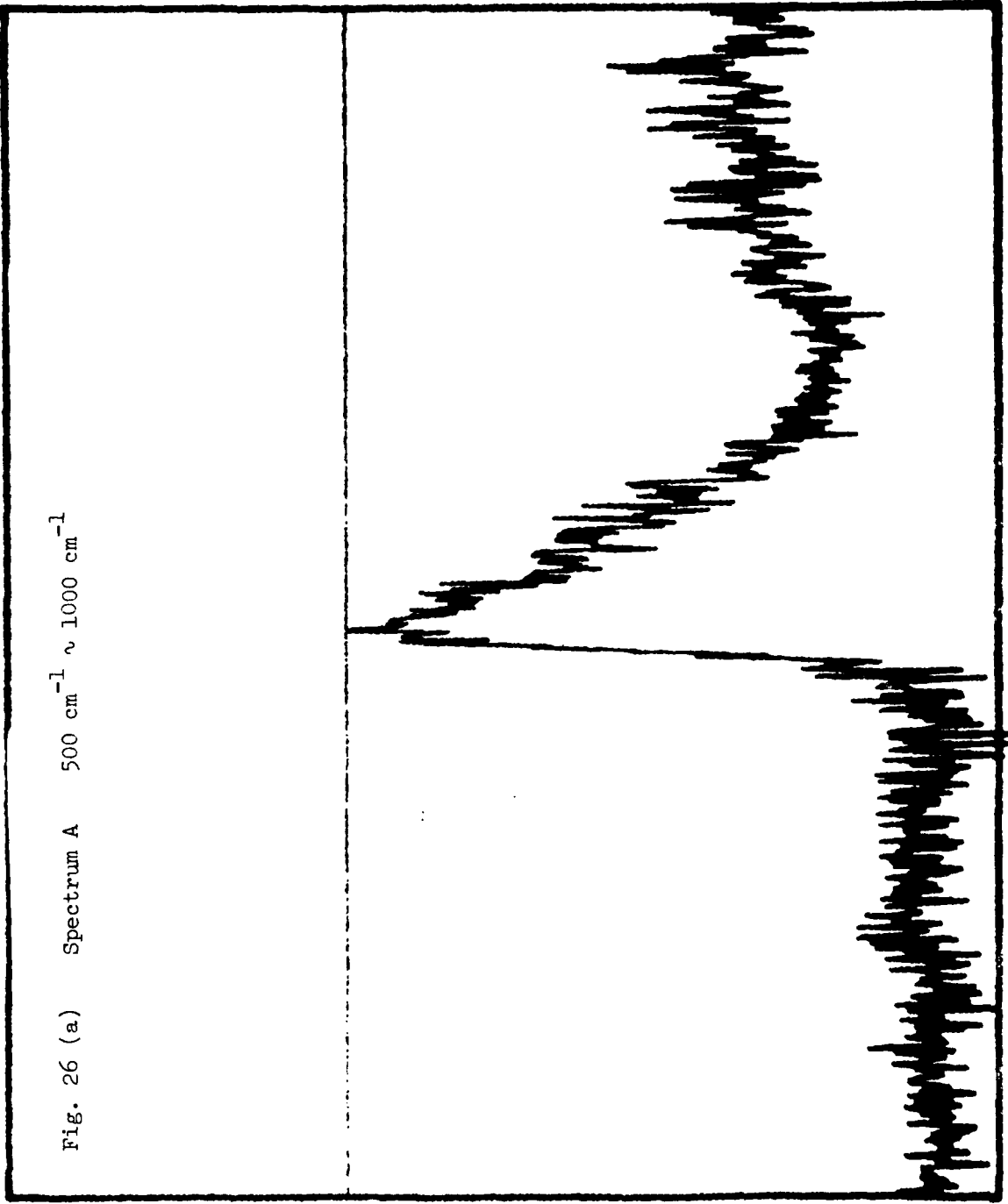


Fig. 26 (b) Spectrum A  $1000\text{ cm}^{-1} \sim 1500\text{ cm}^{-1}$

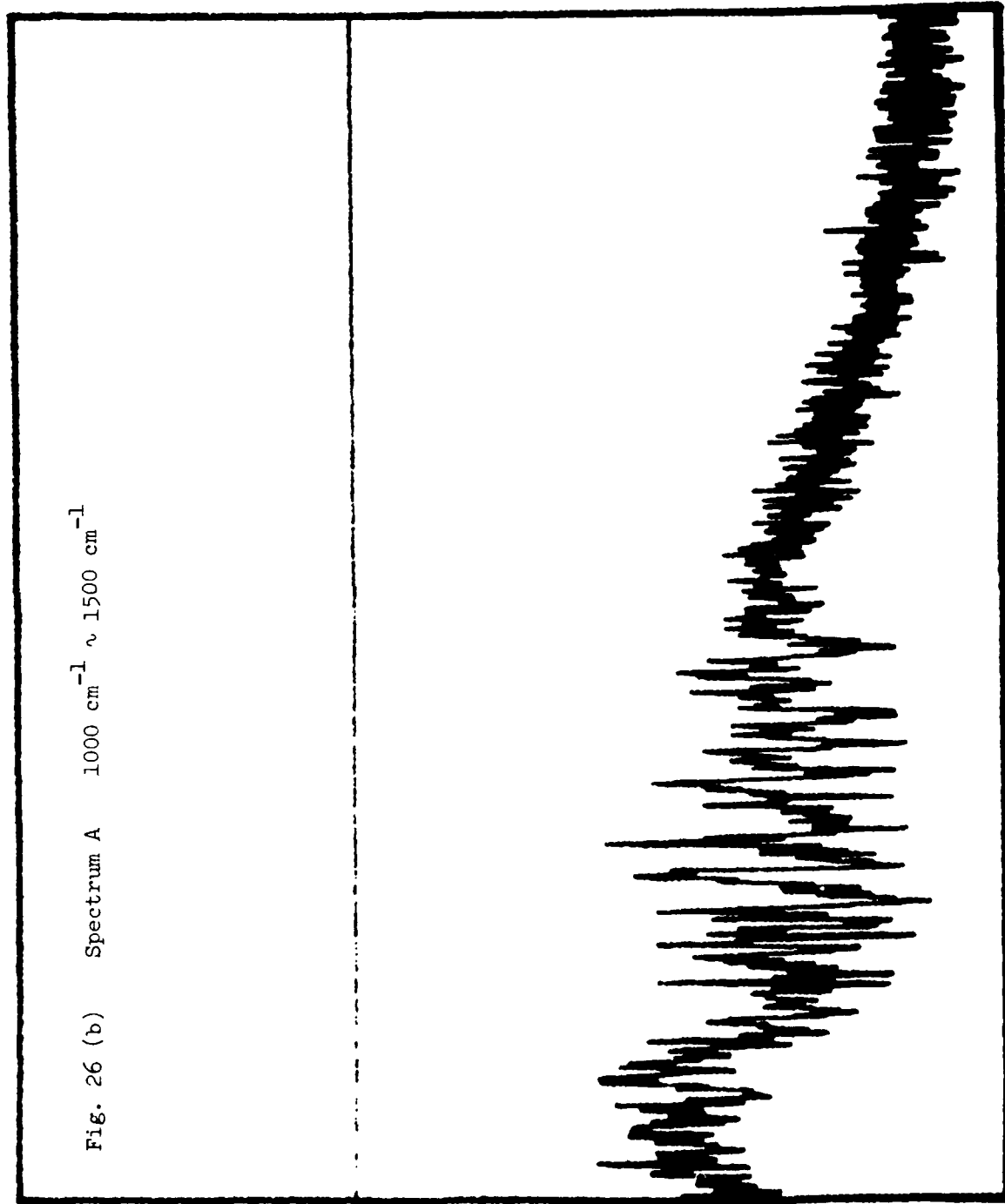


Fig. 27 (a) Spectrum B  $500\text{ cm}^{-1} \sim 1000\text{ cm}^{-1}$

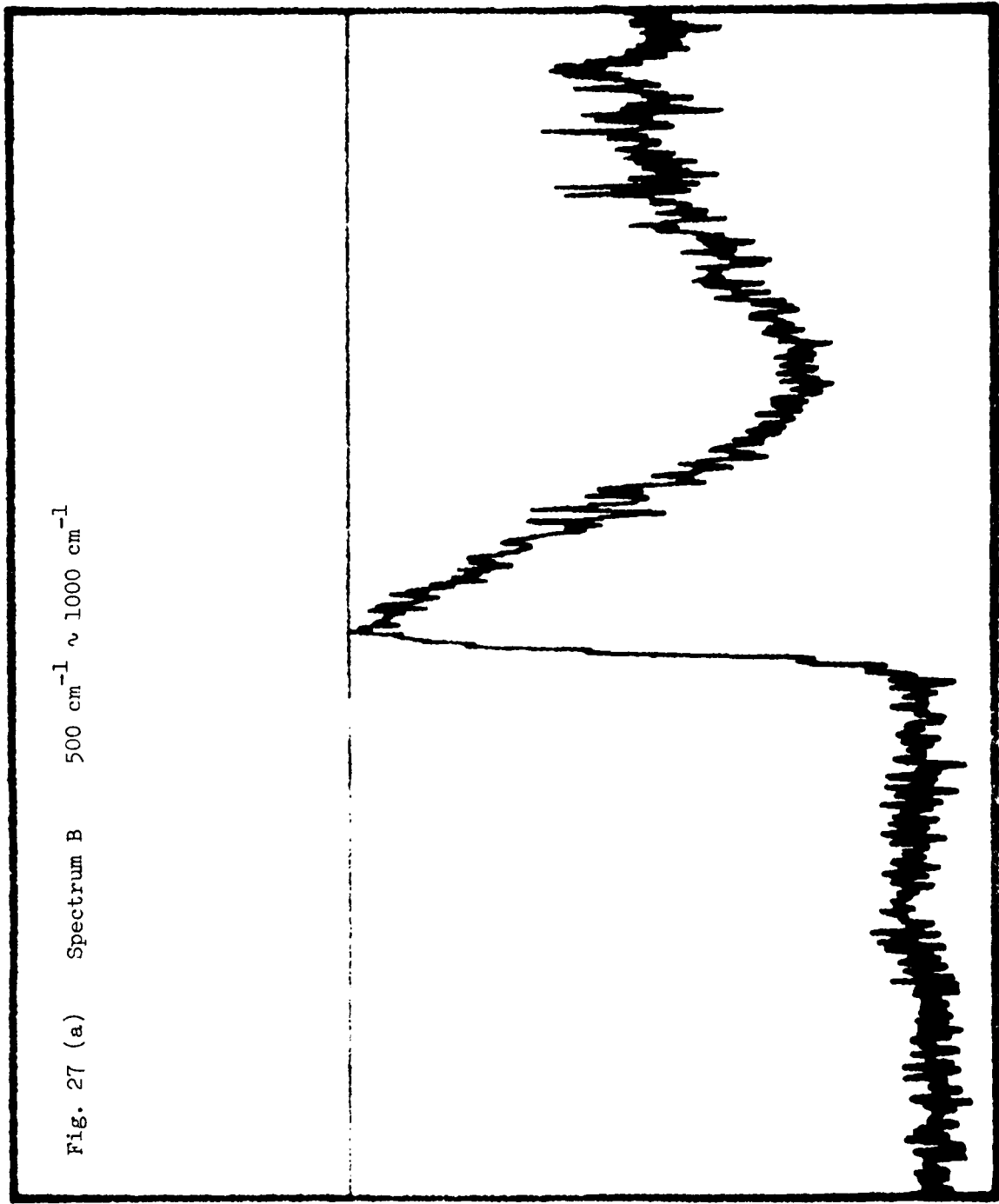


Fig. 27 (b) Spectrum B  $1000\text{ cm}^{-1} \sim 1500\text{ cm}^{-1}$

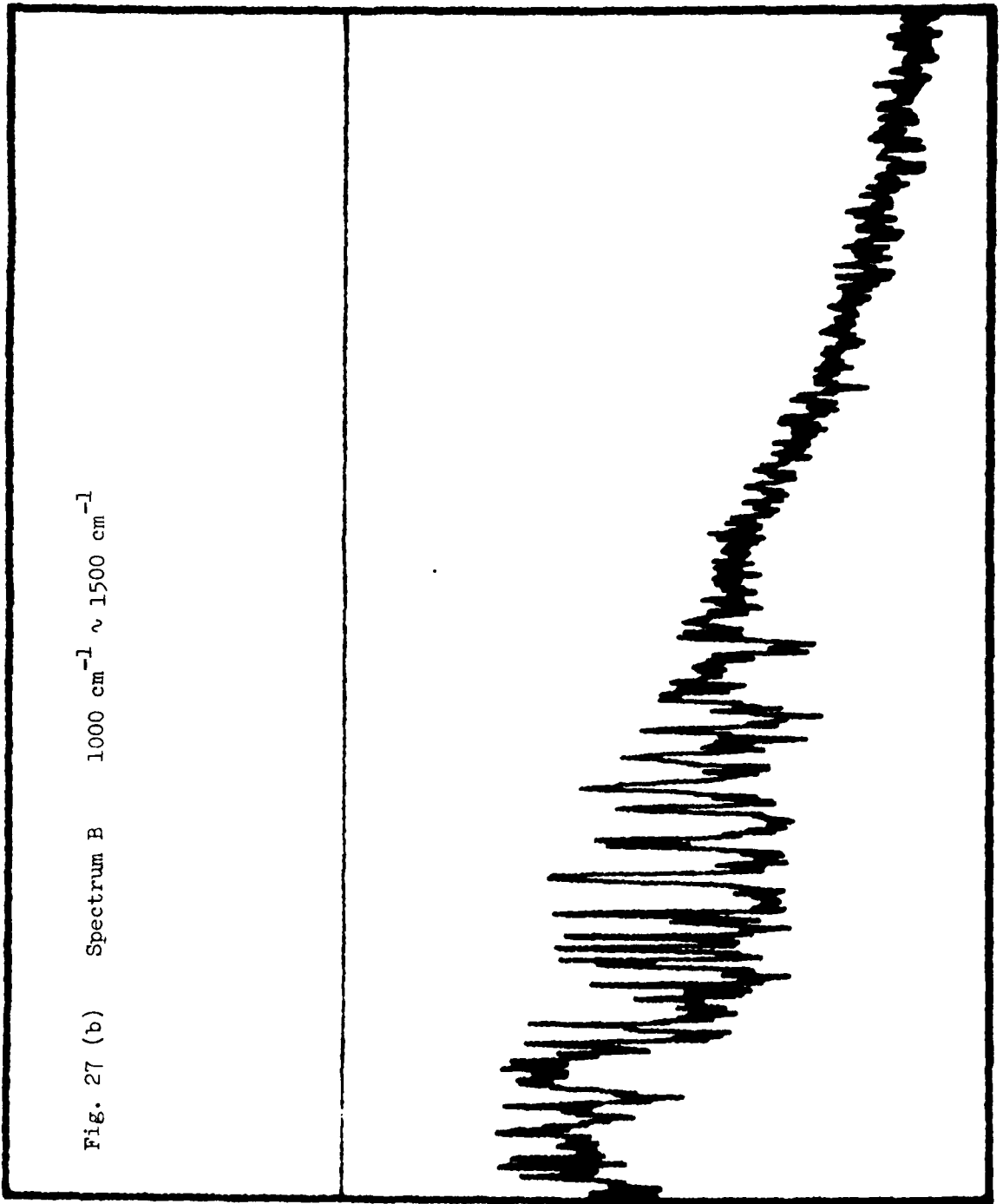


Fig. 28 (a) Spectrum C  $500 \text{ cm}^{-1} \sim 1000 \text{ cm}^{-1}$

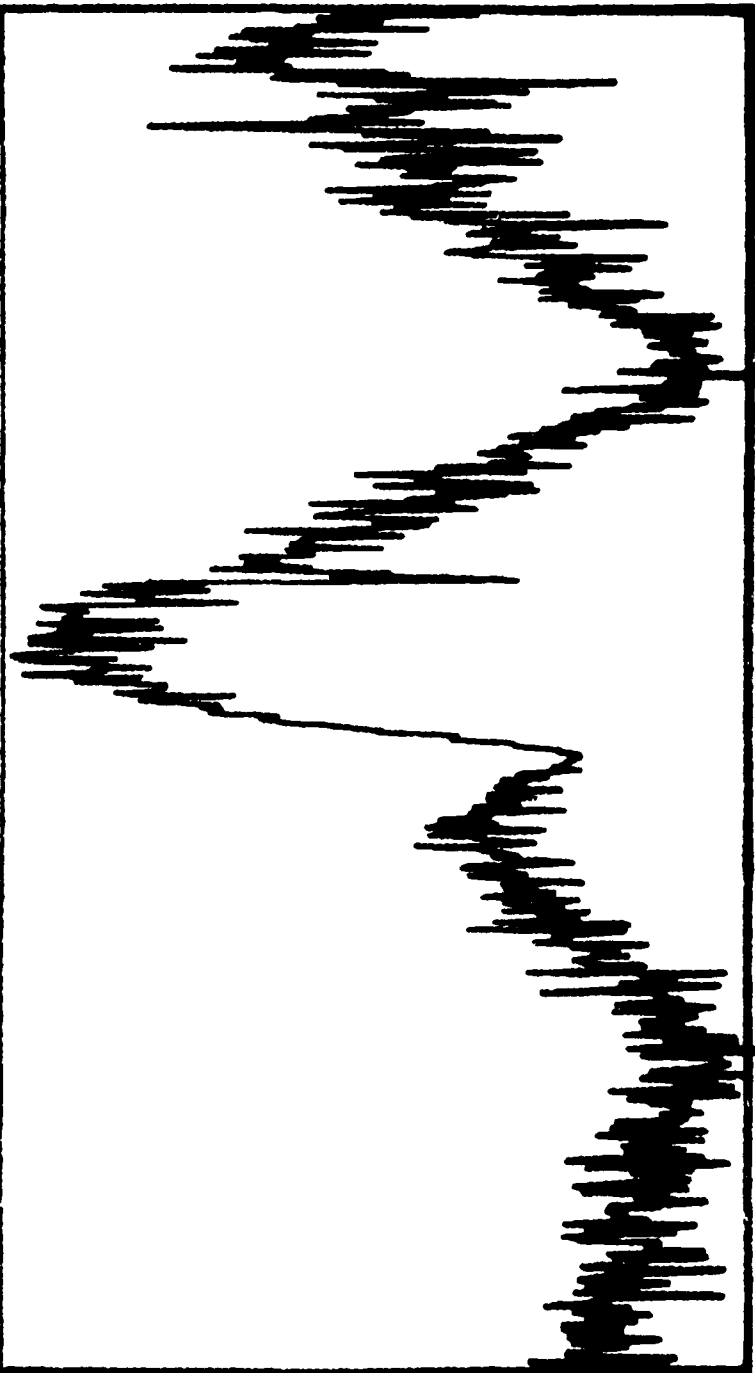


Fig. 28 (b) Spectrum C  $1000\text{ cm}^{-1} \sim 1500\text{ cm}^{-1}$

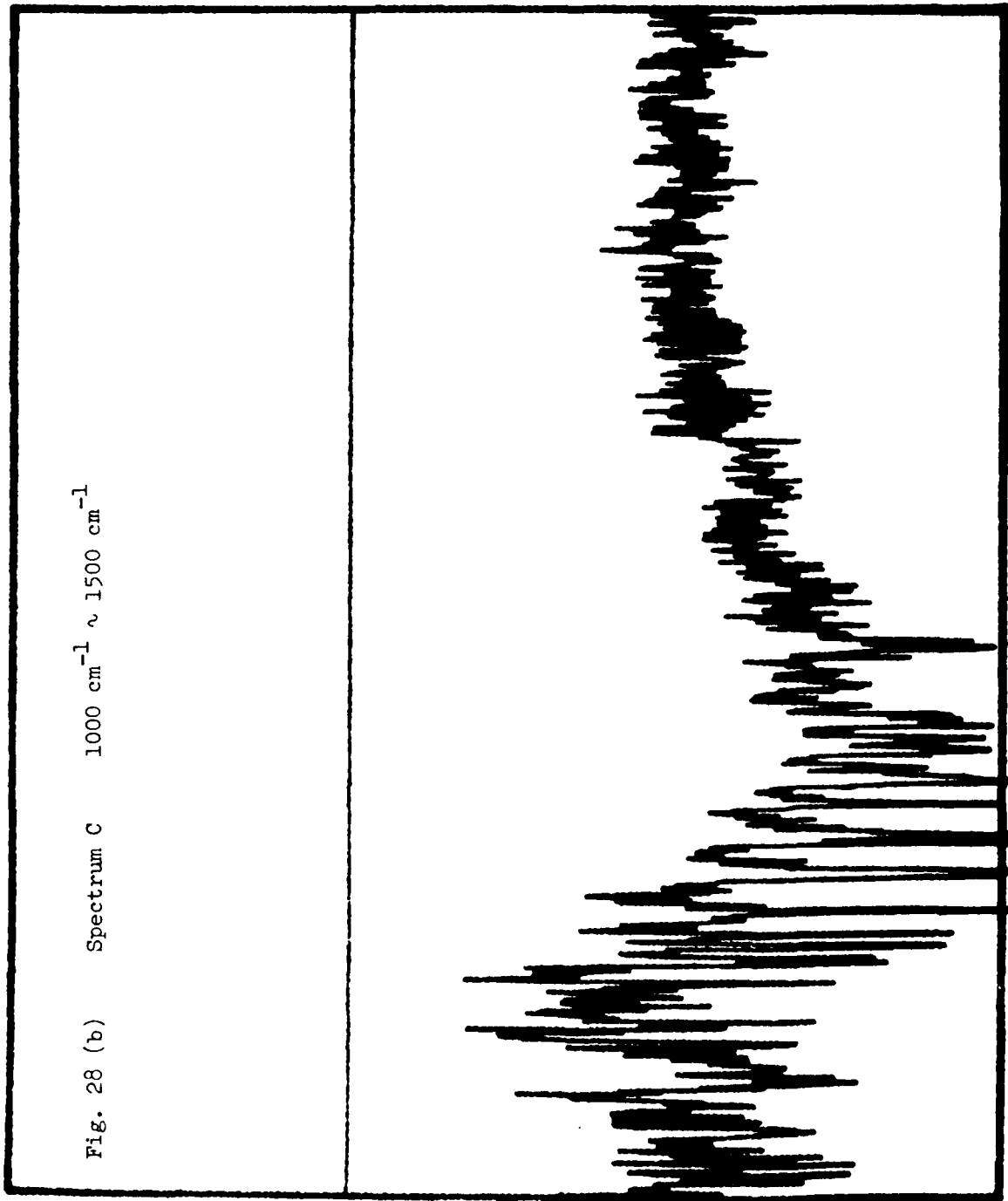


Fig. 29 (a) Spectrum D  $500 \text{ cm}^{-1} \sim 1000 \text{ cm}^{-1}$

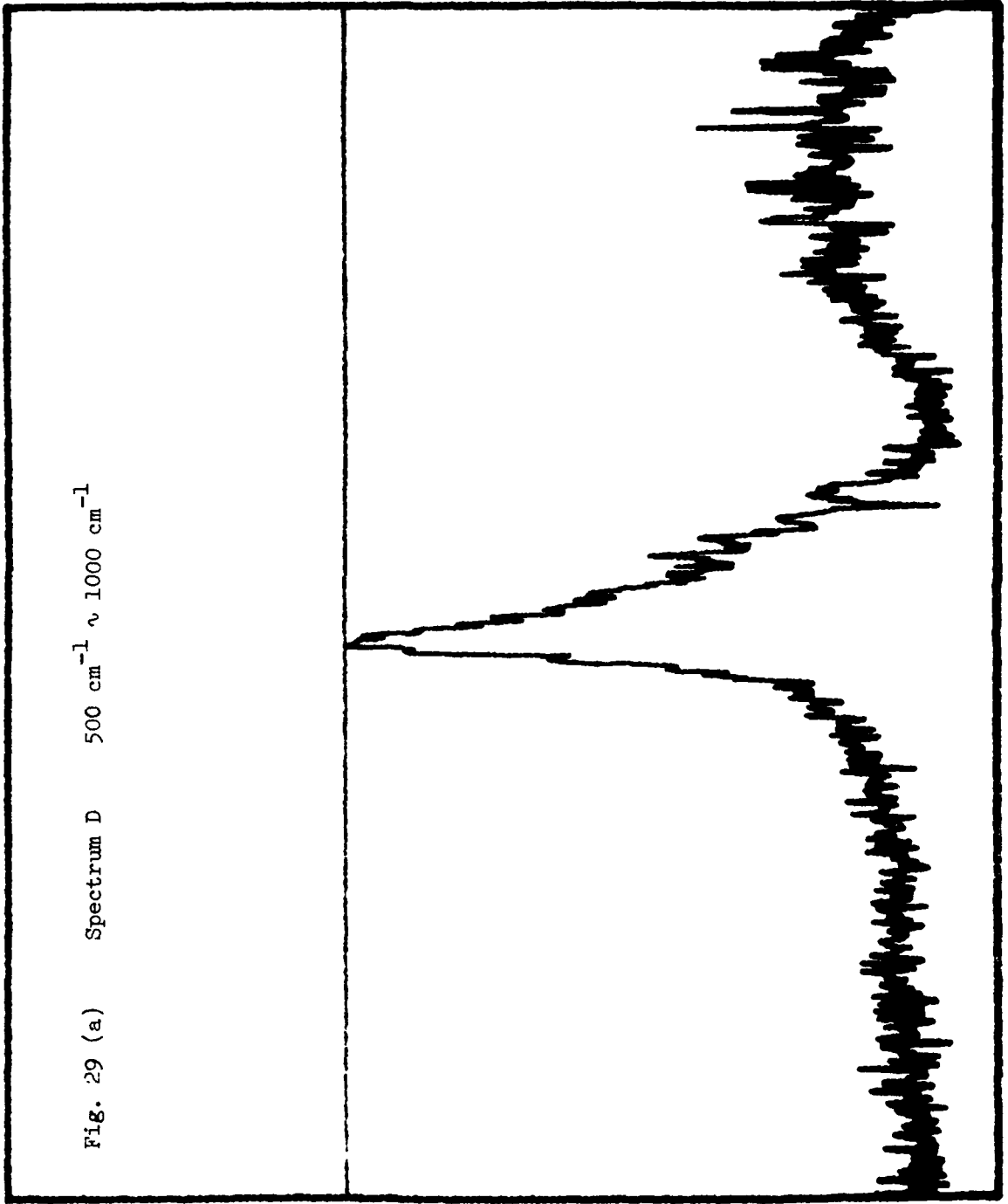


Fig. 29 (b) Spectrum D  $1000\text{ cm}^{-1} \sim 1500\text{ cm}^{-1}$

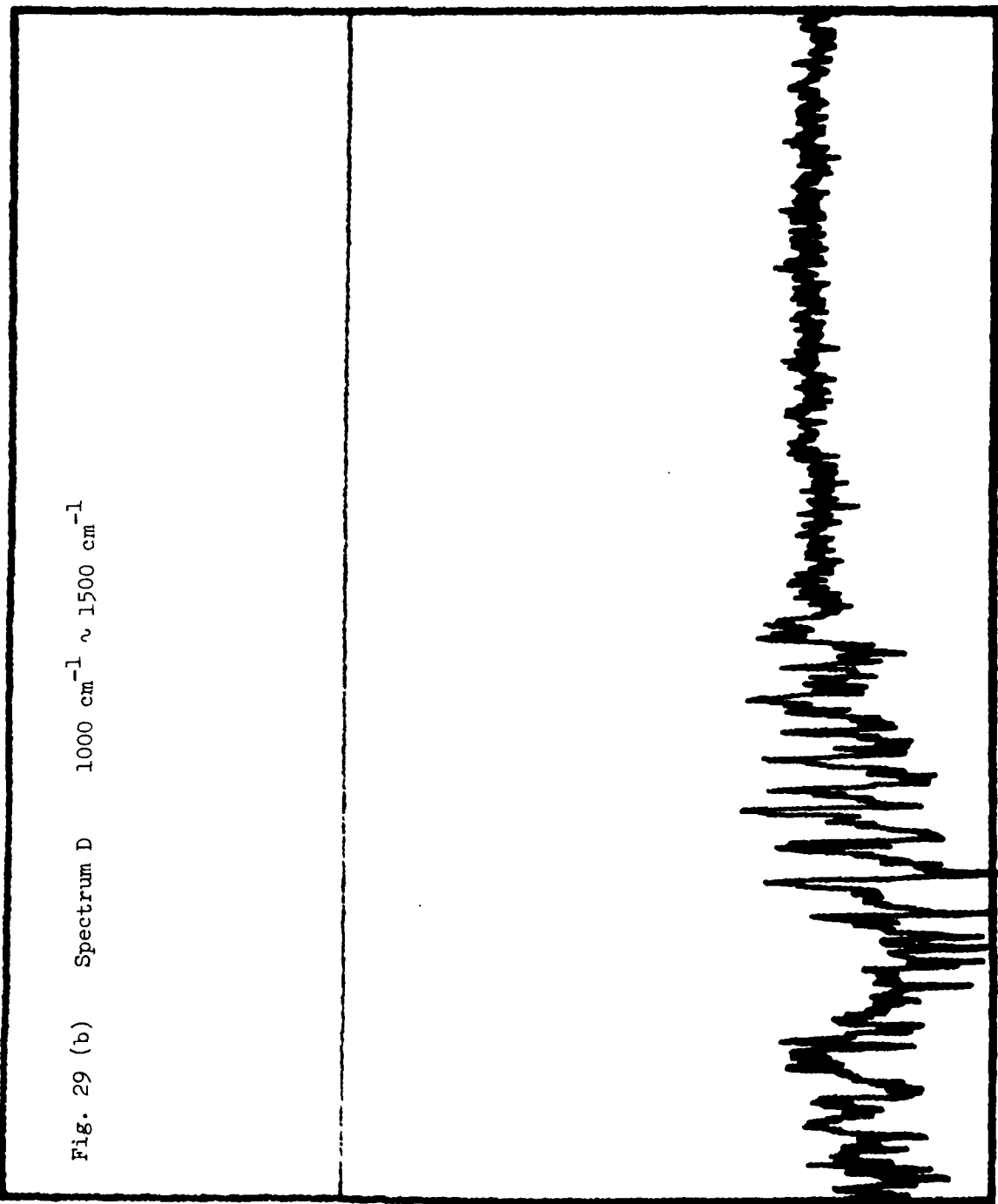


Fig. 30 (a) Spectrum E  $500 \text{ cm}^{-1} \sim 1000 \text{ cm}^{-1}$

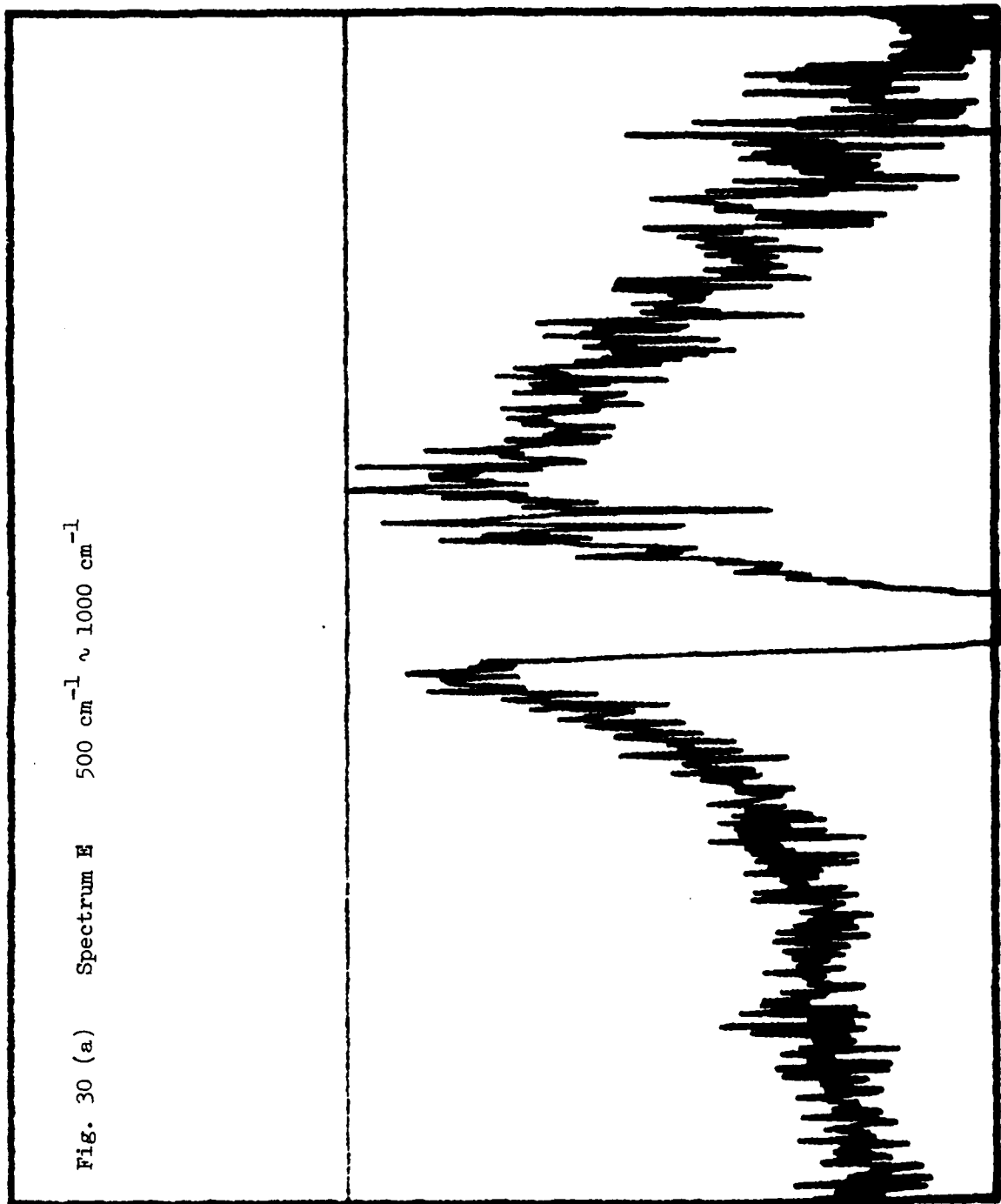


Fig. 30 (b) Spectrum E  $1000\text{ cm}^{-1} \sim 1500\text{ cm}^{-1}$

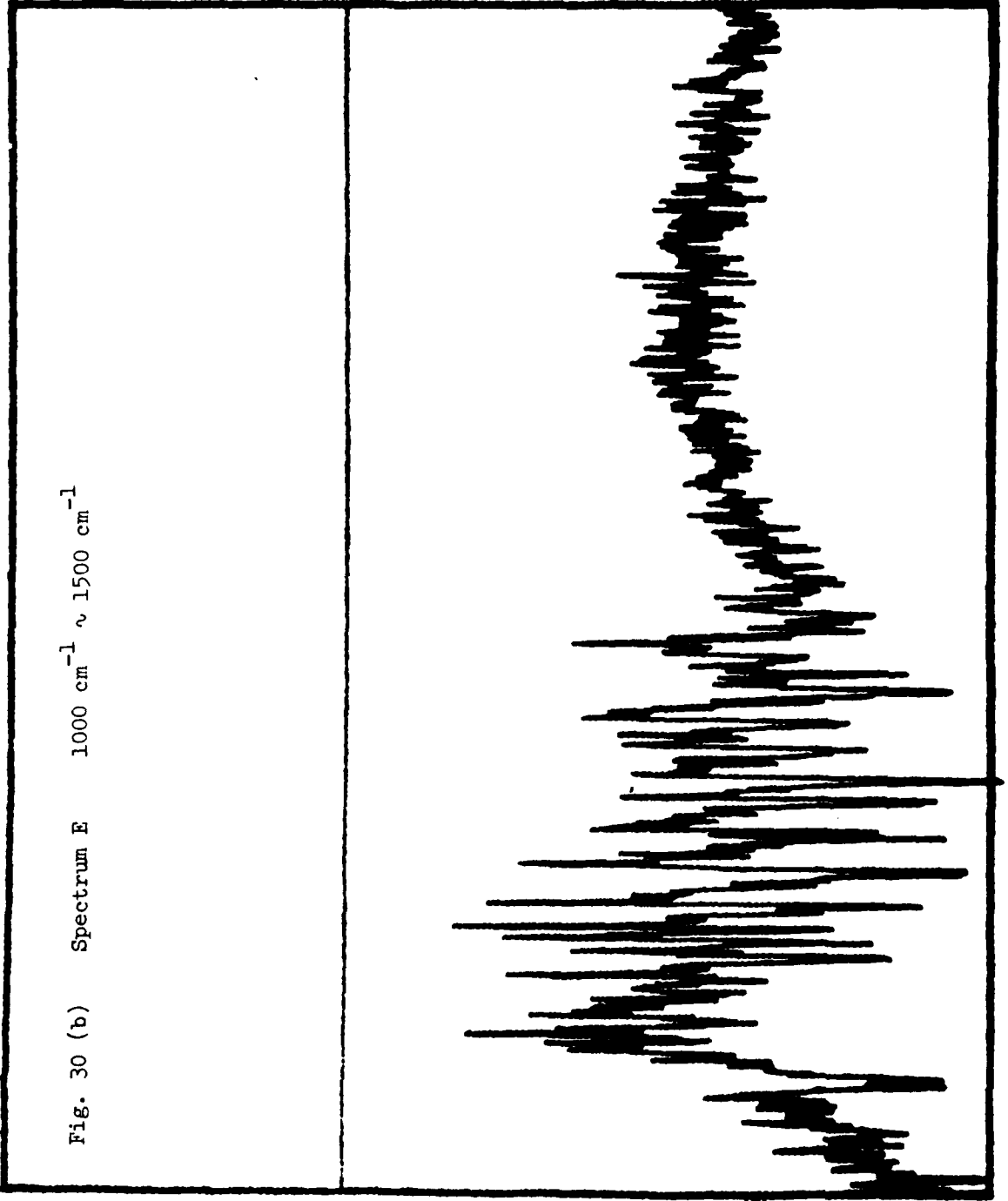


Fig. 31 (a) Spectrum G  $500\text{ cm}^{-1} \sim 1000\text{ cm}^{-1}$

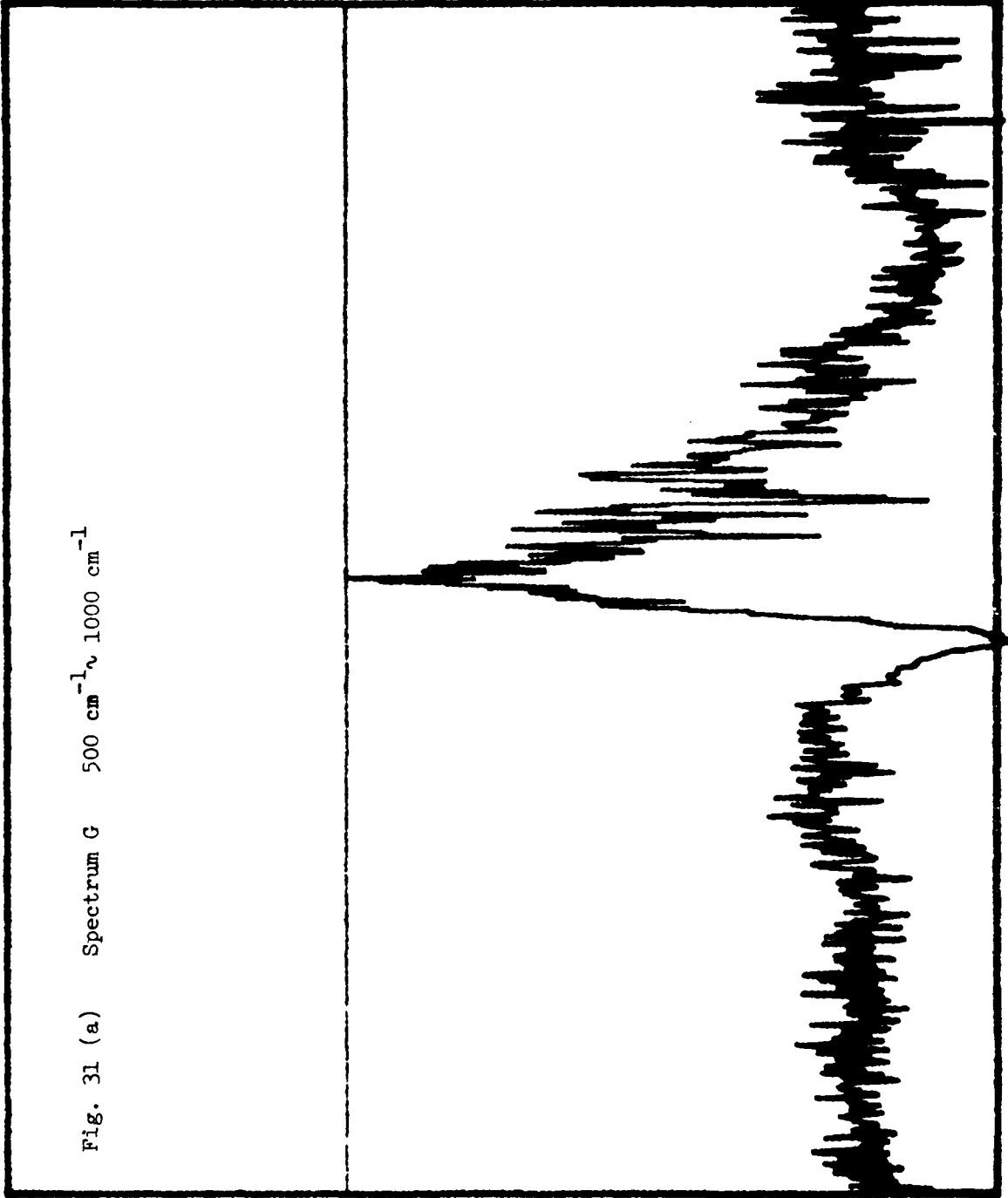


Fig. 31 (b) Spectrum G  $1000\text{ cm}^{-1} \sim 1500\text{ cm}^{-1}$

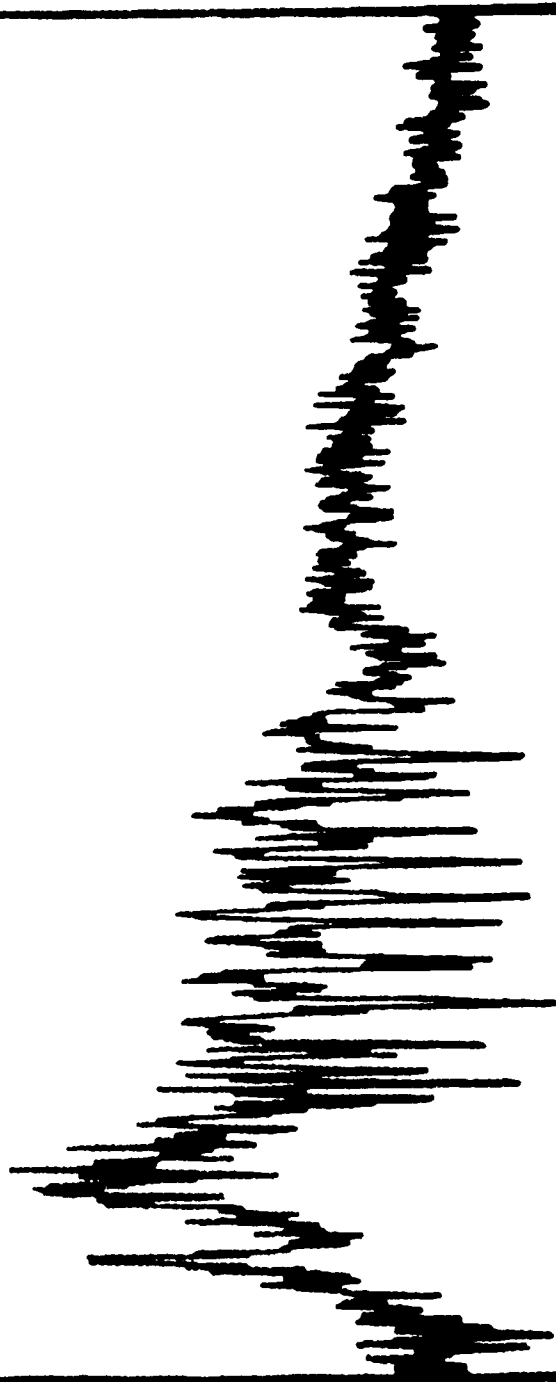


Fig. 32 (a) Spectrum H  $500 \text{ cm}^{-1} \sim 1000 \text{ cm}^{-1}$

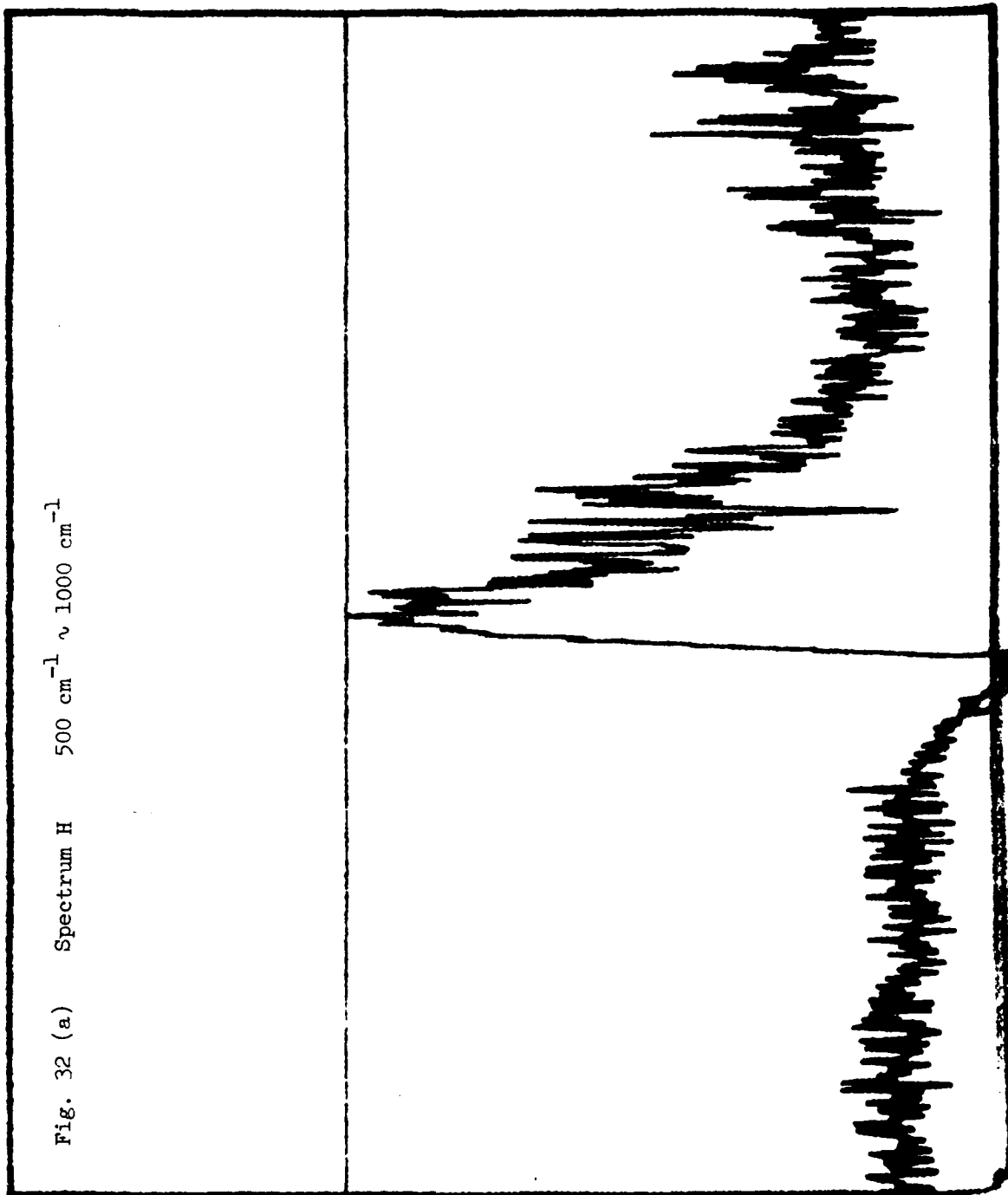


Fig. 32 (b) Spectrum H  $1000\text{ cm}^{-1} \sim 1500\text{ cm}^{-1}$

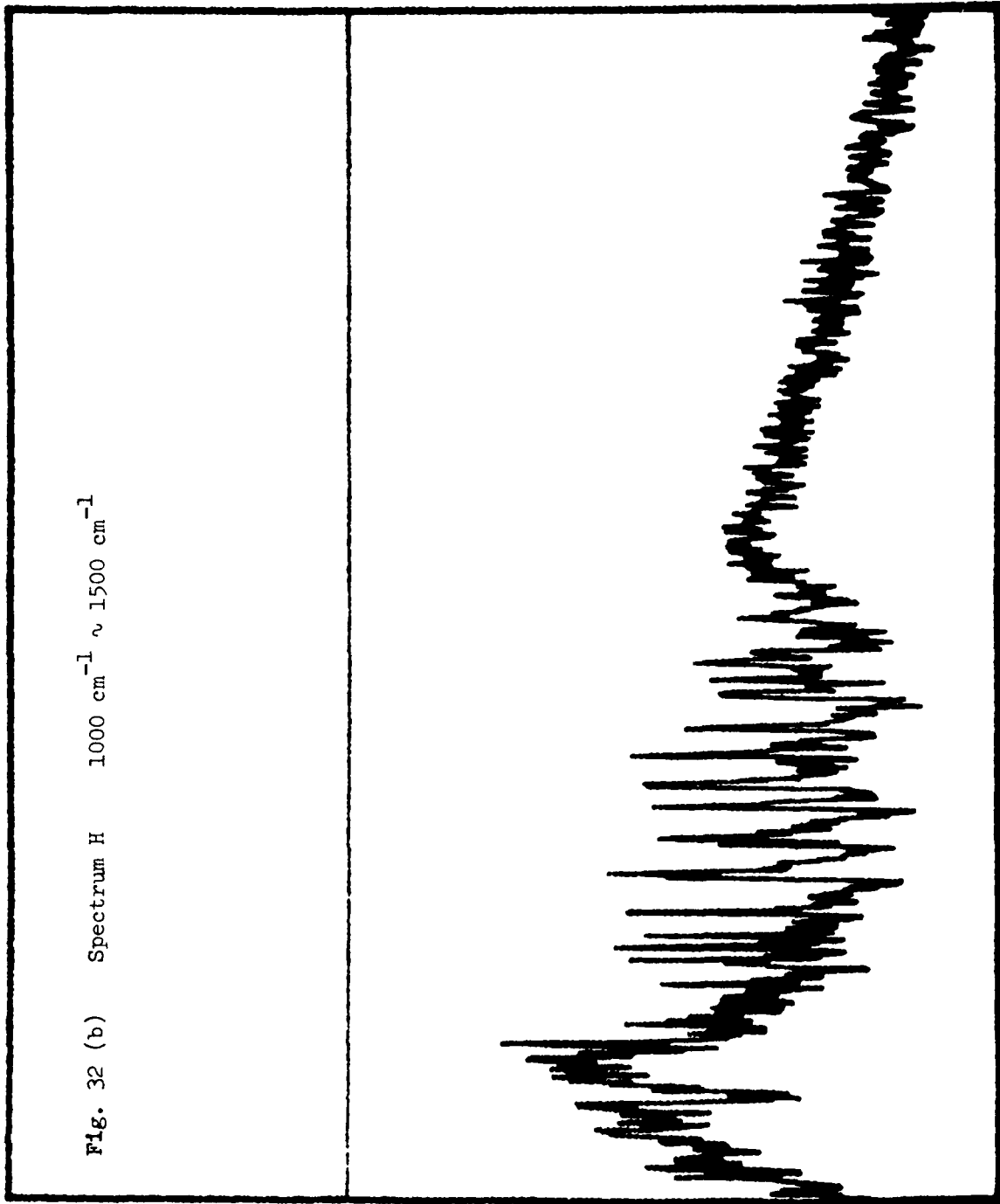


Fig. 33 (a) Spectrum K  $500 \text{ cm}^{-1} \sim 1000 \text{ cm}^{-1}$

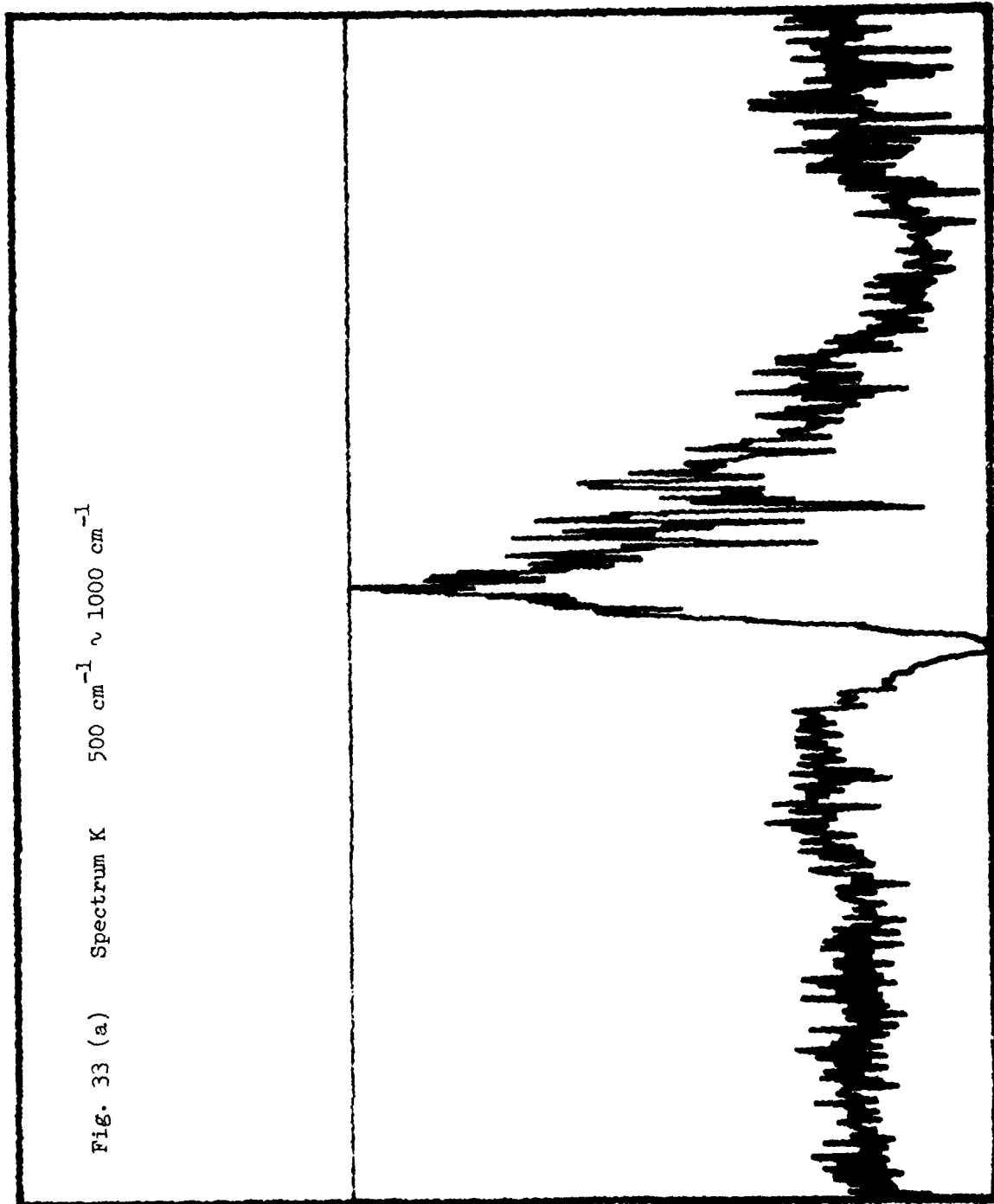


Fig. 33 (b) Spectrum K  $1000\text{ cm}^{-1} \sim 1500\text{ cm}^{-1}$



Fig. 34 (a) Spectrum M  $500 \text{ cm}^{-1} \sim 1000 \text{ cm}^{-1}$

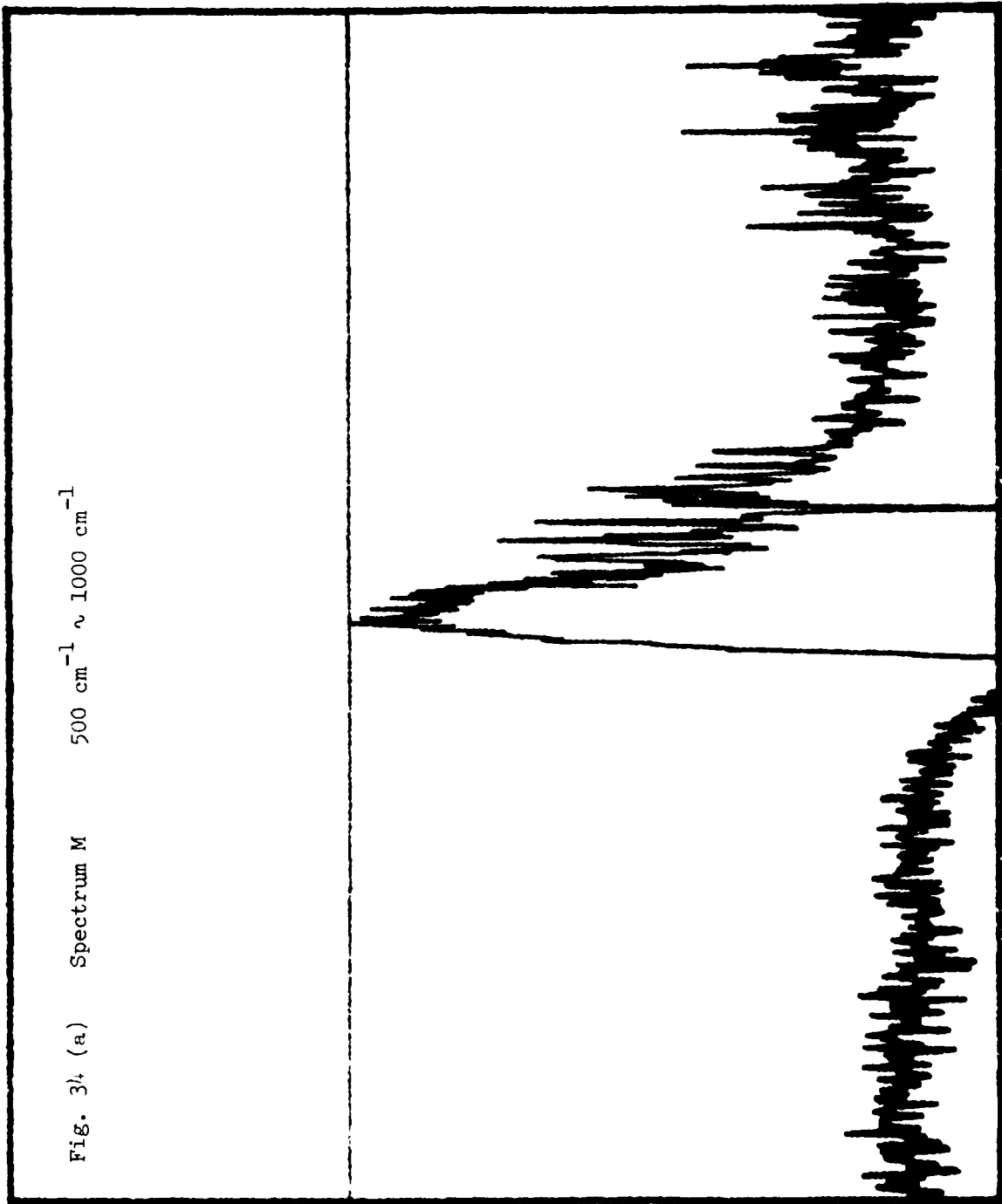


Fig. 34 (b) Spectrum M  $1000\text{ cm}^{-1} \sim 1500\text{ cm}^{-1}$

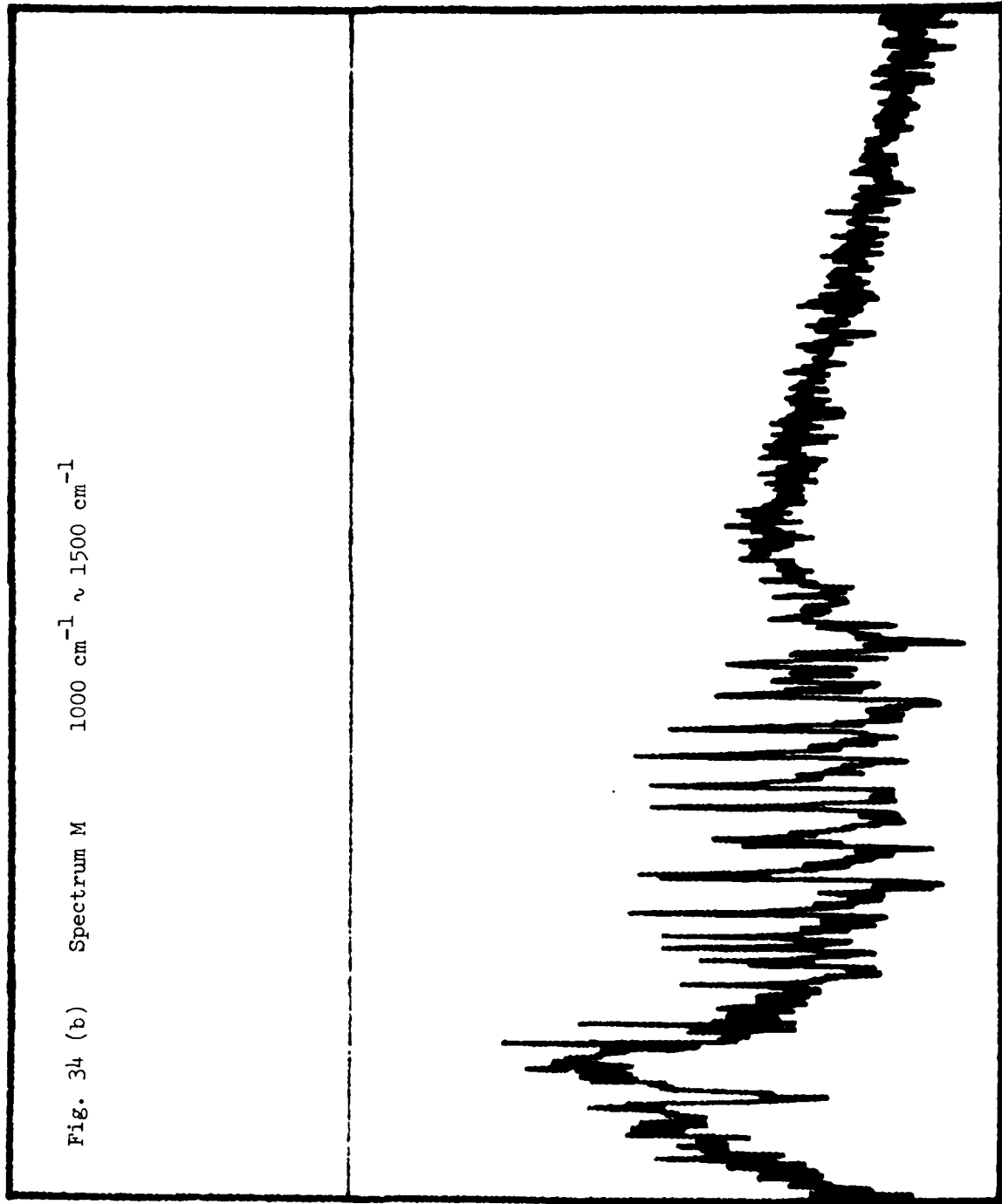


Fig. 35 (a) Spectrum N  $500\text{ cm}^{-1} \sim 1000\text{ cm}^{-1}$

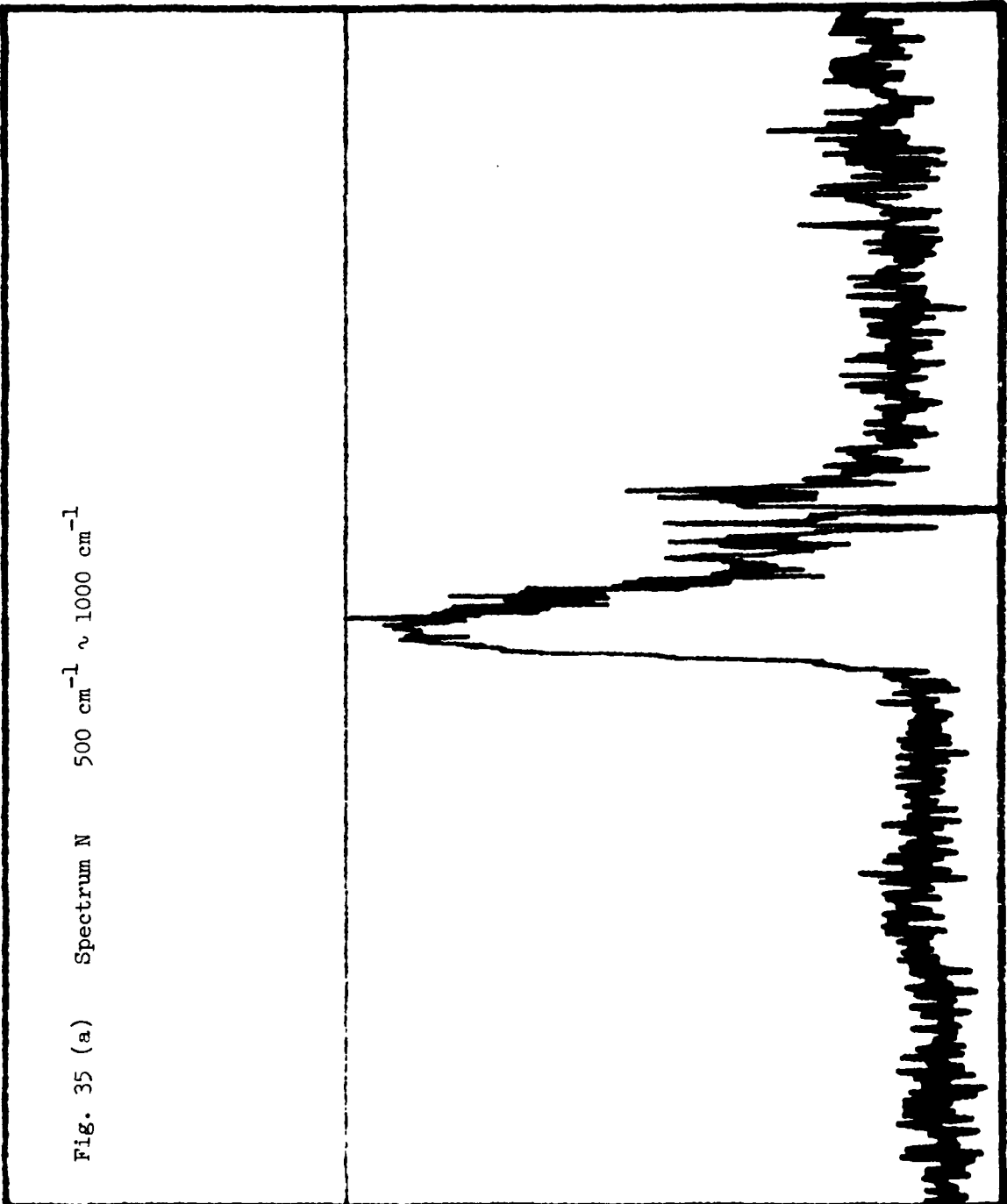


Fig. 35 (b) Spectrum N  $1000\text{ cm}^{-1} \sim 1500\text{ cm}^{-1}$

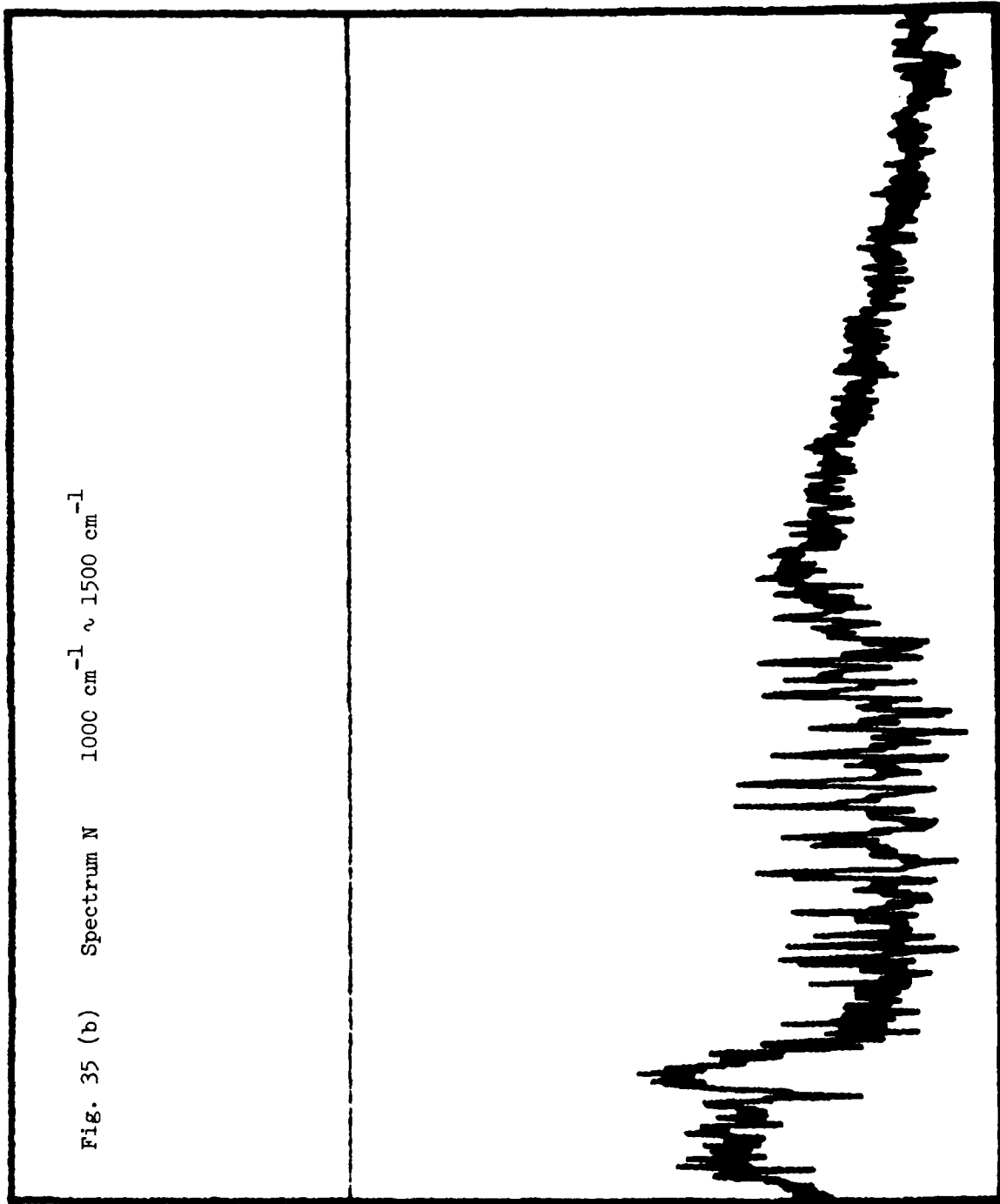


Fig. 36 (a) Spectrum P  $500 \text{ cm}^{-1} \sim 1000 \text{ cm}^{-1}$

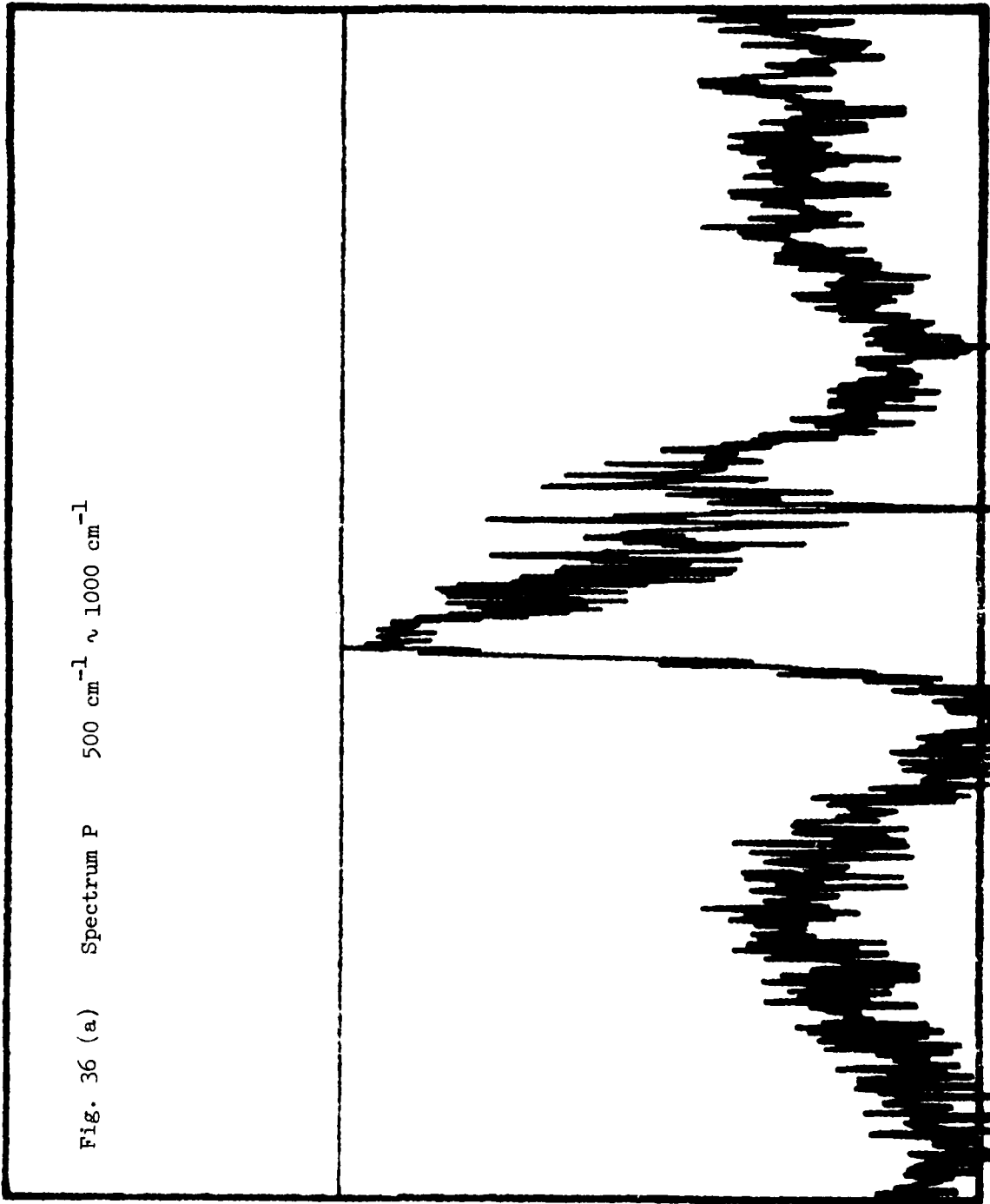


Fig. 36 (b) Spectrum P  $1000\text{ cm}^{-1} \sim 1500\text{ cm}^{-1}$

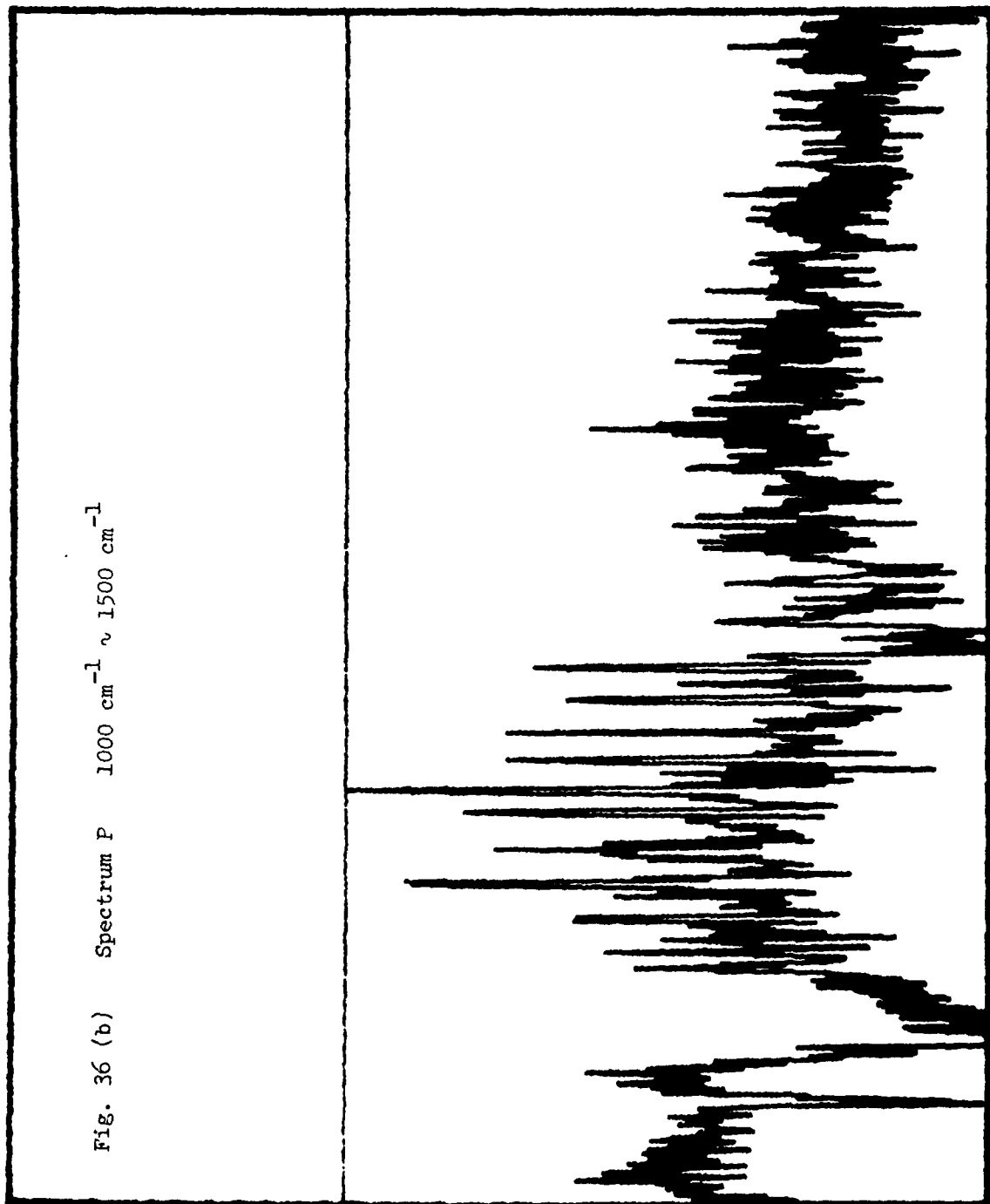


Fig. 37 (a) Spectrum Q  $500 \text{ cm}^{-1} \sim 1000 \text{ cm}^{-1}$

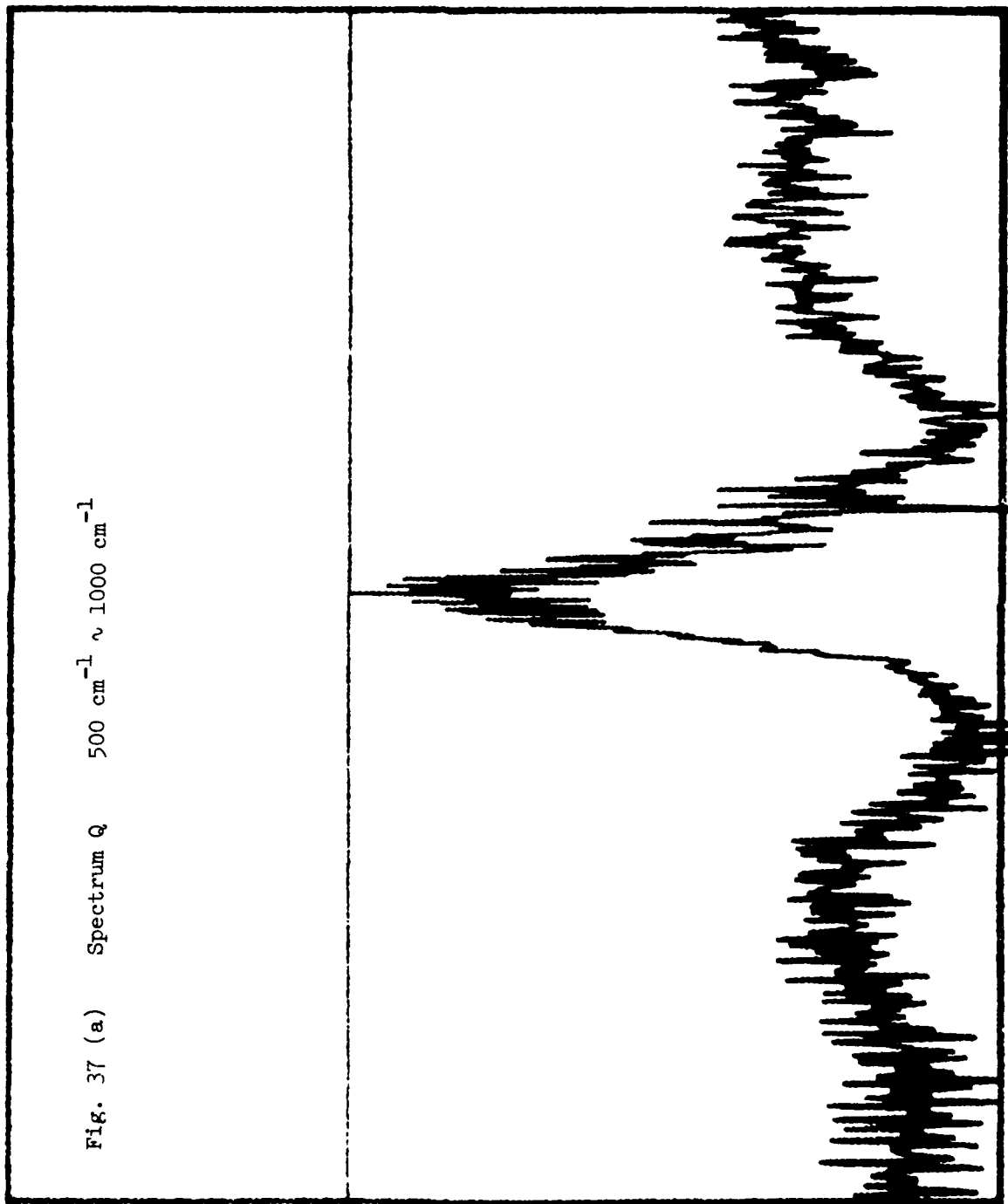


Fig. 37 (b) Spectrum Q  $1000\text{ cm}^{-1} \sim 1500\text{ cm}^{-1}$

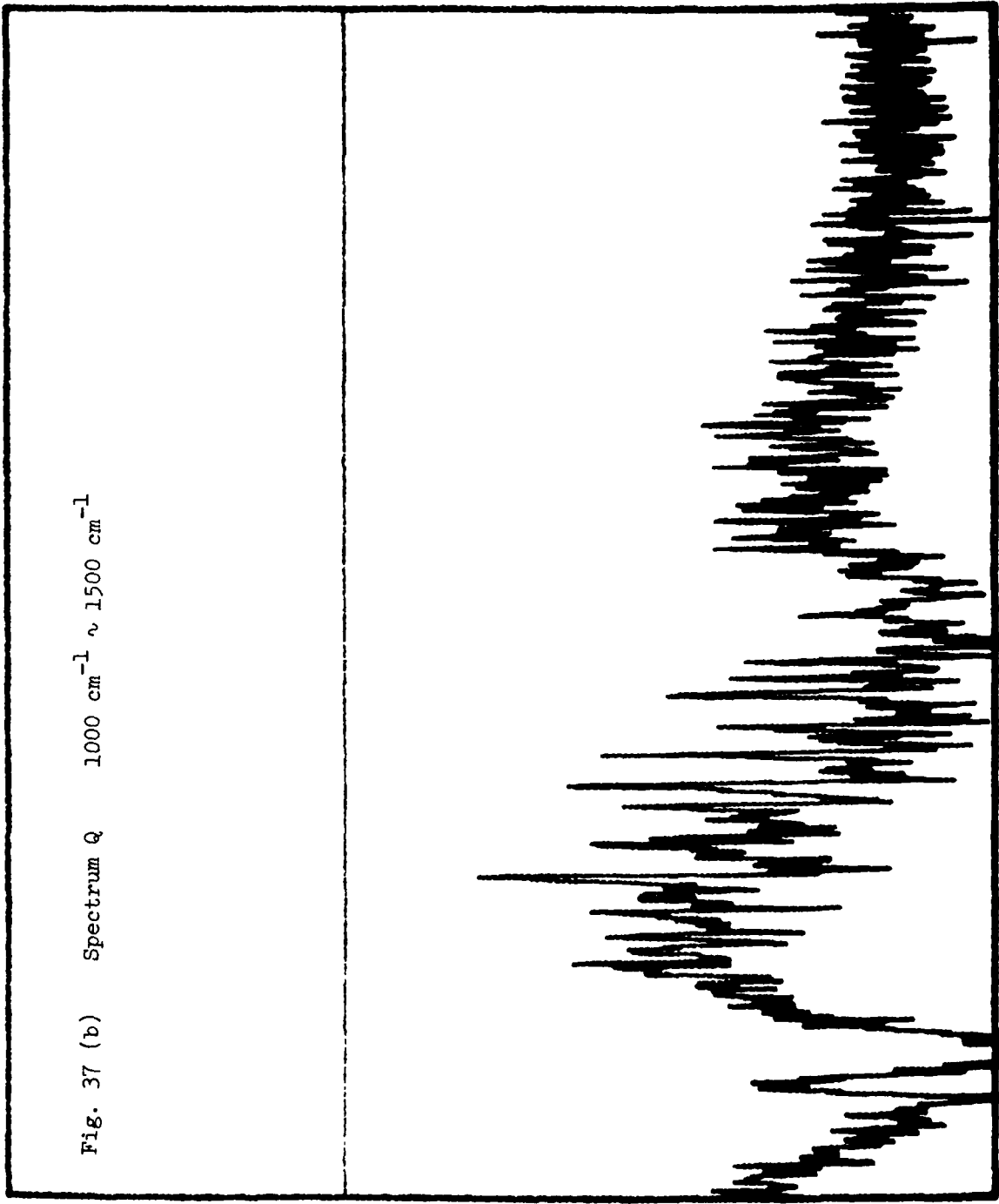


Fig. 38 (a) Spectrum R  $500 \text{ cm}^{-1} \sim 1000 \text{ cm}^{-1}$

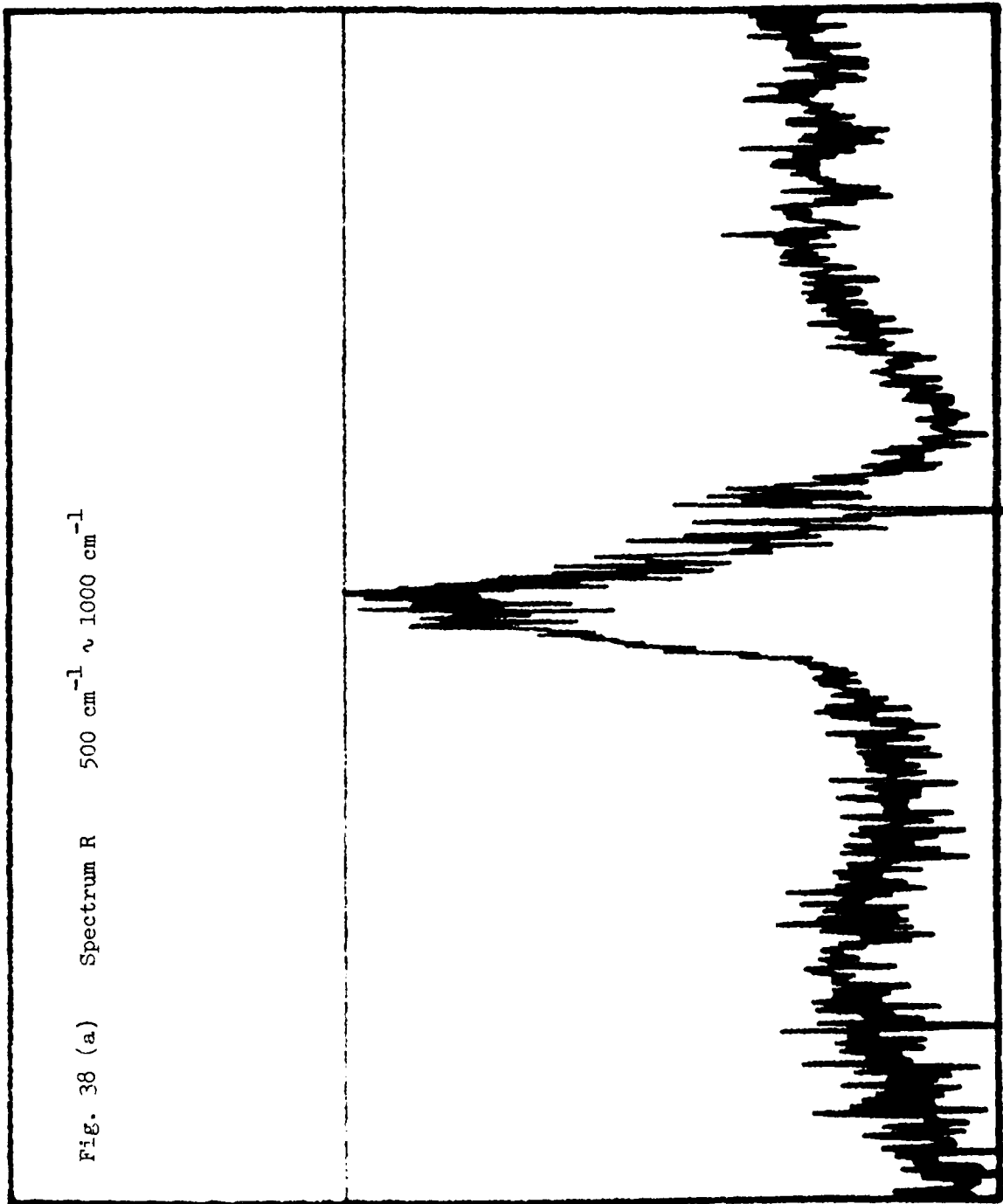
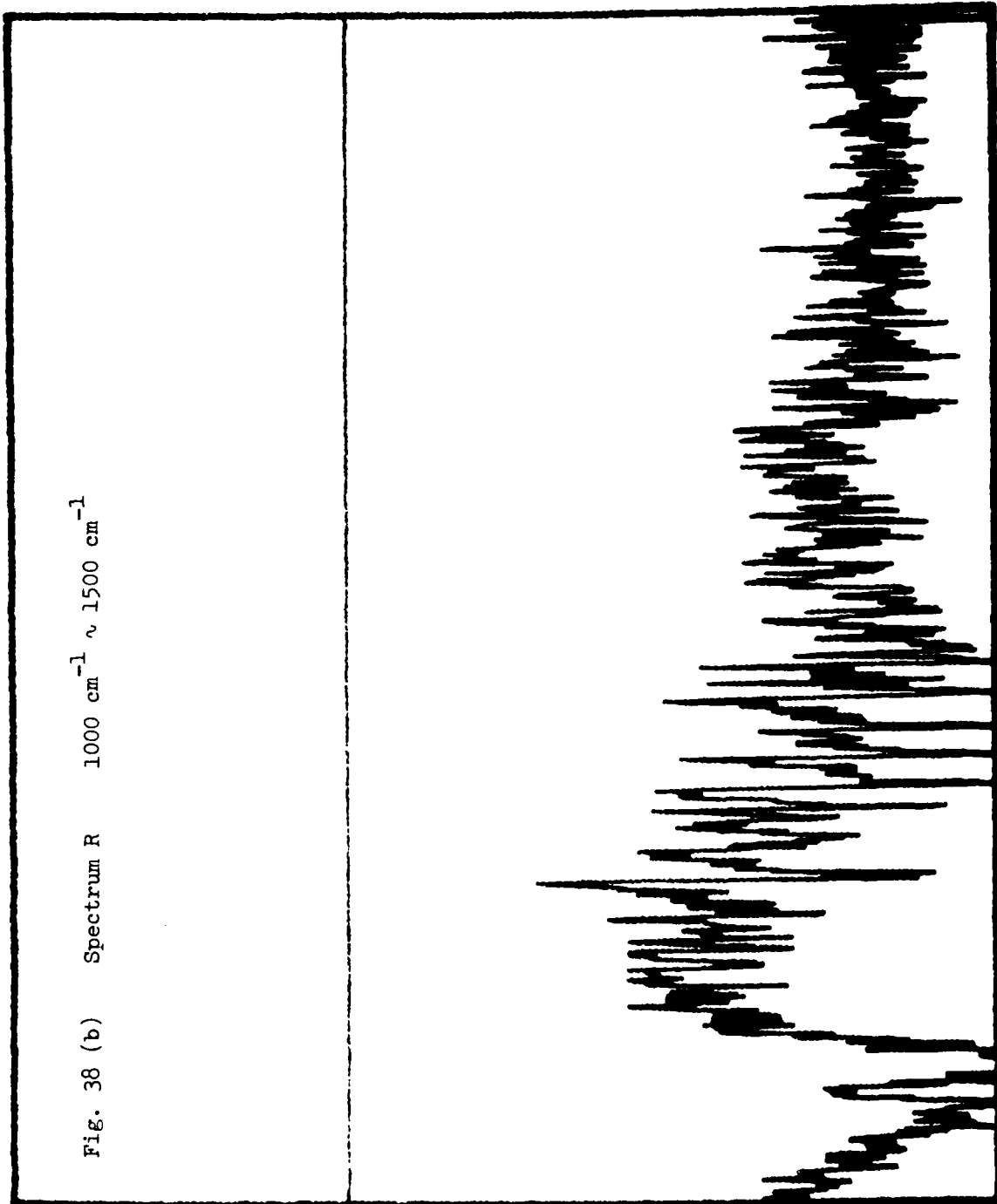


Fig. 38 (b) Spectrum R  $1000\text{ cm}^{-1} \sim 1500\text{ cm}^{-1}$



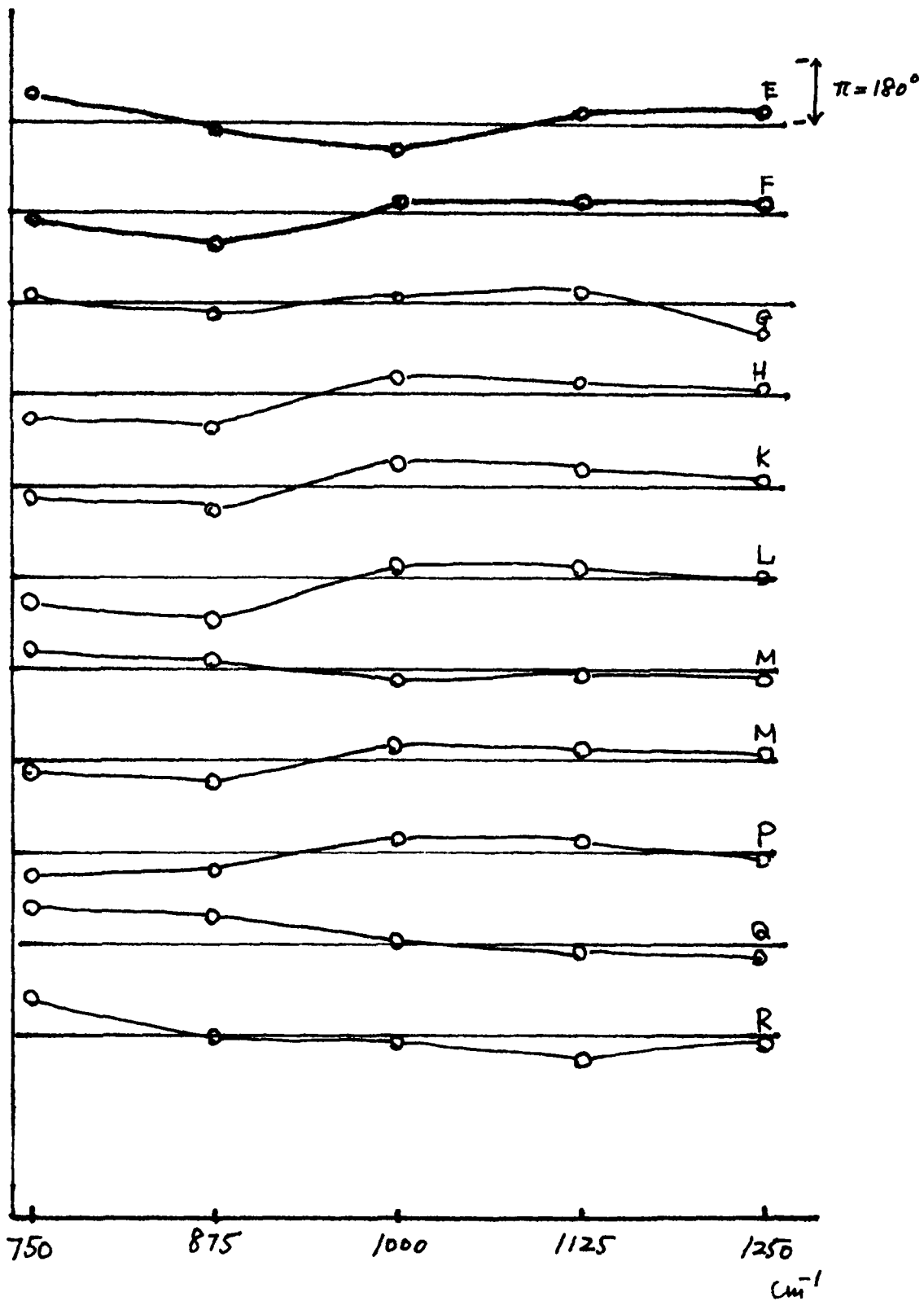


Fig. 39 The phase curves, spectra E through R.

### Spectral Data #N

Figure 40 shows the spectrum recovered from the data N with a resolution of  $0.12 \text{ cm}^{-1}$ . The interferometer was not calibrated for its spectral output as a function of the wavenumber. Thus the radiance value of the detected emission feature is remained undetermined. The detector used in this flight was a Ge:Hg operated at a liquid He temperature. A sharp drop in the spectral feature observed below  $750 \text{ cm}^{-1}$  was caused by the detector's sensitivity loss at that wave number. The spectrum was observed at altitude of approximately 5000 m above sea level. The interferogram was directed about  $10^\circ$  upward with unknown azimuthal orientation. With the observed spectrum, two synthesized spectra, calculated for a single atmospheric layer of  $250^\circ\text{K}$  with the column density given in the figure caption, are shown in Figure 40. The observed spectrum shown in the figure is far noisier than what the instrument was designed to produce at the best condition. A quantitative discussion of the spectral radiance level is not applicable for the present case. The emission features are nonetheless easily identifiable by comparing them with the synthetic spectra.

There are three major peculiarities noticed in the observed spectrum. Since insufficient amount of spectral data were collected, we wish to draw no conclusion regarding a validity of their observation. Nonetheless, they are described below.

The  $\text{H}_2\text{O}$  line feature in  $800 \sim 900 \text{ cm}^{-1}$  is mysteriously weak in the observed data. The beamsplitter should not be held responsible for the unusual feature in this spectral range, because the atmospheric absorption spectrum measured with a globar source prior to the launching showed no peculiarity. The Q branch of the  $800 \text{ cm}^{-1} \text{ CO}_2$  band (12201-10002 of

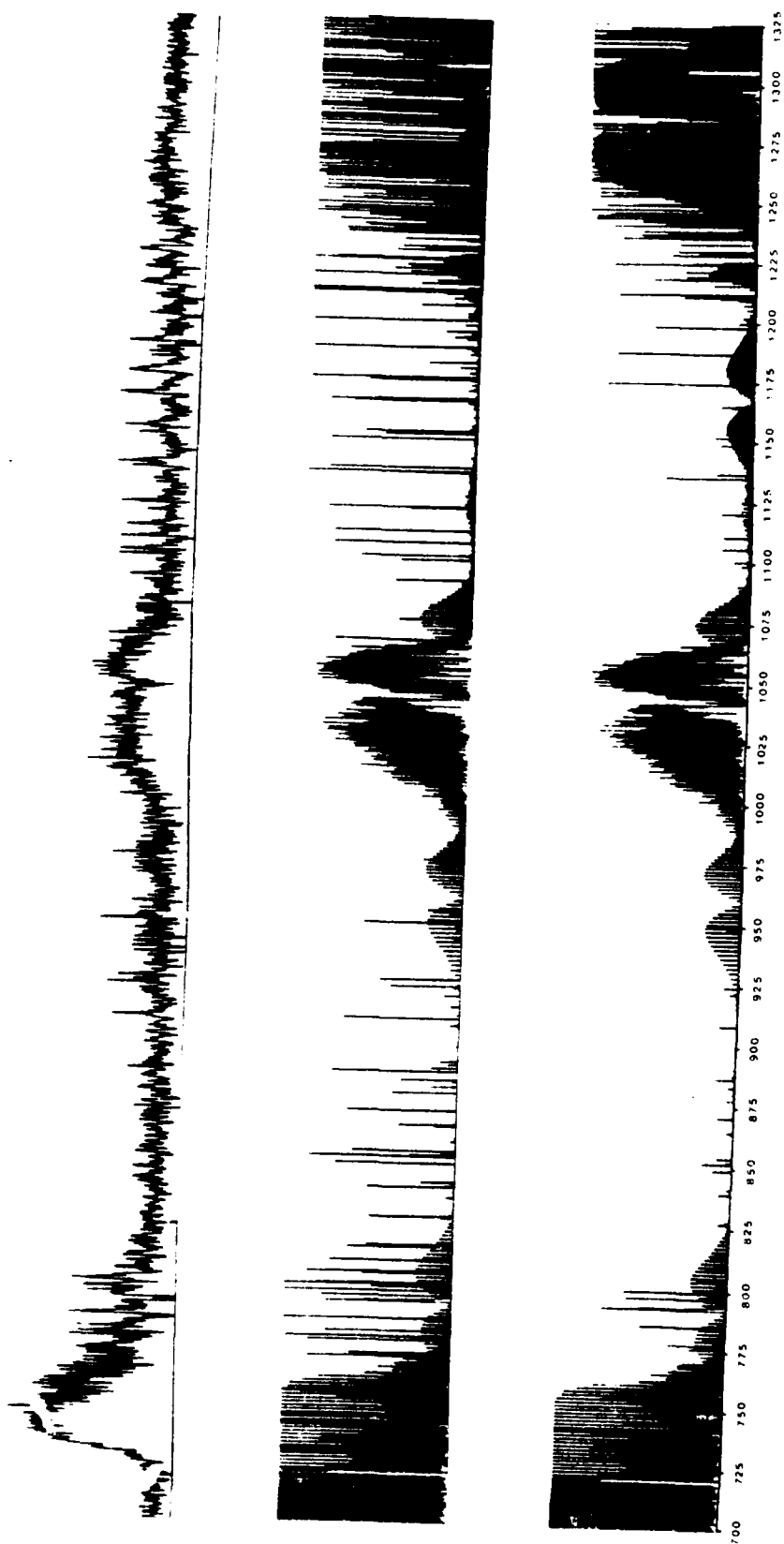
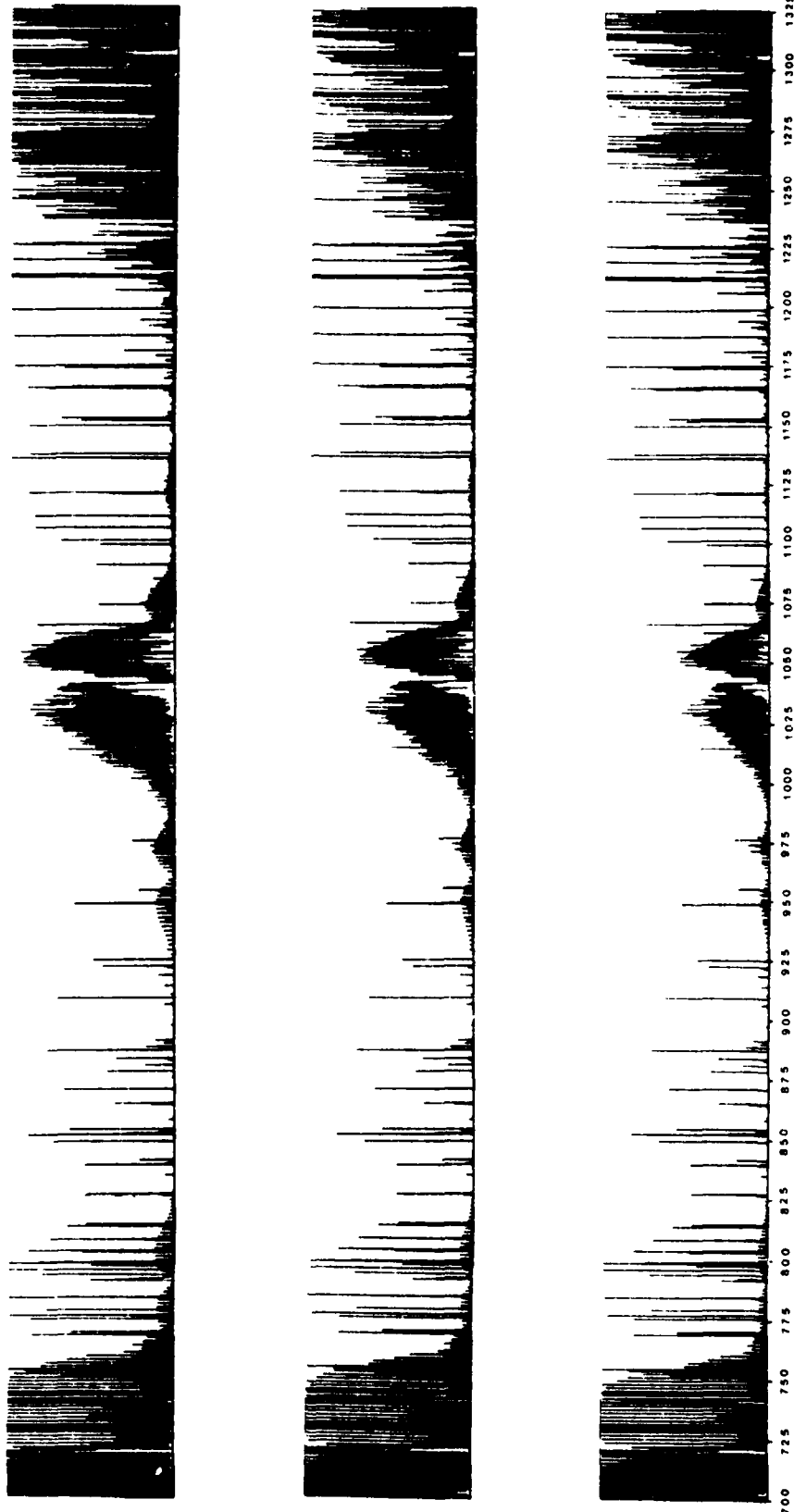


Fig. 40 Spectra observed and synthesized for a resolution of  $0.12 \text{ cm}^{-1}$ .  
 Top: Observed at altitude of 5000 m.  
 Middle: Synthesized assuming a single layer at  $T = 250^\circ\text{K}$ . Total molecular concentration:  
 $\text{H}_2\text{O} = .23 \times 10^{24}$ ;  $\text{CO}_2 = .52 \times 10^{23}$ ;  $\text{N}_2\text{O} = .18 \times 10^{19}$ ;  $\text{O}_3 = .41 \times 10^{20}$ .  
 Bottom: Synthesized assuming a single layer at  $T = 250^\circ\text{K}$ . Total molecular concentration:  
 $\text{H}_2\text{O} = .23 \times 10^{23}$ ;  $\text{CO}_2 = .52 \times 10^{23}$ ;  $\text{N}_2\text{O} = .18 \times 10^{20}$ ;  $\text{O}_3 = .41 \times 10^{20}$ .

$^{12}\text{C}^{16}\text{O}_2$ ) shows an absorptive feature. The band center at  $1040\text{ cm}^{-1}$  of the  $\text{O}_3$  band (001-000) is very narrow in the observed while the synthetic shows a well defined band center.

A semi-quantitative estimate for the column density of detected atmospheric molecules was tried by generating various synthetic spectra which are shown in Figures 41 and 42. All spectra are, as those shown with the observed spectrum, plotted in the emissivity against the black-body emission at the highest temperature of the synthetic model atmosphere. The figure caption details the atmospheric condition for each synthesis.



FREQUENCY  $\text{cm}^{-1}$

Fig. 41

Fig. 41 Caption

Theoretical Spectra

Top: Synthesized assuming a single layer at  $T = 250^{\circ}\text{K}$ ; total molecular concentration:  $\text{H}_2\text{O} = .23 \times 10^{24}$ ,  $\text{CO}_2 = .24 \times 10^{23}$ ,  $\text{O}_3 = 1.42 \times 10^{19}$ ,  $\text{N}_2\text{O} = .24 \times 10^{19}$ .

Middle: Synthesized assuming six layers specified below.

	Temp.	$\text{H}_2\text{O}$	$\text{CO}_2$	$\text{O}_3$	$\text{N}_2\text{O}$
1	250	$.12 \times 10^{24}$	$.4 \times 10^{22}$	$.2 \times 10^{19}$	$.4 \times 10^{18}$
2	245	$.06 \times 10^{24}$	$.4 \times 10^{22}$	$.2 \times 10^{19}$	$.4 \times 10^{18}$
3	240	$.05 \times 10^{24}$	$.4 \times 10^{22}$	$.5 \times 10^{19}$	$.4 \times 10^{18}$
4	230	0	$.4 \times 10^{22}$	$.5 \times 10^{19}$	$.4 \times 10^{18}$
5	240	0	$.4 \times 10^{22}$	$.01 \times 10^{19}$	$.4 \times 10^{18}$
6	250	0	$.4 \times 10^{22}$	$.01 \times 10^{19}$	$.4 \times 10^{18}$

Bottom: Synthesized assuming six layers specified below.

	Temp.	$\text{H}_2\text{O}$	$\text{CO}_2$	$\text{O}_3$	$\text{N}_2\text{O}$
1	250	$.12 \times 10^{24}$	$.4 \times 10^{22}$	$.2 \times 10^{19}$	$.4 \times 10^{18}$
2	245	$.06 \times 10^{24}$	$.4 \times 10^{22}$	$.2 \times 10^{19}$	$.4 \times 10^{18}$
3	240	$.06 \times 10^{24}$	$.4 \times 10^{22}$	$.5 \times 10^{19}$	$.4 \times 10^{18}$
4	230	0	$.4 \times 10^{22}$	$.5 \times 10^{19}$	$.4 \times 10^{18}$
5	220	0	$.4 \times 10^{22}$	$.01 \times 10^{19}$	$.4 \times 10^{18}$
6	220	0	$.4 \times 10^{22}$	$.01 \times 10^{19}$	$.4 \times 10^{18}$

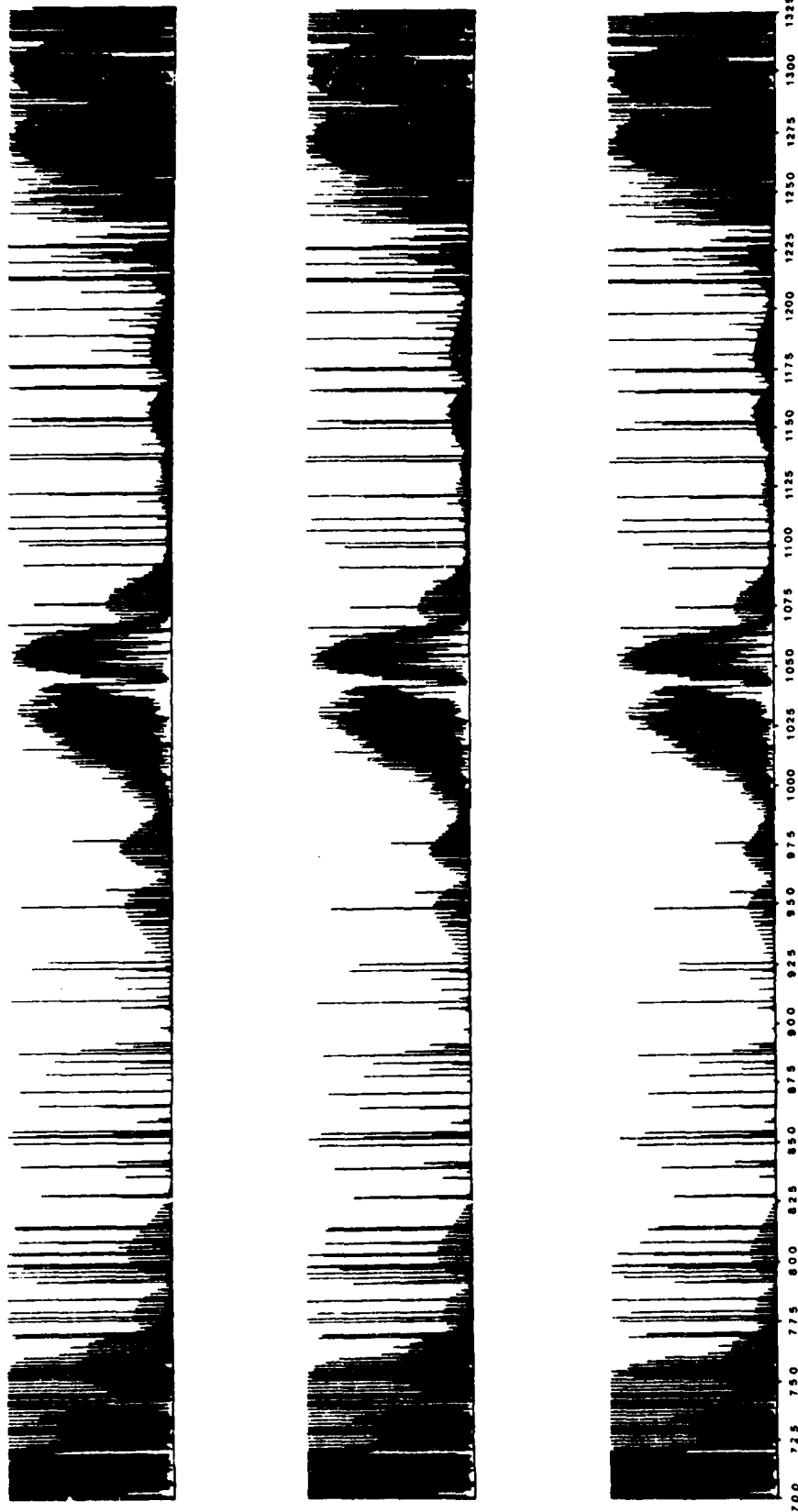


Fig. 1. Theoretical spectra synthesized assuming a single layer with various temperatures. Total molecular concentration:  $H_2O = .23 \times 10^{24}$ ;  $CO_2 = .24 \times 10^{23}$ ;  $O_3 = 1.42 \times 10^{19}$ ;  $N_2O = .1 \times 10^{19}$ . Top: temperature = 280. Middle: temperature = 270. Bottom: temperature = 260.

### Conclusion and Recommendations For Future Flights

The October 1980 flight provided a valuable test for the basic concept of the SCRIBE program. It established a validity of the experiment. The cryogenic interferometer was shown to be very effective for measuring the atmospheric emission. The principal problem which contributed to a degradation of the result was the unstable turn-around behavior in the interferometer scanning. We expect that the problem will be solved in a satisfactory degree by the next flight. With the interferometer scanning problem being solved, several problems related to it will be cured automatically. There are several modifications which we would like to recommend:

(1) Elimination of the gain-adjusting scheme. The radiance level of the emission is known. An on-board calibration scheme for the radiance level is necessary, and it would determine the gain of the detector electronics.

(2) Interferogram sampling interval to be a single laser fringe distance. The present sampling interval of twice the fringe distance could invite more problems.

(3) Improvement of the electronics which generates the 4-bit interferogram status word. The last flight data indicated a poor reliability of the scheme.

Appendix A

```

.TITLE DR11B TO RK1
.CSECT DUMPAL
.GLOBL BASES, HNDLRS

.MCALL ..V2...REGDEF,.PRINT,.EXIT,.CSIGEN
.MCALL .READC,.WRITW,.CLOSE,.SRESET,.ENTER

..V2..
.REGDEF

BLKSIZ = 40 ; # BLOCKS @ RECORD
RECSIZ = < BLKSIZ * 400 > ; # WORDS @ RECORD
FRMSZ = RECSIZ ; # DATA WORDS

ERRWD = 52 ; MONITOR ERROR CODES

DRVEC = 124 ; ADDRESS OF DR INT VECTOR
DRPSW = 340 ; INTERRUPT PRIORITY BR7

DRWC = 172410
DRBA = DRWC + 2
DRST = DRWC + 4
DRDA = DRWC + 6

TKS = 177560 ; TT HARDWARE REGISTERS
TKB = TKS + 2

SWR = 177570
EDTBIT = 2000 ; MT EDT STATUS BIT
CNTRLC = 203 ; ASCII CC

; * * * * *

START: JSR PC,INIT

LO: JSR PC,BELL
JSR PC,PCMIN ; BUFFER LOAD
JSR PC,RKOUT
JSR PC,TRACE

.PRINT #DONE
JSR PC,BELL
JSR PC,CLOSER
.EXIT

DONE: .ASCIZ / DONE/
.EVEN

; * * * * *

; INITIALIZE DEVICES, OPEN FILES, PRESET
; PROGRAM VARIABLES, AND SET INTR VECTOR

INIT: MOV @TKS,TTEMP
CLR @TKS

```

```

        CLR     FRAME
        CLR     BLKNUM

        .ENTER #AREA,#0,#DEV,#-1
        BCS     BADENT
        MOV     #DRINT,@#DRVEC
        MOV     #DRPSW,@#DRVEC+2
        RTS     PC

DEV:    .RAD50  /RK1/
        .RAD50  /PCM/
        .RAD50  /RK1/
        .RAD50  /DAT/

AREA:   .BLKW   10
BADENT: .PRINT  #EMSG
        .EXIT
BADWR:  .PRINT  #WMSG
        .EXIT

EMSG:   .ASCIZ  /BAD ENTER/
WMSG:   .ASCIZ  /BAD WRITE/
        .EVEN

;      *      *      *      *      *      *      *
;
;          RING BELL ON TERMINAL

BELL:   .PRINT  #BELMSG
        RTS     PC

BELMSG: .BYTE   7,7,7,7,7,0
        .EVEN

;      *      *      *      *      *      *      *
;
;          START DR11B WITH INTERRUPT ENABLED
;          ( VECTOR POINTS TO "DRINT" )

PCMIN:  CLR     DRFLG
        MOV     #30,BCOUNT
LOOPA:  BIT     #1,@#SWR          ; LOOP UNTIL "READY"
        BEQ    LOOPA

        MOV     #-FRMSZ,@#DRWC
        MOV     #B0,@#DRBA
        CLR     @#DRST          ; STROBES DRST REGISTER
        MOV     @#177570,@#DRST ; SW REG
        RTS     PC

;      *      *      *      *      *      *      *
;
;          RK1 WRITE

RKOUT:  MOV     #B1,B
AGAIN:  MOV     #B0,BUF
AA:     BIT     #1,DRFLG
        BEQ    AA
        MOV     #B0,B
        .WRITW #AREA,#0,BUF,#20000,BLKNUM
        BCS     BADWR
        ADD     #40,BLKNUM
        MOV     #B1,BUF
AB:     BIT     #1,DRFLG
        BNE    AB

        MOV     #B1,B

```

```

        .WRITW  $AREA,$0,BUF,$20000,BLKNUM
        BCS    BADWR
        ADD    $40,BLKNUM
        DEC    BCOUNT
        BNE    AGAIN
        RTS    PC

DRFLG:  .WORD  0
BCOUNT: .WORD  30
BUF:    .WORD  0

;      *          *          *          *          *
;
;          DR11 INTERRUPT HANDLER
;          TRAP & REPORT ERRORS,
;          START MAGTAPE WRITE.
;

DRINT:  MOV    B,@$DRBA
        MOV    $-FRMSZ,@$DRWC
        MOV    @$SWR,@$DRST
        INC    DRFLG

DRDONE: RTI

;      *          *          *          *          *
;
;          DUMPS DR11B REGISTERS
;

DRDUMP: MOV    R0,-(SP)
        MOV    R1,-(SP)

        MOV    @$DRWC,R0
        MOV    $DRWCM,R1
        JSR    PC,BASEB

        MOV    @$DRBA,R0
        MOV    $DRBAM,R1
        JSR    PC,BASEB

        MOV    @$DRST,R0
        MOV    $DRSTM,R1
        JSR    PC,BASEB

        MOV    @$DRDA,R0
        MOV    $DRDAM,R1
        JSR    PC,BASEB

        .PRINT $DRMSG
        MOV    (SP)+,R1
        MOV    (SP)+,R0
        RTS    PC

DRMSG:  .ASCII  / DR DUMP/
        .BYTE  12, 15

        .ASCII  / WC /
DRWCM:  .BLKB  6

        .ASCII  / BA /
URBAM:  .BLKB  6

        .ASCII  / ST /

```

```

DRSTM: .BLKB 6
      .ASCII / DA /
DRDAM: .BLKB 6
      .BYTE 0
      .EVEN

```

```

; * * * * *

```

```

; DISPLAYS CURRENT FRAME NUMBER IF
; TTY KEY IS PRESSED. ALSO STOPS
; PROGRAM ON ^C

```

```

TRACE: TSTB @TKS
      BEQ TRACND

      .PRINT #TRDUMP
      MOV R1,-(SP)
      MOV @TKB,-(SP)

      MOV BCOUNT,R0
      MOV #FRMNUM,R1
      JSR PC,BASEB

      .PRINT #TRACEM
      MOV (SP)+,R0
      CMPB #CNTRLC,R0
      BNE TRACNM

      .PRINT #TRACEX
      MOV TSTEMP,@TKS
      JSR PC,CLOSER
      .EXIT

```

```

TRACNM: MOV (SP)+,R1

```

```

TRACND: RTS PC

```

```

TRDUMP: .ASCIZ / TR DUMP /
TRACEM: .ASCII / FRAME # /
FRMNUM: .BLKB 6
      .BYTE 0
TRACEX: .ASCIZ / ABORT/
      .EVEN

```

```

; * * * * *

```

```

; REPORT ERRORS & ABORTS PROGRAM

```

```

ERRORS: MOV ERRNUM,R0
      MOV #ERRSUB,R1
      JSR PC,BASEB

```

```

      MOV ERRWD,R0
      MOV #ERRWRD,R1
      JSR PC,BASEB

```

```

; .PRINT #ERRMSG
; JSR PC,CLOSER
; .EXIT

```

```

ERRMSG: .ASCII / ERROR: SUB /

```

```
ERRSUB: .BLKB 6
        .ASCII /, CODE /
ERRWRD: .BLKB 6
        .BYTE 0
        .EVEN
```

```
; * * * * *
;
; CLOSE FILES, RESET SYSTEM
```

```
CLOSER: .CLOSE #0
        .CLOSE #3
        .CLOSE #4
        .SRESET
        RTS PC
```

```
: * * * * *
```

```
; STATUS BLOCK
```

```
STATUS = .
FRAME: 0
BLANUM: 0
ERRNUM: 0
RK1FLG: 0
SPTEMP: 0
TSTEMP: 0
EMT1: .BLKW 5
EMT2: .BLKW 5
EMT3: .BLKW 5
EMT4: .BLKW 5
```

```
ENDBUF: . = STATUS+1000 ; 400 WORDS
```

```
B0: .BLKW RECSIZ
B1: .BLKW RECSIZ
B: .WORD 0
```

```
.END START
```

```
*
```

```

DIMENSION IDATA(4096),IBUFF(4096),NAME1(4),NAME2(4),NAME3(1)
DATA NAME1/3RRK1,3RPCM,3RRK1,3RDAT/
DATA NAME2/3RDT0,3RPCM,3RDAT,3RDAT/
DATA NAME3/3RDT0/
DO 70 I=1,4096
  IDATA(I)=0.
70  CONTINUE
C
C READ FROM RK1
C
      JSIZE=4096
      IC=IGETC()
      IF(LOOKUP(IC,NAME1).LT.0)STOP 'BAD LOOK UP'
      JC=IGETC()
      IF (IFETCH(NAME3).NE.0)STOP 'FATAL ERRER FETCHING HANDLER'
      IC1=IENTER(JC,NAME2,0,0)
      IF(IC1.EQ.-1)STOP 'ENTER FAILURE NO CHANNEL'
      IF(IC1.EQ.-2)STOP 'NO SPACE'
      ISTART=1
      IEND=0
      INDEX=0
      NB=0
      IAA=4096
      ICOUNT=18
      INB=1
10  CALL IREADW (4096,IDATA,NB,IC)
      ICODE=IREADW (4096,IDATA,NB,IC)
      IF (ICODE.EQ.-1) GO TO 100
      NB=NB+16
      CALL SLECT (IDATA,IBUFF,JSIZE,ISTART,IEND)
      IF (IEND.LT.IAA)GO TO 10
      K=1
      DO 20 I=ISTART,IAA
        IBUFF(I)=IDATA(K)
        K=K+1
20  CONTINUE
      IF(ICOUNT.NE.1) GO TO 25
      DO 22 I=2049,4096
        IBUFF(I)=0
22  CONTINUE
25  CALL IWRITW(4096,IBUFF,INB,JC)
      INB=INB+16
      J=1
      KEND=IEND-ISTART
      DO 30 I=K,KEND
        IBUFF(J)=IDATA(I)
        J=J+1
30  CONTINUE
      IEND=J-1
      ICOUNT=ICOUNT-1
      IF(ICOUNT.NE.0) GO TO 10
100 CALL CLOSEC(IC)
      CALL IFREEC(IC)
      CALL CLOSEC(JC)
      CALL IFREEC(JC)
      CALL EXIT
      STOP
      END

```

```

SUBROUTINE SLECT (IDATA,IBUFF,JSIZE,ISTART,IEND)
DIMENSION IDATA(1),IBUFF(1)
DATA ITEST /5/
INDEX=1
ISTART=IEND+1
J=1
DO 10 I=1,JSIZE
IX=IDATA(I).AND.ITEST
IF (IX.NE.5) GO TO 10
CALL ZEROUT (IDATA(I),INDEX)
IF (INDEX.EQ.0) GO TO 10
IDATA(J)=IDATA(I)
J=J+1
10 CONTINUE
J=J-1
IEND=ISTART+J-1
IF (IEND.GT.4096)GO TO 30
J=1
DO 20 I=ISTART,IEND
IBUFF(I)=IDATA(J)
J=J+1
20 CONTINUE
30 RETURN
END

```

```

*
;TAKE ZERO DATA OFF THE TAPE (DATA,INDEX)
.MCALL ..V2...REGDEF
..V2..
.REGDEF
.GLOBL ZEROUT
ZEROUT: TST    (R5)+
MOV     @ (R5)+,R2
MOV     #1,@ (R5)

        RIC    #17,R2
        ROR   R2
        ROR   R2
        ROR   R2
        ROR   R2
        TST   R2
        BNE  OUT
        CLR  @ (R5)
;
OUT:    RTS    PC
;
        .END  ZEROUT
*

```



```

PROGRAM MFX(TAPE1,TAPER,OUTPUT,TAPER)
DIMENSION IA(4096)
100 FORMAT(14F7)
101 FORMAT(10F4X,05)
102 FORMAT(6F7)
READ(6,100) JUNK
READ(6,100) JUNK
READ(6,102) JUNK
READ(6,101)(IA(I),I=1,4096)
IAVER1=0
IAVER2=0
J=4096
DO 10 I=1,256
IAVER1=IAVER1+IA(I)
IAVER2=IAVER2+IA(I)
J=J-1
10 CONTINUE
IAVER1=IAVER1/256
IAVER2=IAVER2/256
PRINT 100,IAVER1,IAVER2
IDIFF=(IAVER2-IAVER1)/2
DO 15 I=1,1024
IA(I)=IA(I)-IAVER1
IF(IA(I) .LT. IDIFF) GO TO 10
15 CONTINUE
16 CONTINUE
PRINT 100, I
IJ=I+15
IJJ=I+15
PRINT 100,(IA(J),J=IJ,IJJ)
IK=I-1
DO 19 K=1+IK
A=FLOAT(IA(K))*5.6
IA(K)=ITTY(A)
19 CONTINUE
IKK=IK+1
IA(KK)=IA(KK)-IAVER2+IAVER1
IKK=IKK+1
DO 21 K=IKK,4096
IA(K)=IA(K)-IAVER2
21 CONTINUE
WRITE(1,100)(IA(I),I=1,4096)
DO 17 K=1,8
READ(6,101)(IA(I),I=1,4096)
DO 18 I=1,4096
IA(I)=IA(I)-IAVER2
18 CONTINUE
WRITE(1,100)(IA(I),I=1,4096)
17 CONTINUE
CALL EXIT
STOP
END

```

